

MODIS
Thermal Emissive Band
RVS Measurement Data Analysis

Outline

- Basic equations to retrieve RVS
- Drifting of the linear coefficient b_1
- Error sources and analysis in RVS retrieval
- RVS fitting equation and procedure

Basic RVS retrieval equations (1)

$$f(DN_{bcs}) = L_{bcs} \cdot RVS_{bcs} + (\tau - RVS_{bcs}) \cdot L_{sm} + \delta_{bkg} \quad (\text{Eq.1})$$

$$f(DN_{obc}) = \varepsilon \cdot L_{obc} \cdot RVS_{obc} + (\tau - RVS_{obc}) \cdot L_{sm} + \delta_{bkg} \quad (\text{Eq.2})$$

$$f(DN_{svs}) = L_{svs} \cdot RVS_{svs} + (\tau - RVS_{svs}) \cdot L_{sm} + \delta_{bkg} \quad (\text{Eq.3})$$

$$f(DN) = a_0 + a_1 \cdot DN + a_2 \cdot DN^2 \quad (\text{Eq.4})$$

where τ is the MODIS fixed optics total throughput, and L is the Planck function radiance integrated over each bandwidth.

Basic RVS retrieval equations (2)

(Eq.1) - (Eq.3) gives

$$b_1 \cdot dn_{bcs} + (L_{svs} - L_{sm}) \cdot RVS_{svs} + a_2 \cdot dn_{bcs}^2 = (L_{bcs} - L_{sm}) \cdot RVS_{bcs} \quad (\text{Eq.5})$$

(Eq.2) - (Eq.3) gives

$$b_1 \cdot dn_{obc} + (L_{svs} - L_{sm}) \cdot RVS_{svs} + a_2 \cdot dn_{obc}^2 = (\varepsilon \cdot L_{obc} - L_{sm}) \cdot RVS_{obc} \quad (\text{Eq.6})$$

where

$$b_1 = a_1 + 2a_2 \cdot DN_{svs} \quad (\text{Eq.7})$$

Basic RVS retrieval equations (3)

(Eq.5) / (Eq.6) gives

$$\frac{RVS_{bcs}}{RVS_{obc}} = \frac{\varepsilon \cdot L_{obc} - L_{sm}}{L_{bcs} - L_{sm}} \cdot \frac{dn_{bcs}}{dn_{obc}} \cdot (1 + \Delta_1 + \Delta_2) \quad (\text{Eq.8})$$

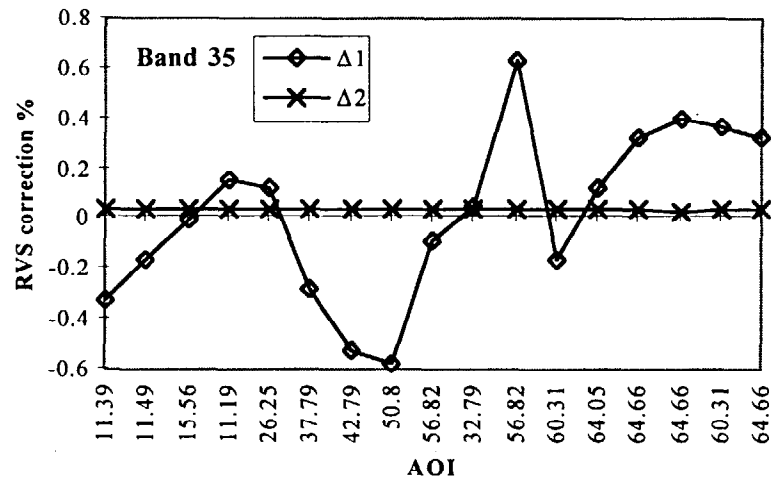
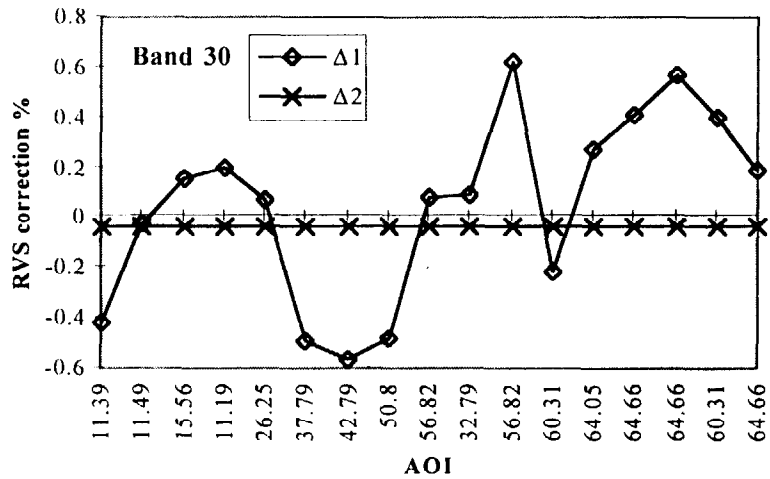
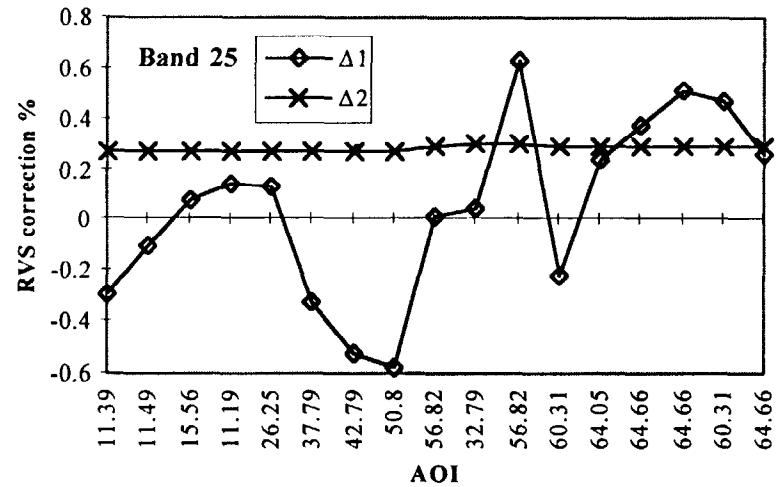
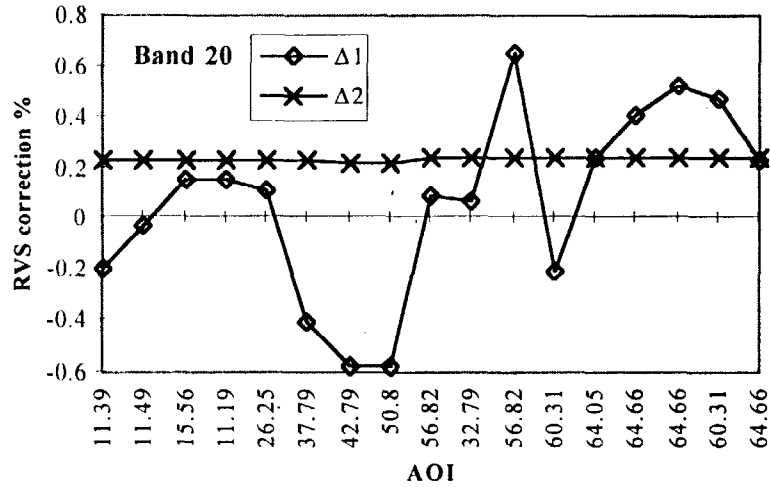
where correction due to temperature difference between sm and svS is

$$\Delta_1 = \frac{RVS_{svs} \cdot (L_{sm} - L_{svs})}{b_1 \cdot dn_{bcs} \cdot dn_{obc}} \cdot (dn_{bcs} - dn_{obc}) \quad (\text{Eq.9})$$

and the correction due to non-linear term is

$$\Delta_2 = \frac{a_2}{b_1} \cdot (dn_{bcs} - dn_{obc}) \quad (\text{Eq.10})$$

Δ_1 , Δ_2 Evaluation



Drifting of linear coefficient b_1

As shown in (Eq.7)

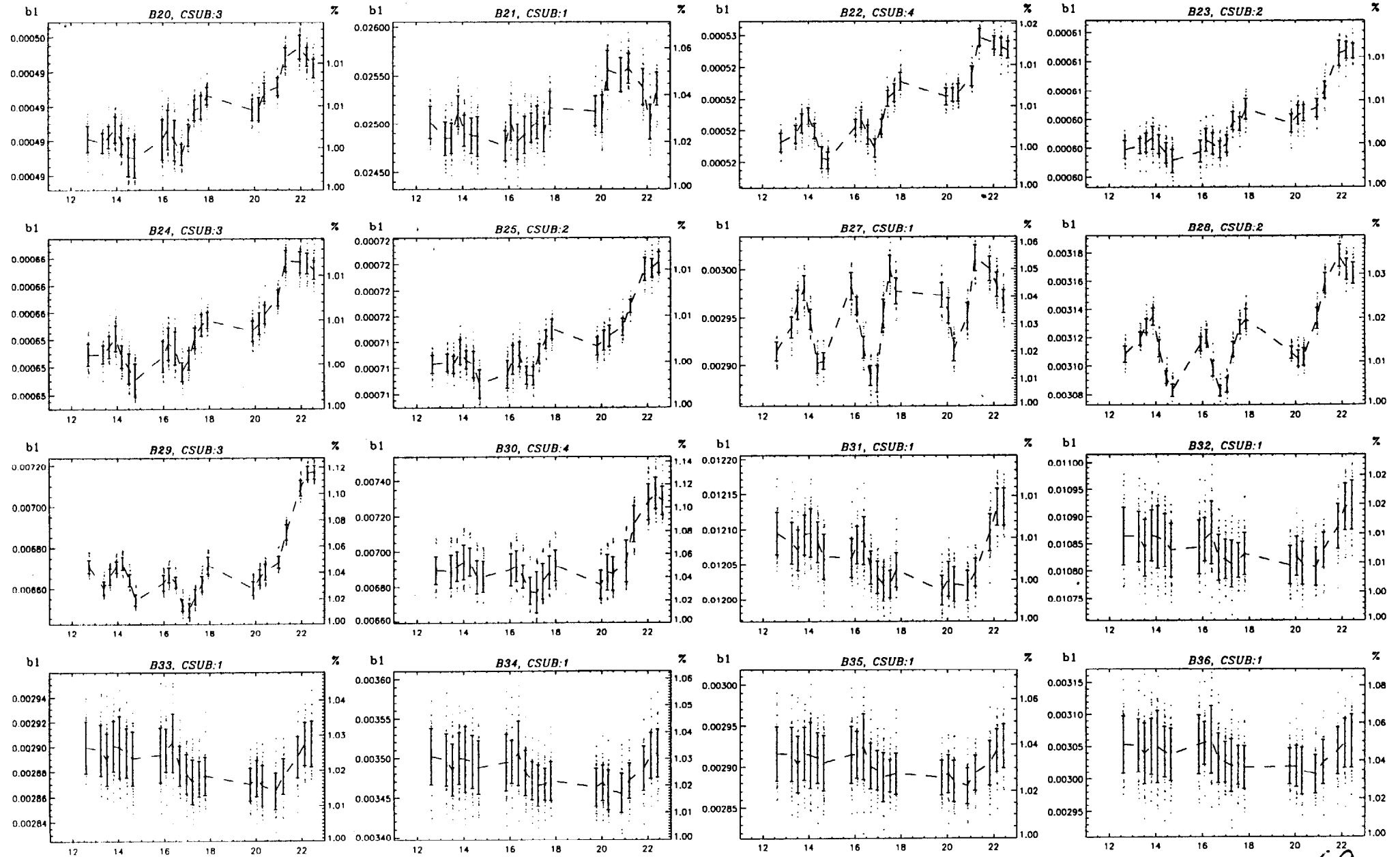
$$b_1 = a_1 + 2a_2 \cdot DN_{svs}$$

where the a_1 is a function of FPA temperature, and DN_{svs} drifts as background fluctuates, thus, b_1 will fluctuate as DN_{svs} and FPA temperature drift, and hence needs to be retrieved scan by scan as

$$b_1 = RVS_{obc} \cdot \frac{(\varepsilon \cdot L_{obc} - L_{sm})}{dn_{obc}} + \text{higher order terms, (Eq.11)}$$

FM1 RVS Highbay Measurement (PC20); Data set [320_2]

Linear Gain $\langle b1 \rangle_{50 \text{ frames}}$ vs. Time(hours of the day; 3/30/98); ch5, 40 scans, side A; T_bcs=320K



Error sources in RVS retrieval

- Temperature measurement error in

$$T_{\text{bcs}}, T_{\text{obc}}, T_{\text{sm}}, T_{\text{svs}}$$

- OBC effective emissivity ϵ_{obc}
- DN measurement errors due to

cross-talk, finite resolution, ...

Error Analysis in RVS (1)

From (Eq.8), the complete *rvs* differential equation is
(correction terms are ignored in this analysis)

$$\begin{aligned} \frac{d(rvs)}{rvs} = & \frac{\partial \ln(rvs)}{\partial \varepsilon_{obc}} \Delta \varepsilon_{obc} \\ & + \frac{\partial \ln(rvs)}{\partial T_{bcs}} \Delta T_{bcs} + \frac{\partial \ln(rvs)}{\partial T_{obc}} \Delta T_{obc} + \frac{\partial \ln(rvs)}{\partial T_{sm}} \Delta T_{sm} \\ & + \frac{\partial \ln(rvs)}{\partial DN_{bcs}} \Delta DN_{bcs} + \frac{\partial \ln(rvs)}{\partial DN_{obc}} \Delta DN_{obc} + \frac{\partial \ln(rvs)}{\partial DN_{svs}} \Delta DN_{svs} \end{aligned}$$

(Eq.12)

Error Analysis in RVS (2) (due to the error in ϵ_{obc})

$$\frac{\partial \ln(rvs)}{\partial \epsilon_{obc}} \Delta \epsilon_{obc} = \left(\frac{L_{obc}}{\epsilon_{obc} L_{obc} - L_{sm}} \right) \cdot \Delta \epsilon_{obc} \quad (\text{Eq.13})$$

This is a systematic bias error, which is independent of the AOI. Since rvs will be renormalized later at a particular AOI angle, this bias error will essentially be “renormalized out” and thus will not contribute to the total rvs error.

Error Analysis in RVS (3)

(due to the error in T_{bcs} , T_{obc} , T_{sm} measurements)

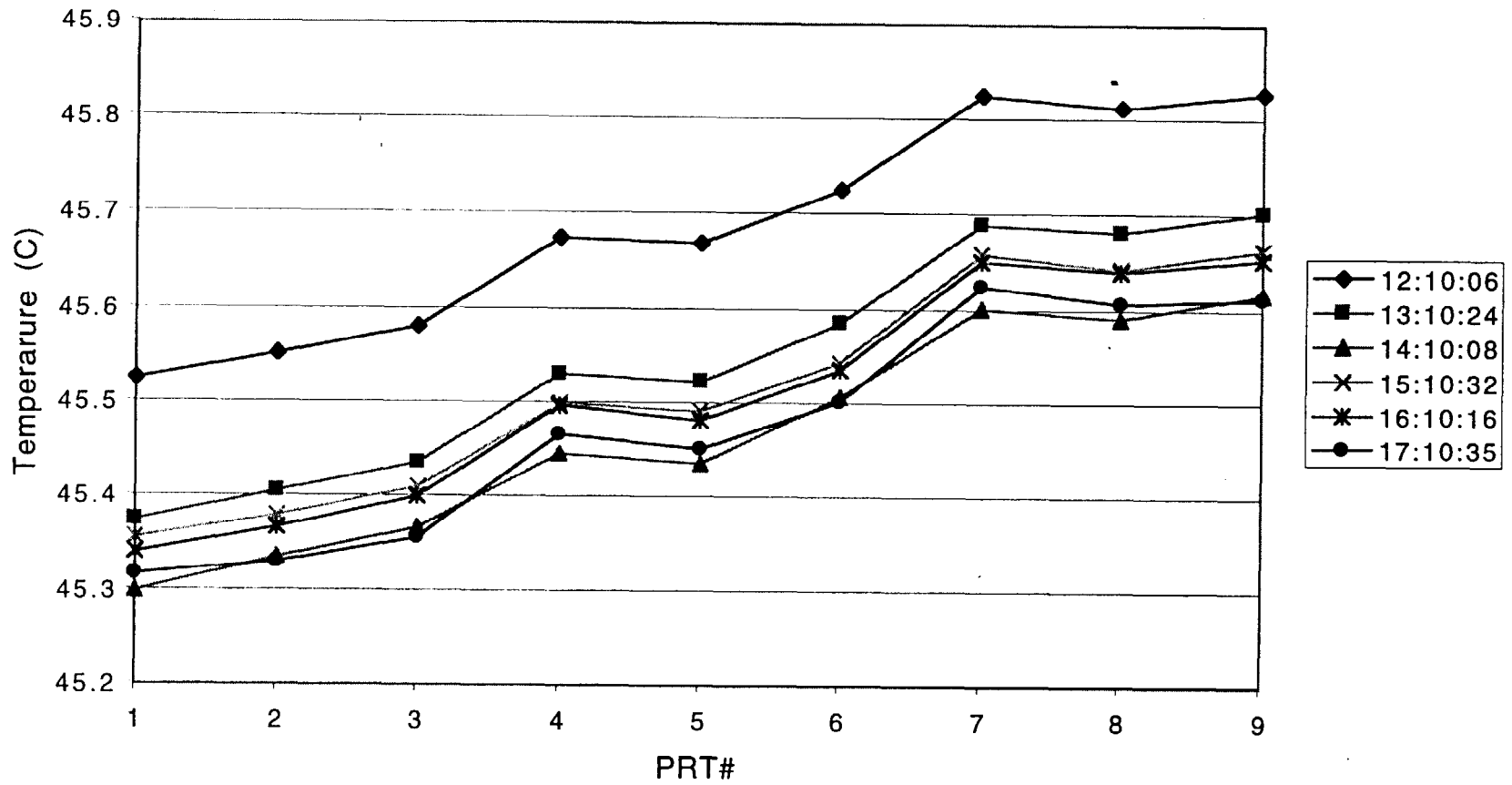
$$\frac{\partial \ln(rvs)}{\partial T_{bcs}} \Delta T_{bcs} = \left(\frac{-L'_{bcs}}{L_{bcs} - L_{sm}} \right) \cdot \Delta T_{bcs} \quad (\text{Eq.14})$$

$$\frac{\partial \ln(rvs)}{\partial T_{obc}} \Delta T_{obc} = \left(\frac{\epsilon_{obc} L'_{obc}}{\epsilon_{obc} L_{obc} - L_{sm}} \right) \cdot \Delta T_{obc} \quad (\text{Eq.15})$$

$$\frac{\partial \ln(rvs)}{\partial T_{sm}} \Delta T_{sm} = \left(\frac{-L'_{sm}}{\epsilon_{obc} L_{obc} - L_{sm}} + \frac{L'_{sm}}{L_{bcs} - L_{sm}} \right) \cdot \Delta T_{sm} \quad (\text{Eq.16})$$

A system bias error in ΔT , combining with the terms in (..), will be constant across the AOIs, thus won't effect the renormalized rvs , only the local fluctuated error in ΔT will contribute to the errors in rvs .

9 PRTs Output from BCS 1st Bounce Plate on RVS Test [320K_3]
12-5 pm, 3-31-1998; BDATB93.OUT



Error Analysis in RVS (4)

(due to the errors in DN_{bcs} , DN_{obc} , DN_{svs})

$$\frac{\partial \ln(rvs)}{\partial DN_{bcs}} \cdot \Delta DN_{bcs} = \left(\frac{1}{DN_{bcs} - DN_{svs}} \right) \cdot \Delta DN_{bcs} \quad (\text{Eq.17})$$

$$\frac{\partial \ln(rvs)}{\partial DN_{obc}} \cdot \Delta DN_{obc} = \left(\frac{-1}{DN_{obc} - DN_{svs}} \right) \cdot \Delta DN_{obc} \quad (\text{Eq.18})$$

$$\frac{\partial \ln(rvs)}{\partial DN_{svs}} \Delta DN_{svs} = \left(\frac{-1}{DN_{bcs} - DN_{svs}} + \frac{1}{DN_{obc} - DN_{svs}} \right) \cdot \Delta DN_{svs} \quad (\text{Eq.19})$$

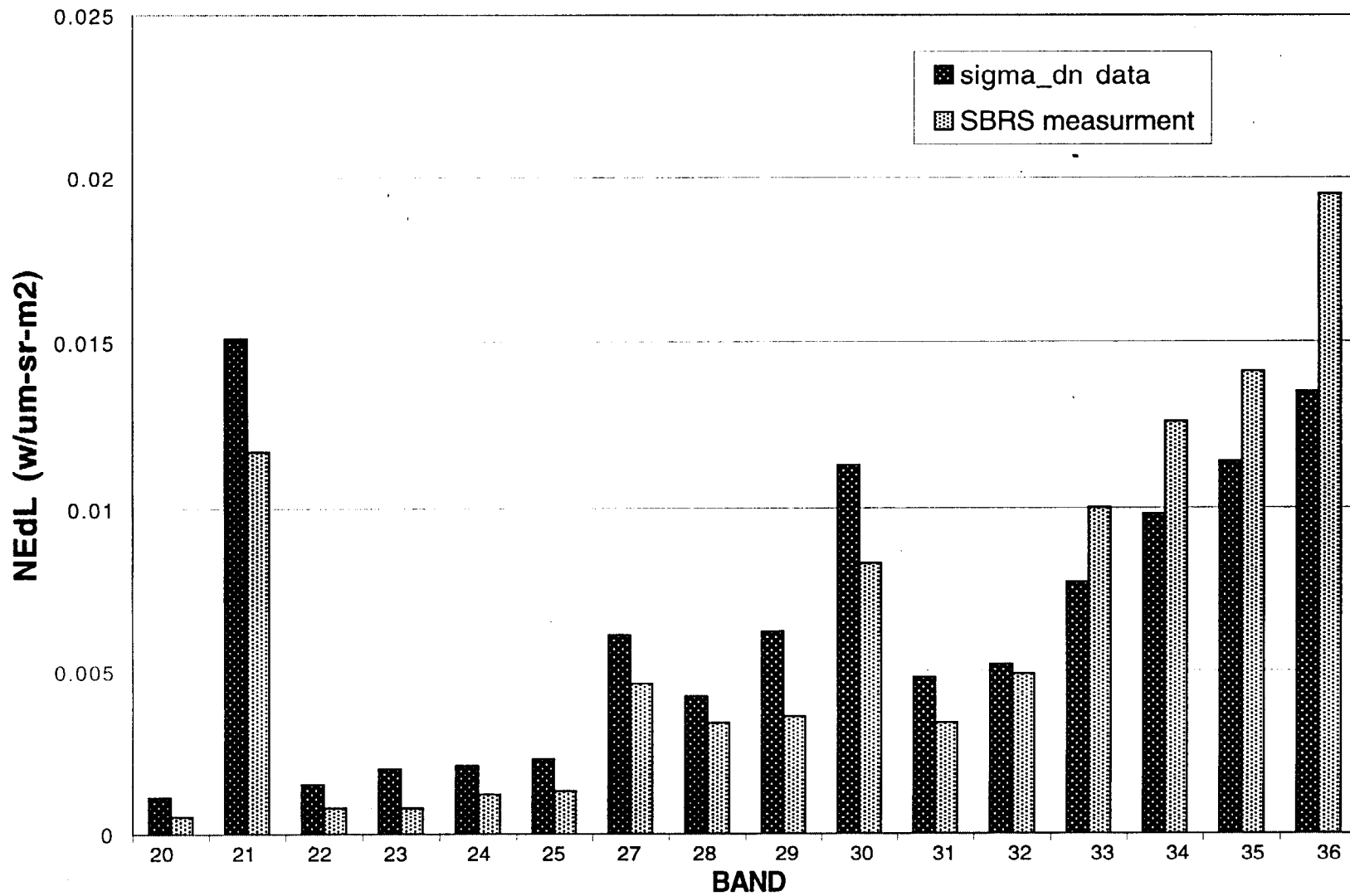
Error Analysis in RVS (5)

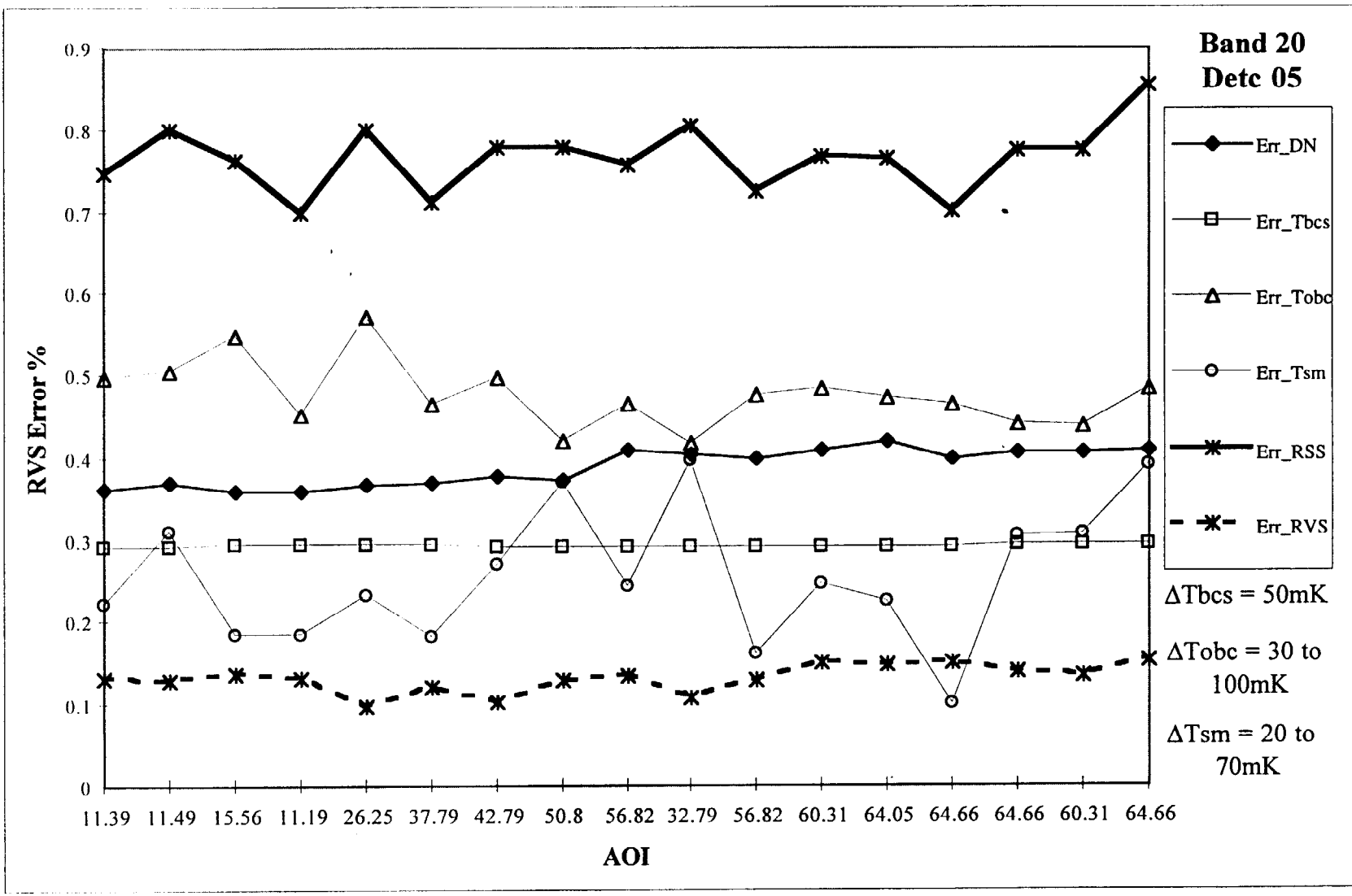
$\sigma(\text{RVS})$

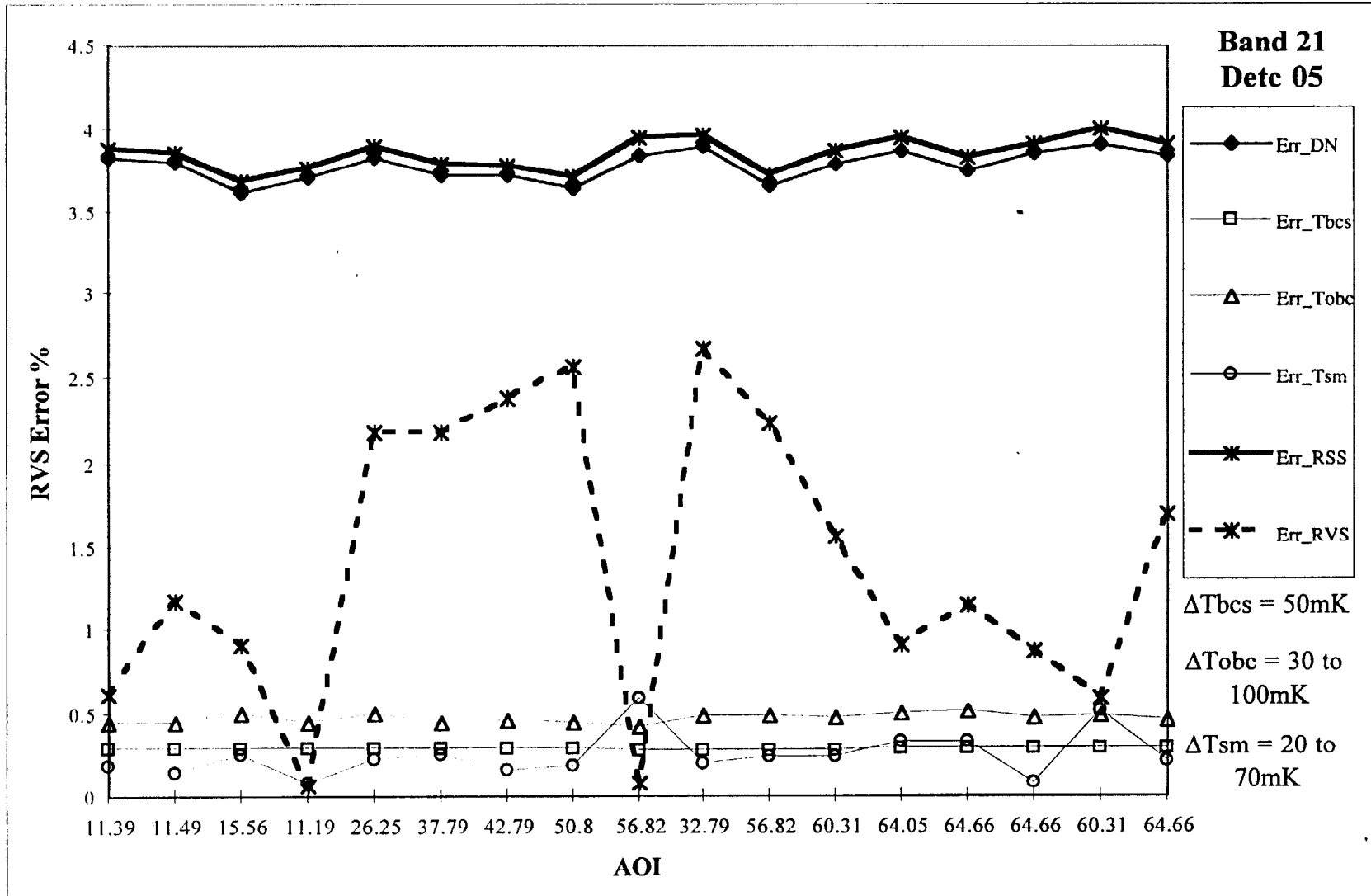
$$\sigma(\text{rvs}) = \sqrt{\sigma_{T_{bcs}}^2 + \sigma_{T_{obc}}^2 + \sigma_{T_{svs}}^2 + \sigma_{DN_{bcs}}^2 + \sigma_{DN_{obc}}^2 + \sigma_{DN_{svs}}^2}$$

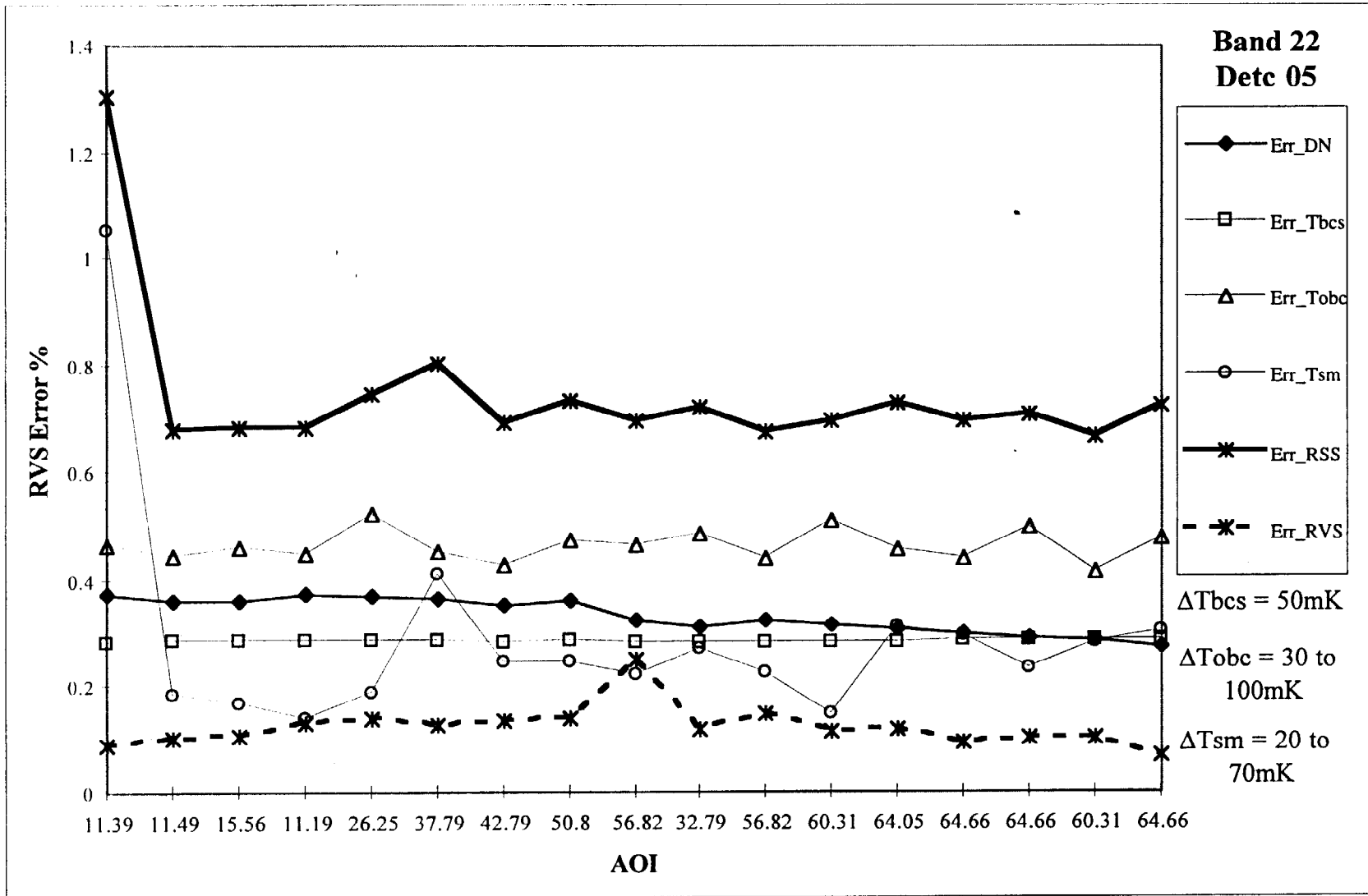
The RSS ignores the correlation relationship between the variables, thus will result in either over-estimating or under-estimating the total 1-sigma error in *rvs*.

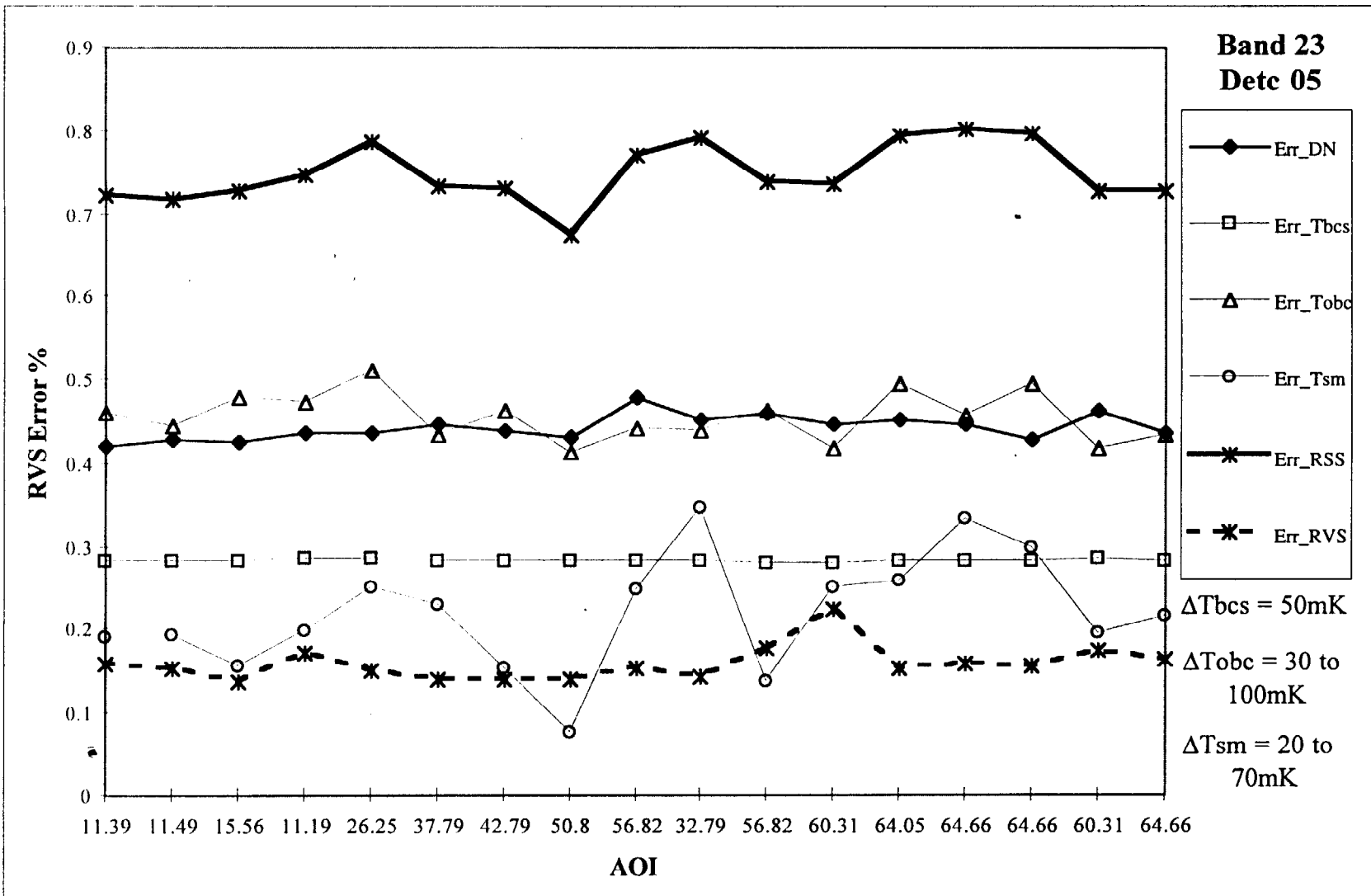
NEdL from [linear gain * σ (dn)] compared with SBRS measured value

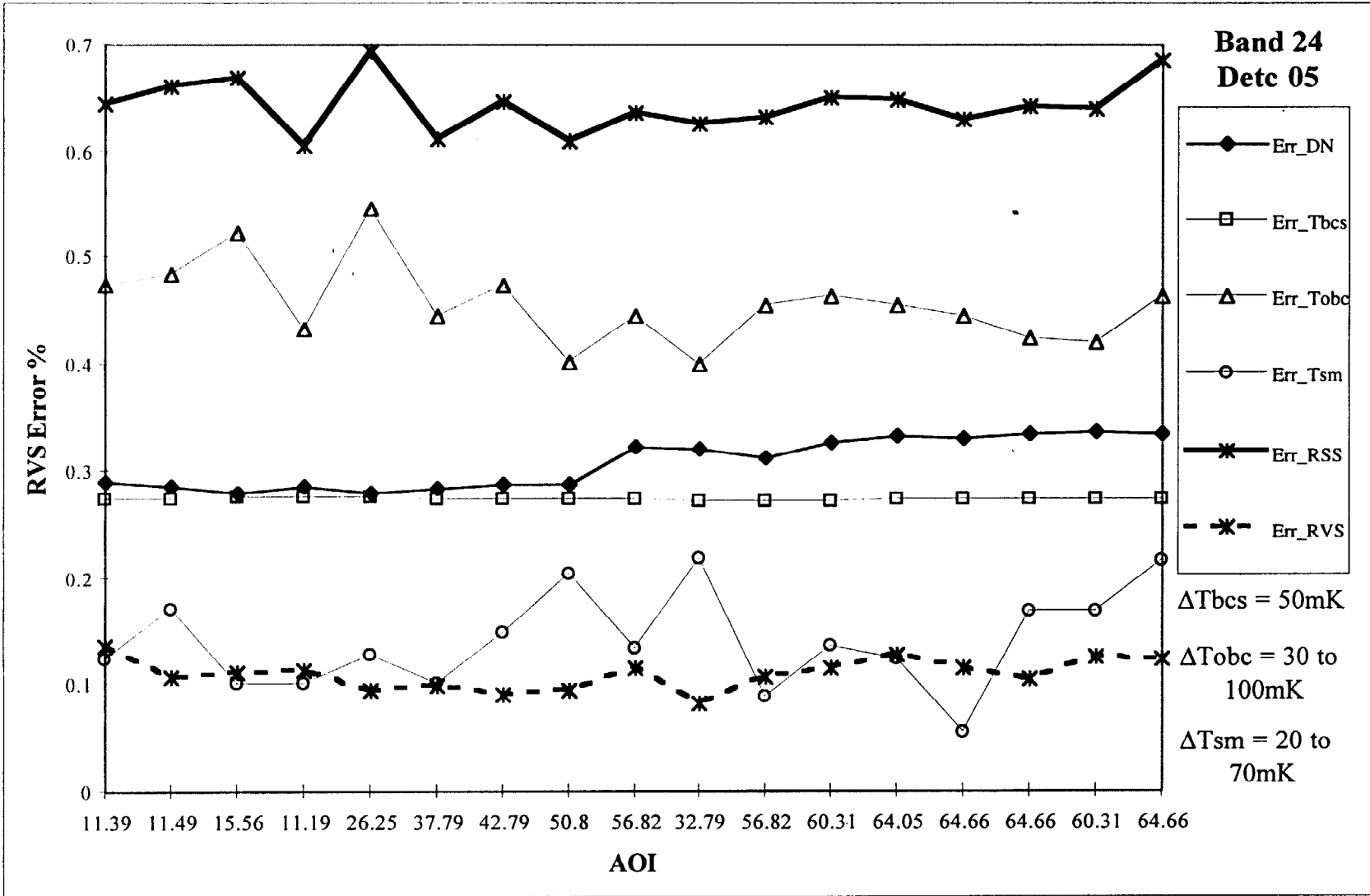


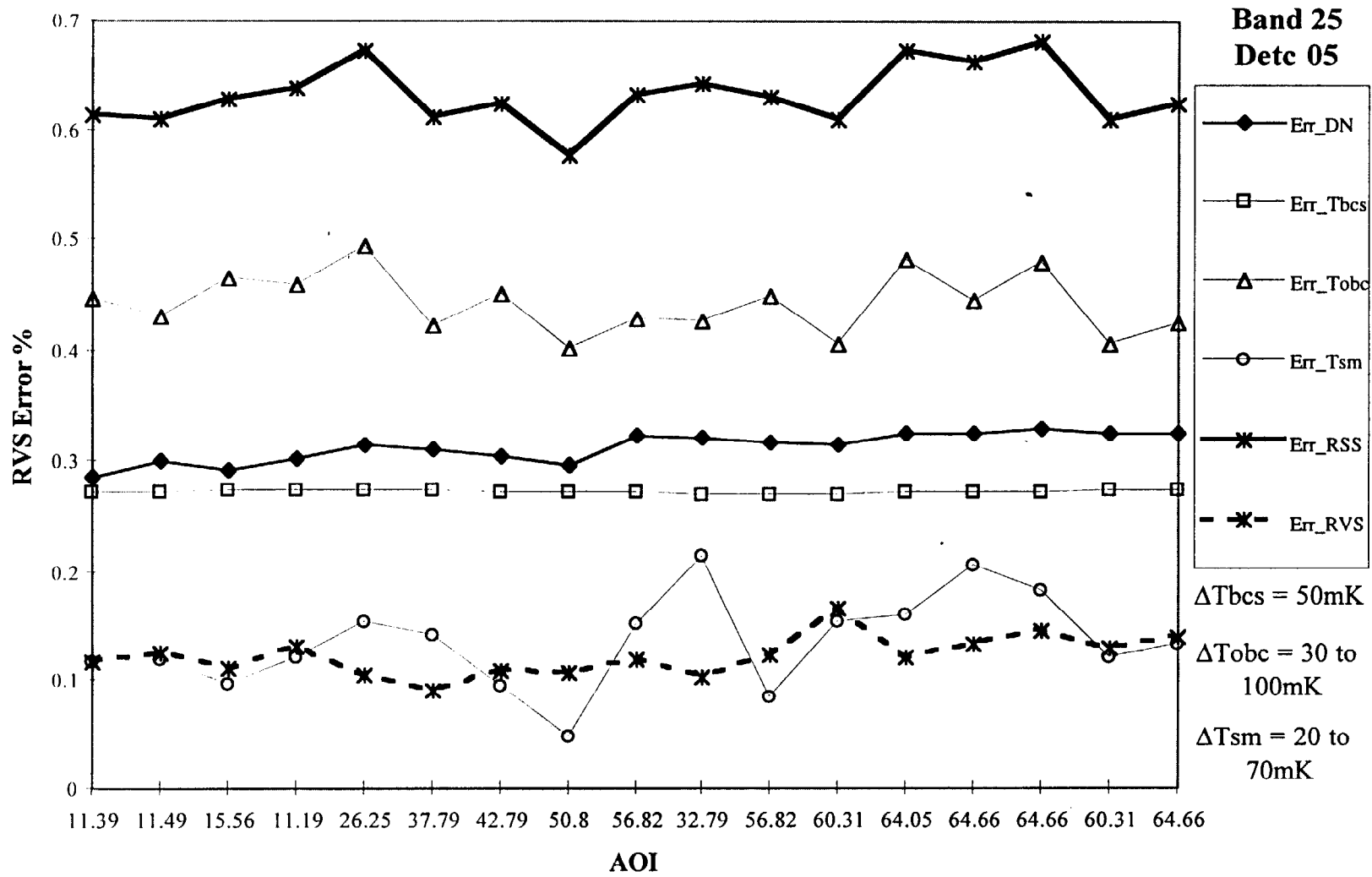


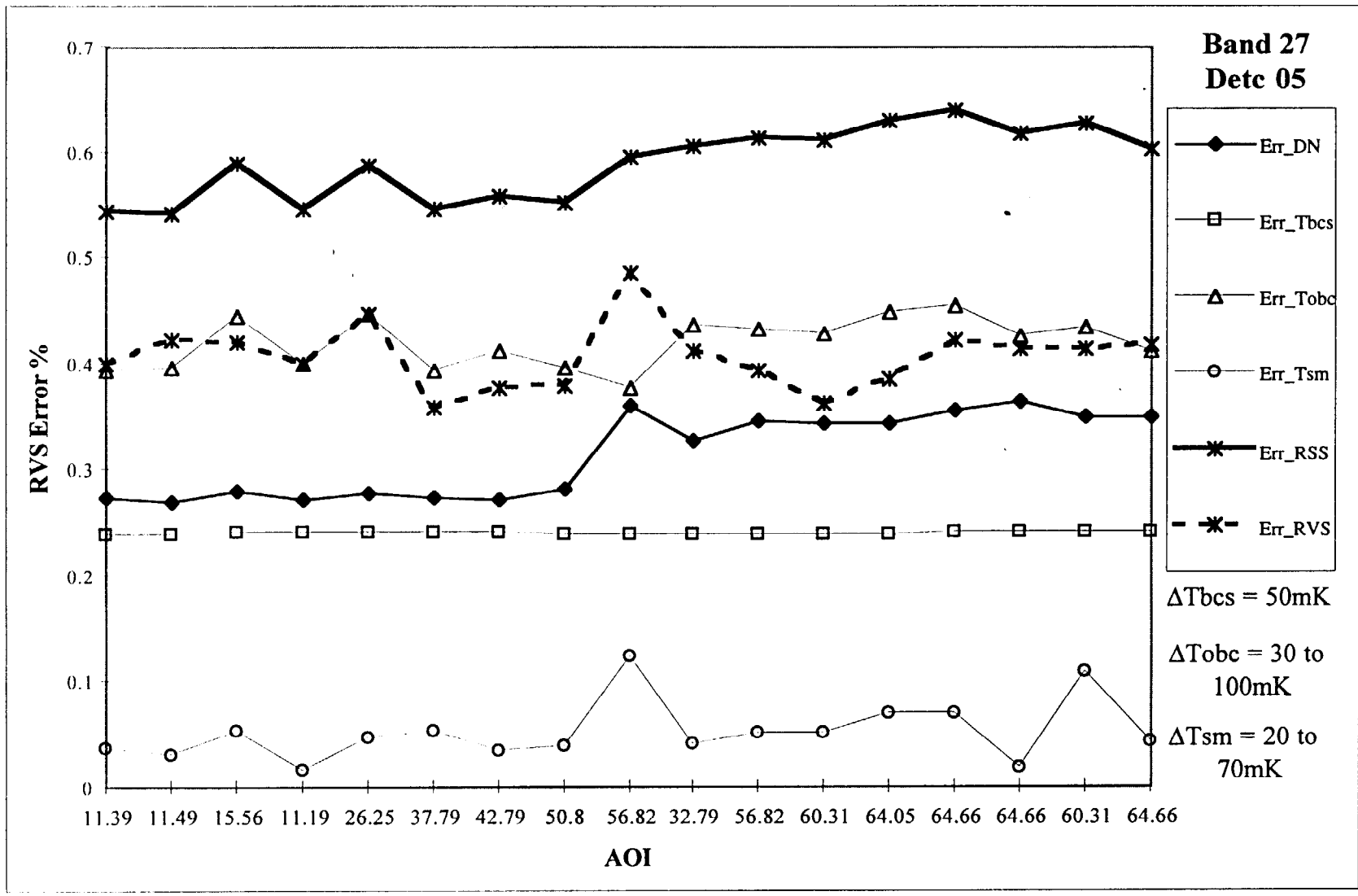


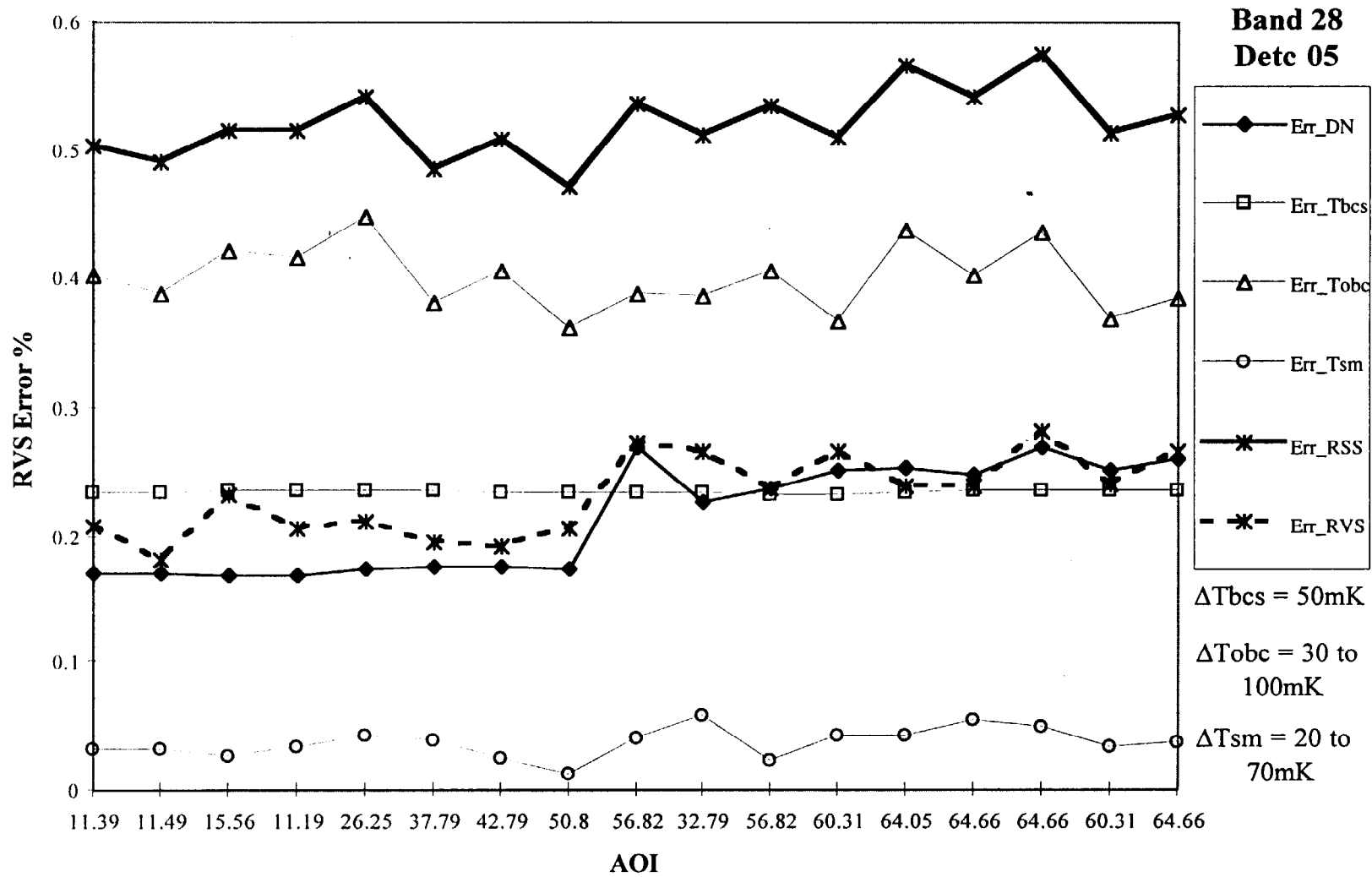


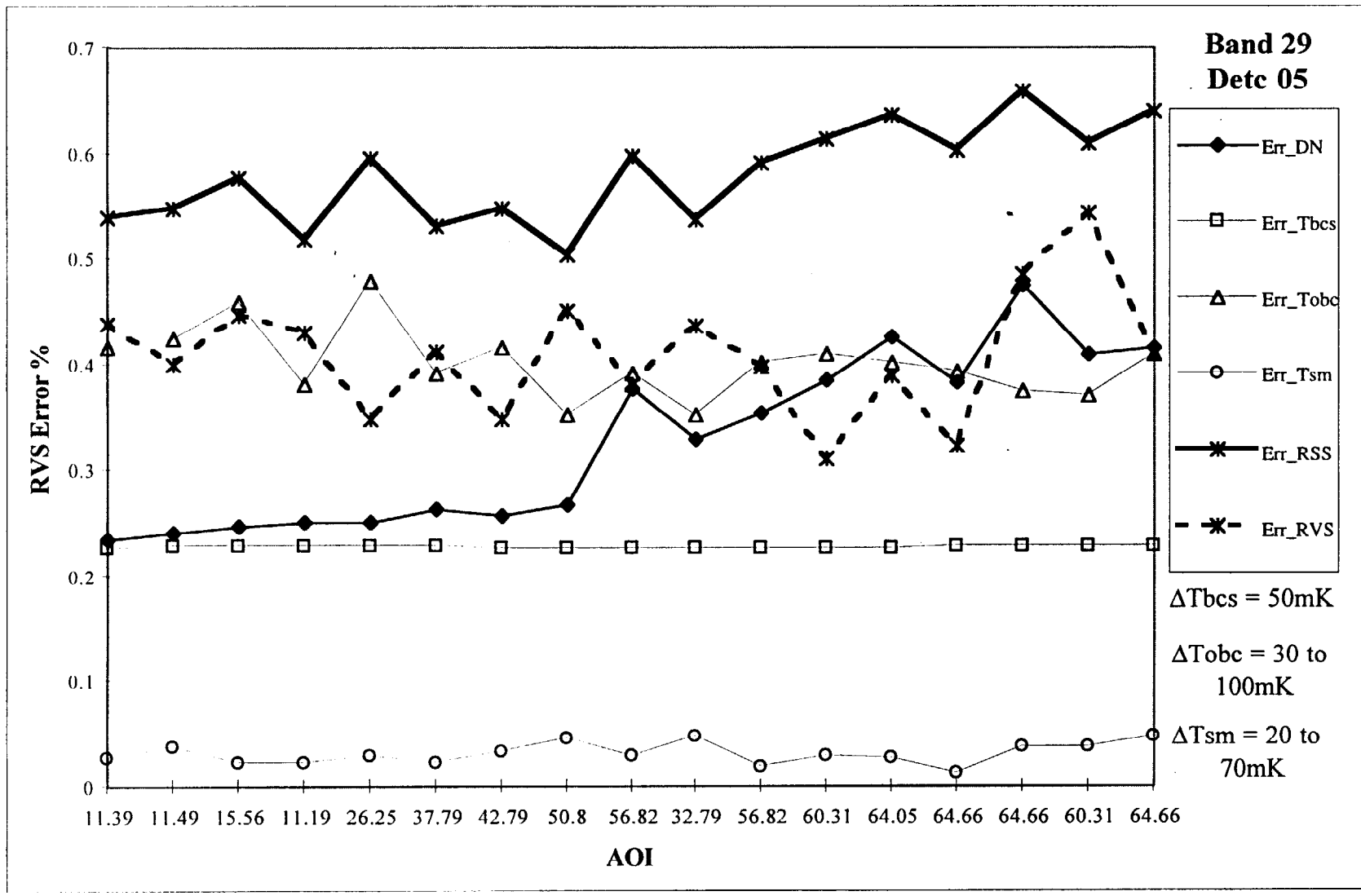


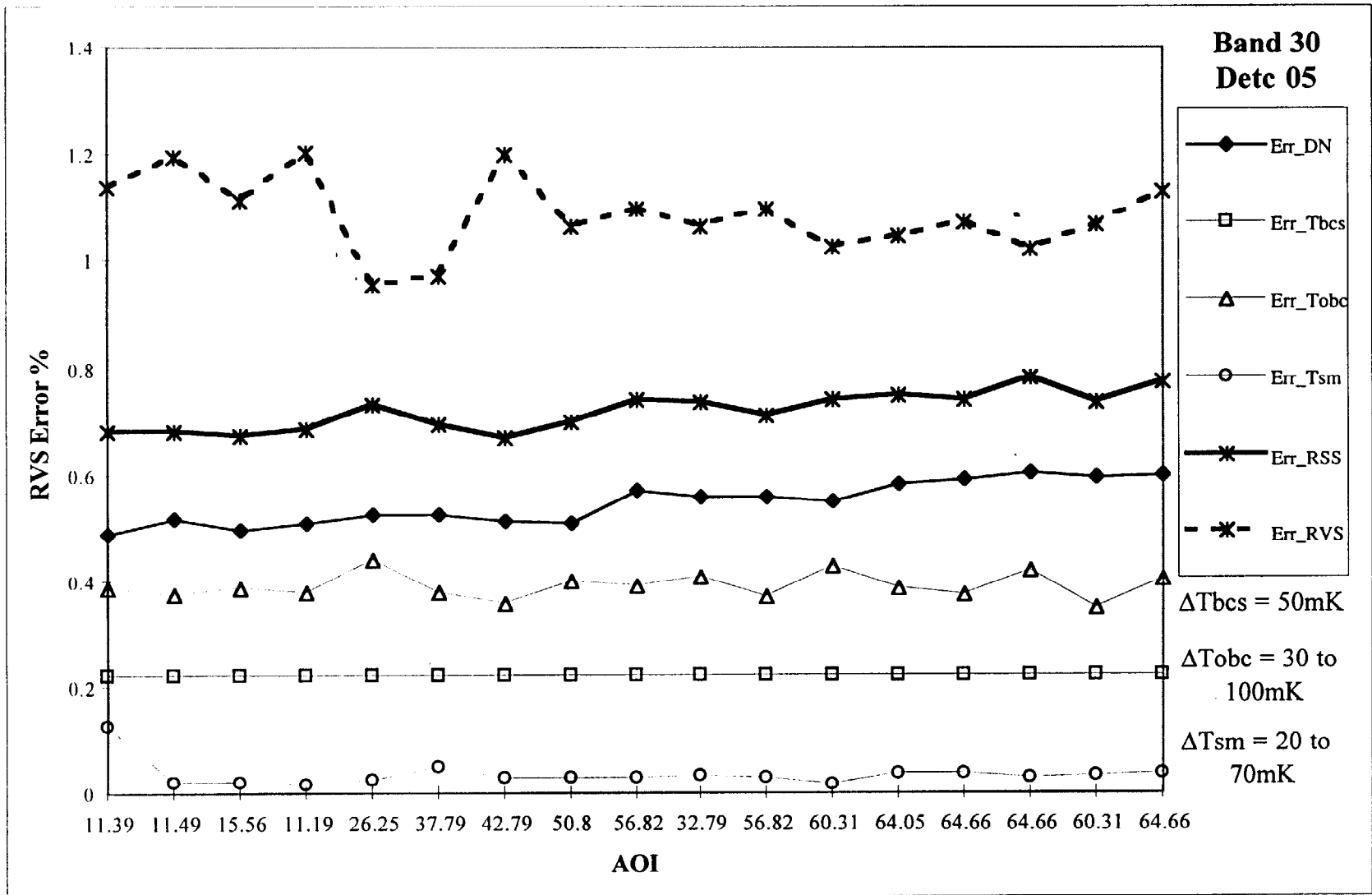


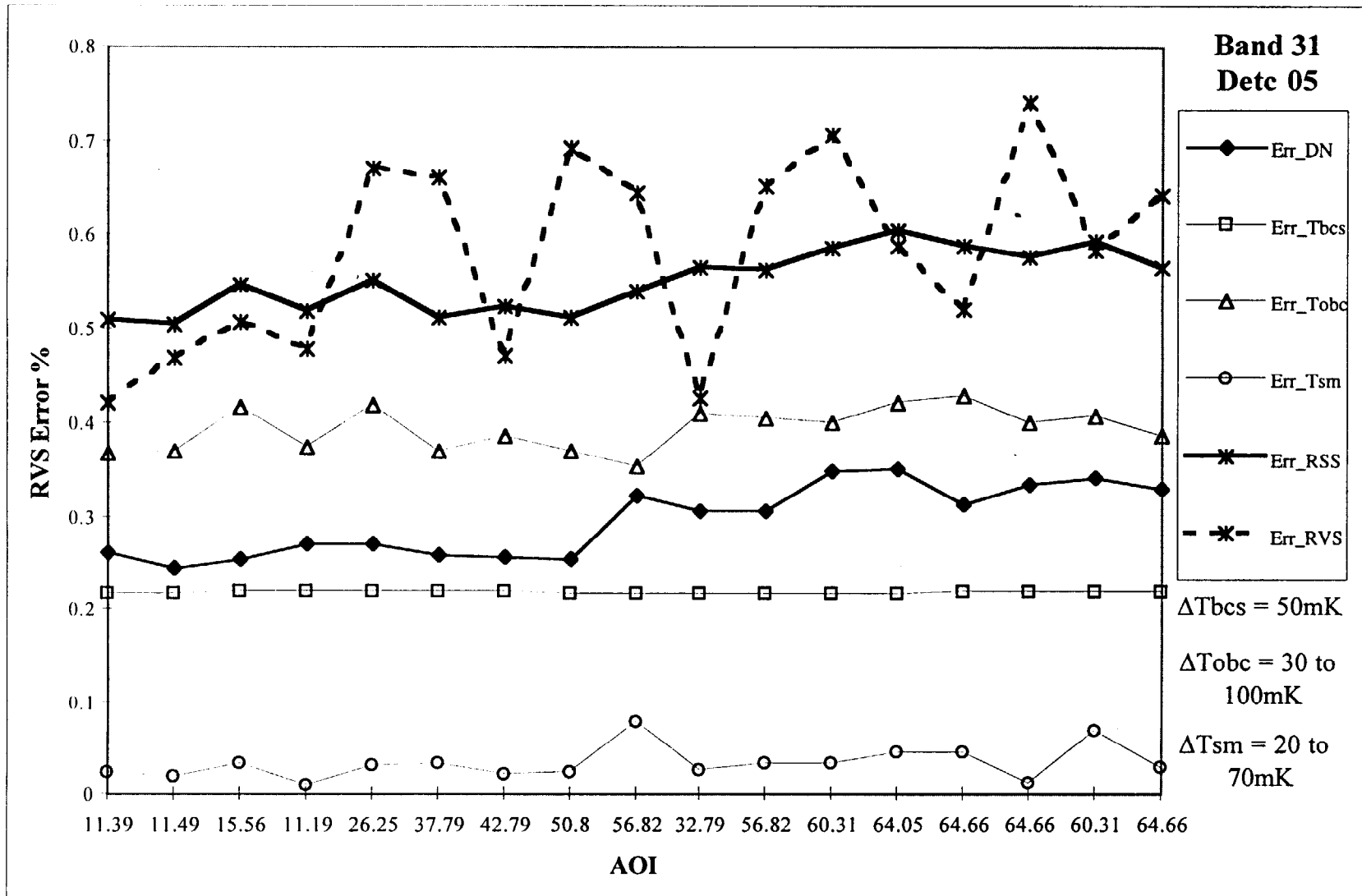


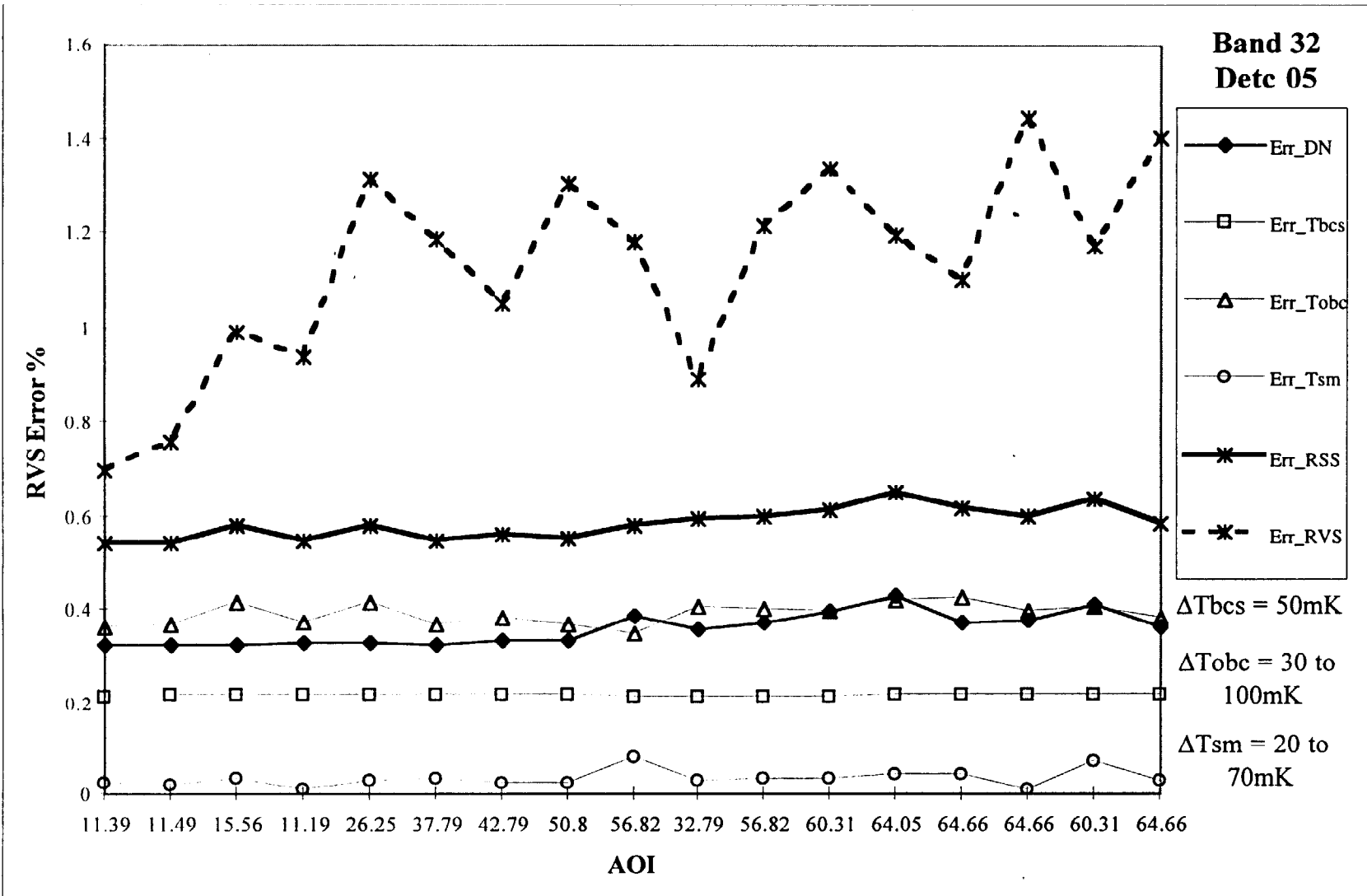


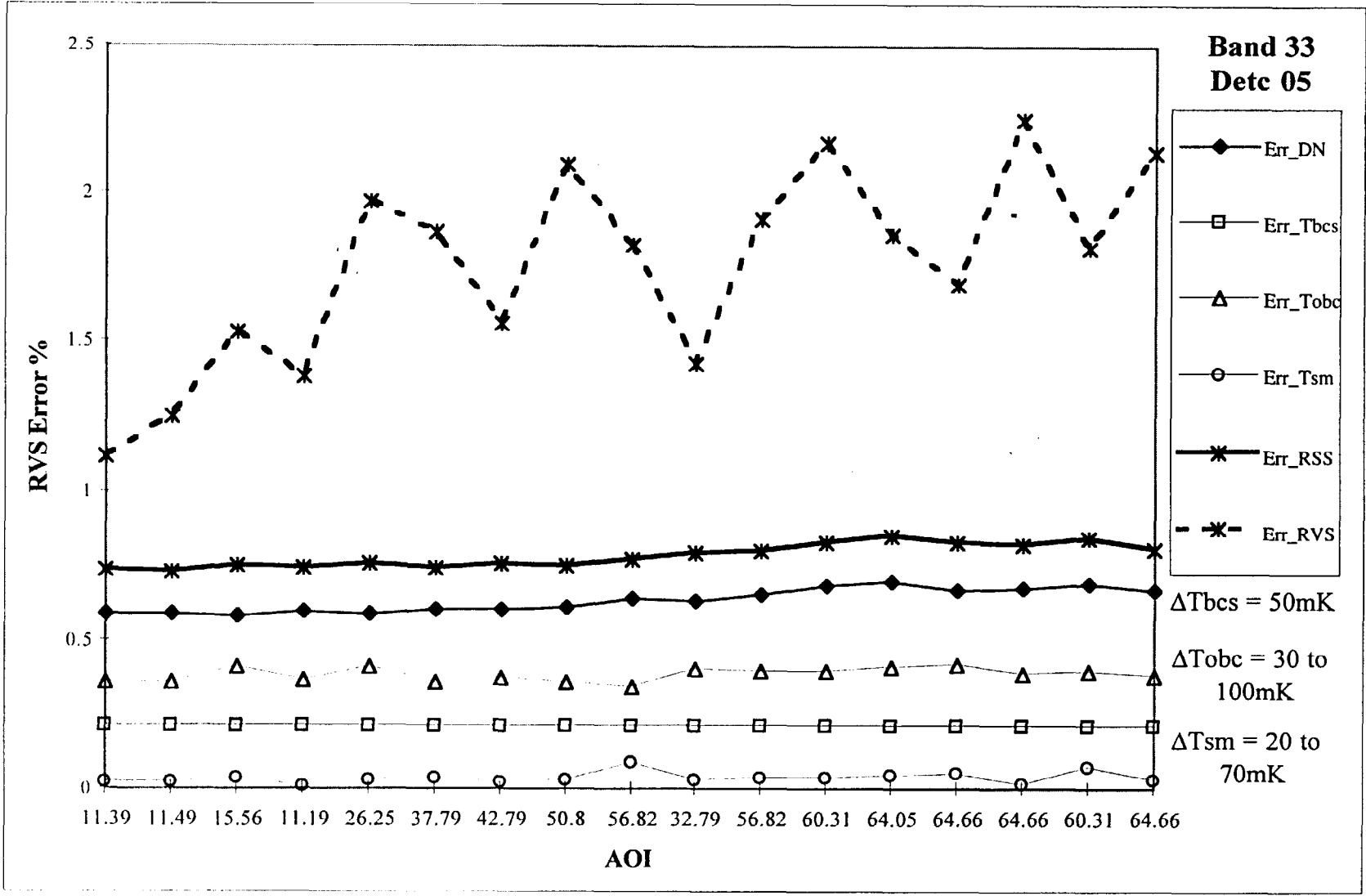


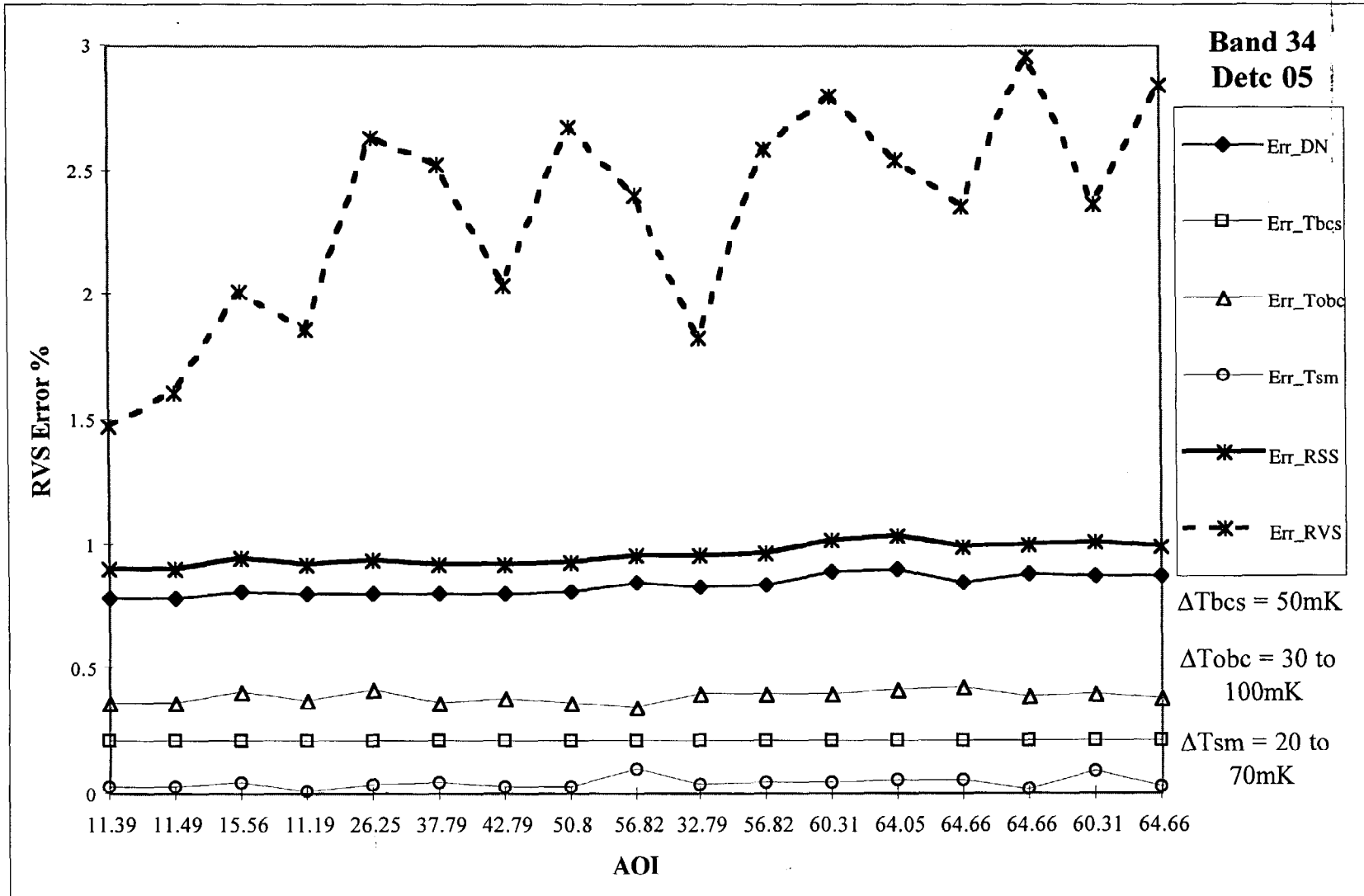


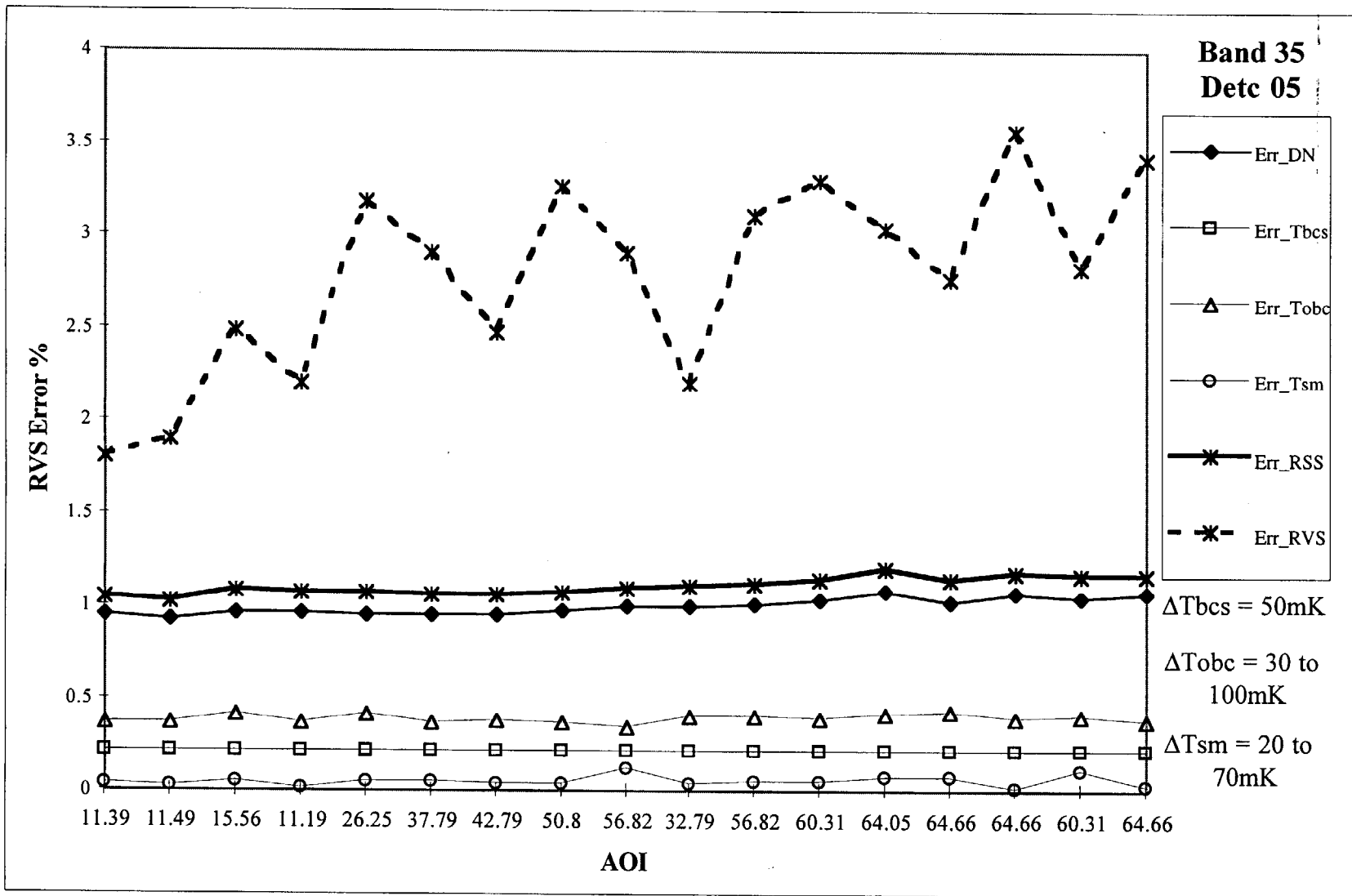


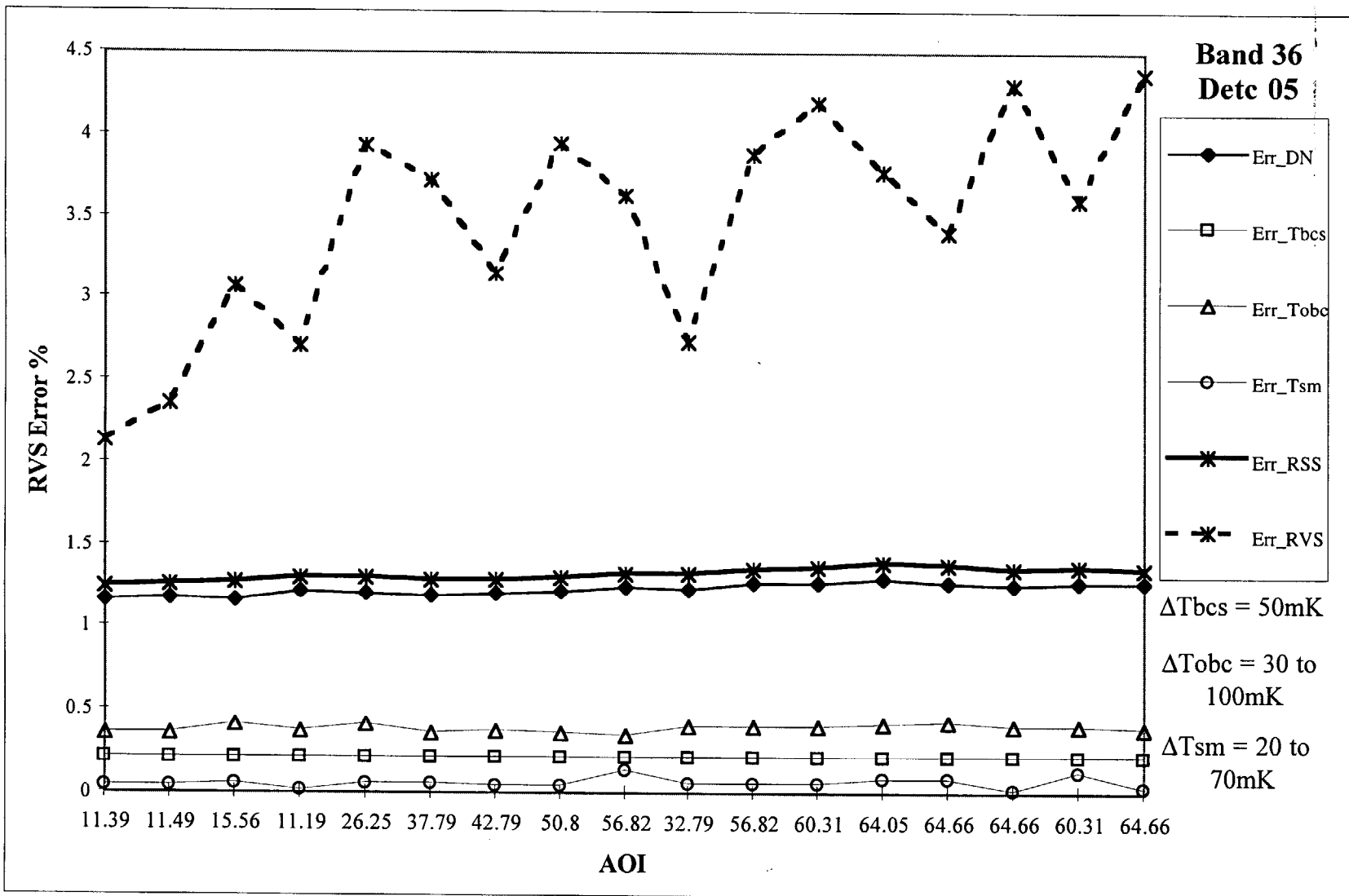












RVS fitting equations and procedure (1)

The MODIS polarization theory (Appendx A) gives

$$RVS = \tau \cdot \bar{\rho} + \eta \cdot \overline{\delta\rho} \quad \text{or,} \quad rvs = \bar{\rho} + C \cdot \overline{\delta\rho} \quad (\text{Eq.20})$$

where τ is the MODIS fix-optics total throughput (or A_{11} component of the fixed-optics 4x4 Mueller matrix), and η is the A_{12} component of the matrix, and rvs is the re-normalized RVS, and

$$\bar{\rho} = \frac{\rho_s + \rho_p}{2} \quad , \quad \overline{\delta\rho} = \frac{\rho_s - \rho_p}{2} \quad (\text{Eq.21})$$

Using (Eq.12), together with RVS data and ρ_s and ρ_p functions fitted to the NPL scan mirror reflectivity data, τ and η can be determined by Least-Square fitting procedure, thus, completes the RVS fitting.

RVS fitting equations and procedure (2)

- This procedure assumes that reflectivity measurement accuracy is comparable or better than that of the RVS measurement. Given this presumption, this fitting procedure can be proved to be superior to the direct fitting (e.g., quadratic fitting) of the RVS data, which is primarily due to the fact that Eq.12 is an exact relationship between the RVS and scan mirror reflectivities.
- If we assume that the fixed-optics parameter C is the same for both the FM1 and PFM, then PFM RVS can be retrieved from the PFM scan mirror reflectivity measurement from NPL as

$$r_{VS_{PFM}} = \bar{\rho}_{PFM} + C_{FM1} \cdot \overline{\delta\rho}_{PFM} \quad (\text{Eq.22})$$

Appendix A: MODIS Polarization Theory (1)

$$S = \mathbf{D} \cdot \mathbf{A} \cdot \mathbf{M} \cdot \mathbf{L}$$

S = at-detector radiance (a scalar quantity)

$\mathbf{D} = [D, 0, 0, 0]$ is the detector vector

\mathbf{A} = the Mueller matrix for the fixed optics

\mathbf{M} = the Mueller matrix for the rotating scan mirror

\mathbf{L} = the Stokes vector for the at-aperture radiance field

$$S_{ev} = \mathbf{D} \cdot \mathbf{A} \cdot \mathbf{M}(\rho_{ev}) \cdot \mathbf{L}_{ev} + \mathbf{D} \cdot \mathbf{A} \cdot \mathbf{M}(\epsilon_{ev}) \cdot \mathbf{L}_{sm} + \delta_{bkg}$$

$$S_{sv} = \mathbf{D} \cdot \mathbf{A} \cdot \mathbf{M}(\epsilon_{sv}) \cdot \mathbf{L}_{sm} + \delta_{bkg}$$

$$\Delta S_{ev} = \mathbf{D} \cdot \mathbf{A} \cdot \mathbf{M}(\rho_{ev}) \cdot \mathbf{L}_{ev} + \mathbf{D} \cdot \mathbf{A} \cdot \mathbf{M}(\epsilon_{ev}) \cdot \mathbf{L}_{sm} - \mathbf{D} \cdot \mathbf{A} \cdot \mathbf{M}(\epsilon_{sv}) \cdot \mathbf{L}_{sm}$$

Appendix A: MODIS Polarization Theory (2)

$$\mathbf{L}_{ev} = [L_{ev}, 0, 0, 0]^T \quad \mathbf{L}_{sm} = [L_{sm}, 0, 0, 0]^T$$

$$\Delta S_{ev} = D \left\{ \sum_{j=0}^3 A_{0j} M_{j0}(\rho_{ev}) \right\} L_{ev} + D \left\{ \sum_{j=0}^3 A_{0j} [M_{j0}(\varepsilon_{ev}) - M_{j0}(\varepsilon_{sv})] \right\} L_{sm}$$

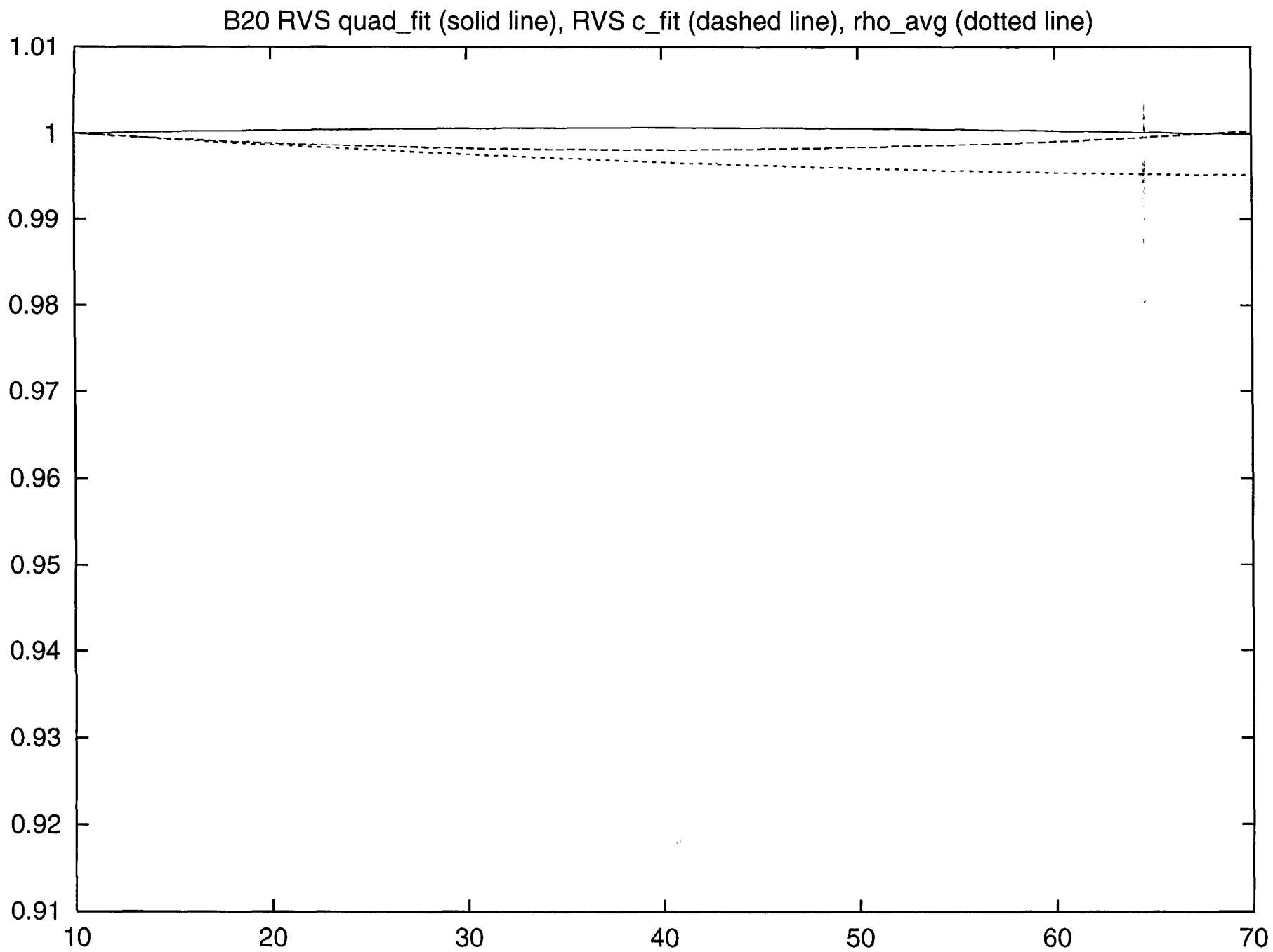
$$\Delta S_{ev} = RVS_{ev} L_{ev} + (RVS_{sv} - RVS_{ev}) L_{sm}$$

$$RVS = D \sum_{j=0}^3 A_{0j} M_{j0}(\rho)$$

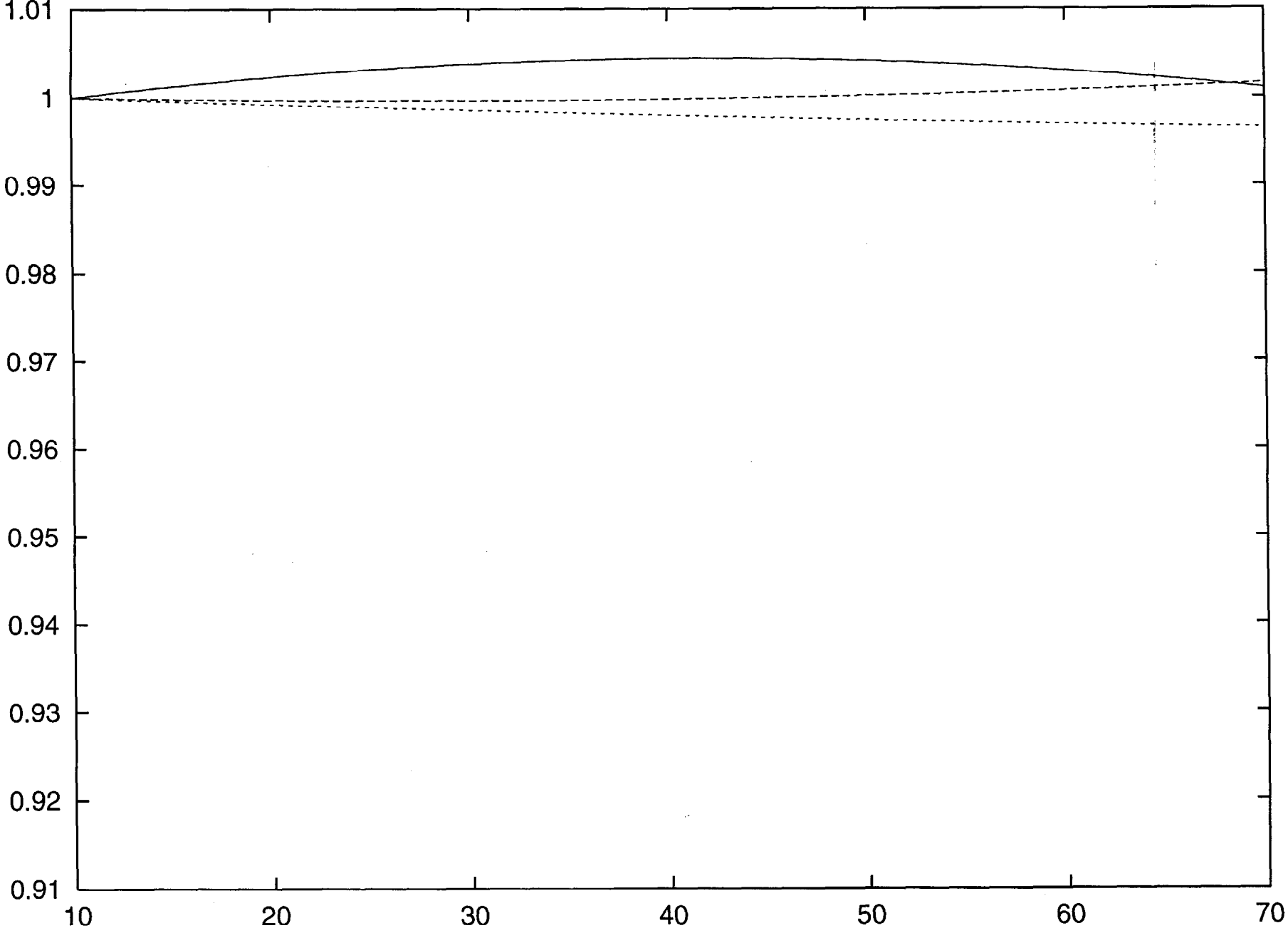
$$M_{10} = \frac{1}{2}(\rho_s - \rho_p) \quad M_{00} = \frac{1}{2}(\rho_s + \rho_p)$$

$$RVS = A_{00} \left[\frac{\rho_s + \rho_p}{2} \right] + A_{01} \left[\frac{\rho_s - \rho_p}{2} \right] = \tau_{fix}^{pol} \cdot \bar{\rho} + A_{01} \cdot \delta \bar{\rho}$$

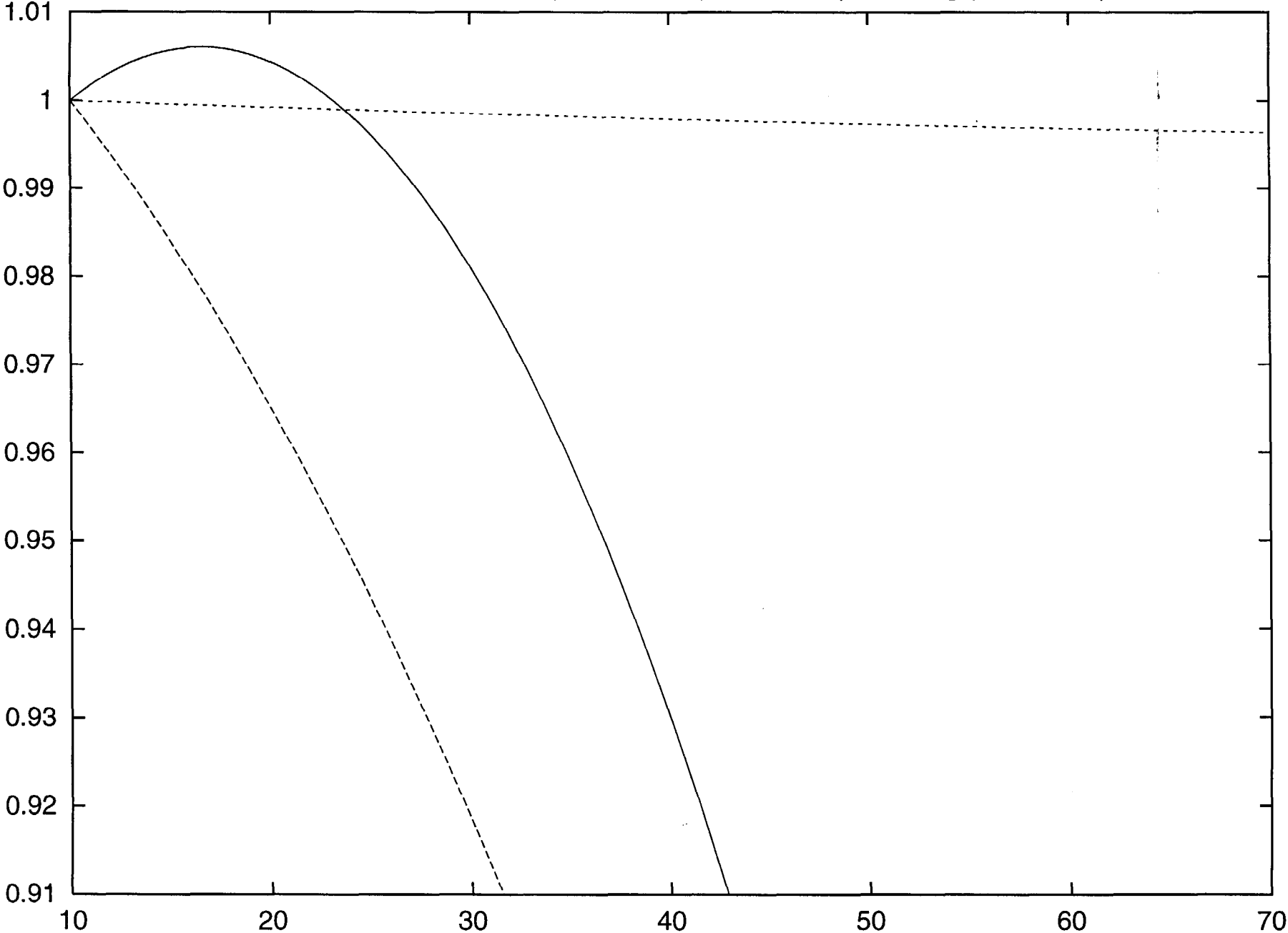
Comparison of Highbay polarized RVS,
quadratic fit to Highbay RVS and quadratic fit
to NPL average reflectance data



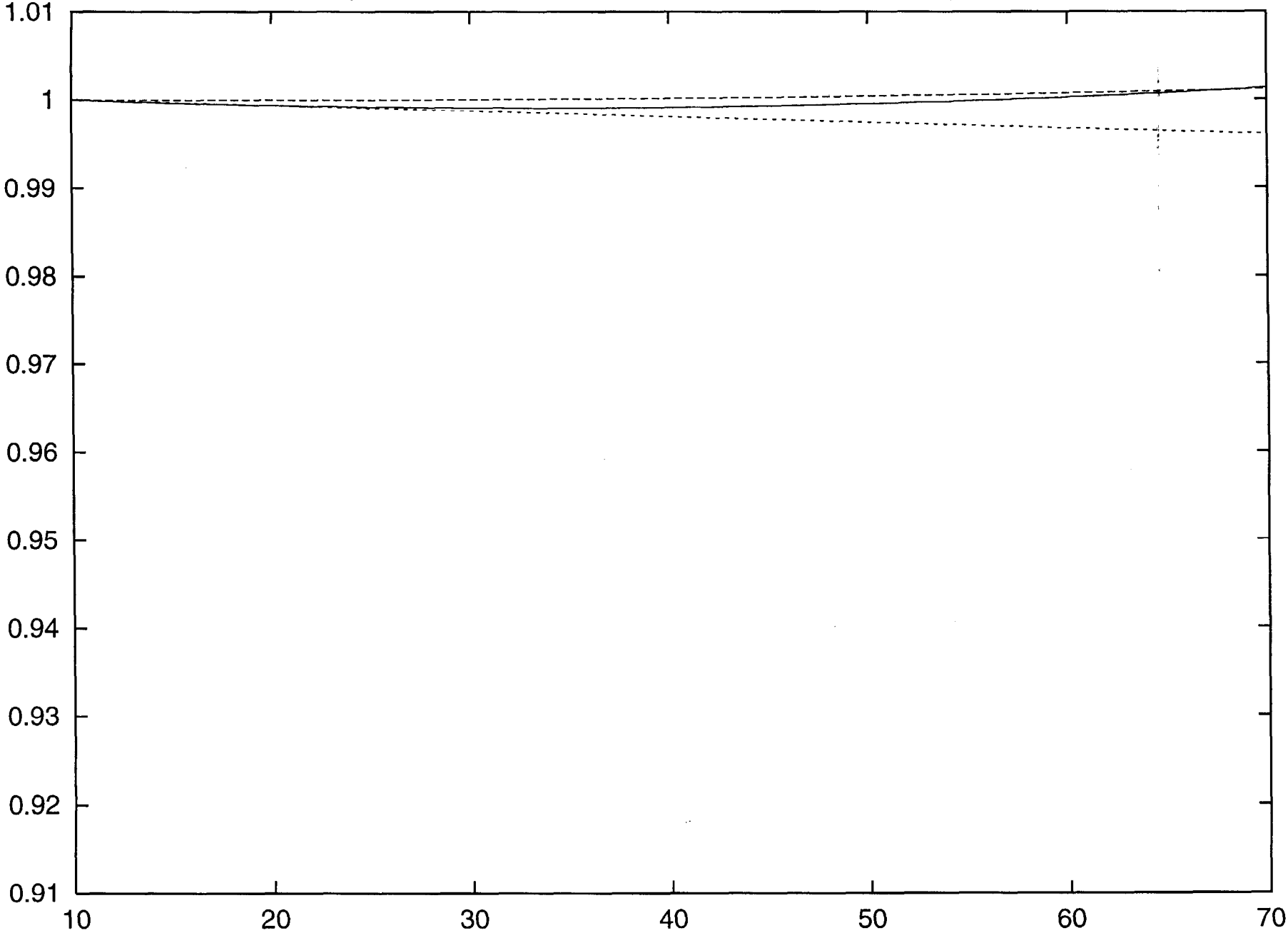
B21 RVS quad_fit (solid line), RVS c_fit (dashed line), rho_avg (dotted line)



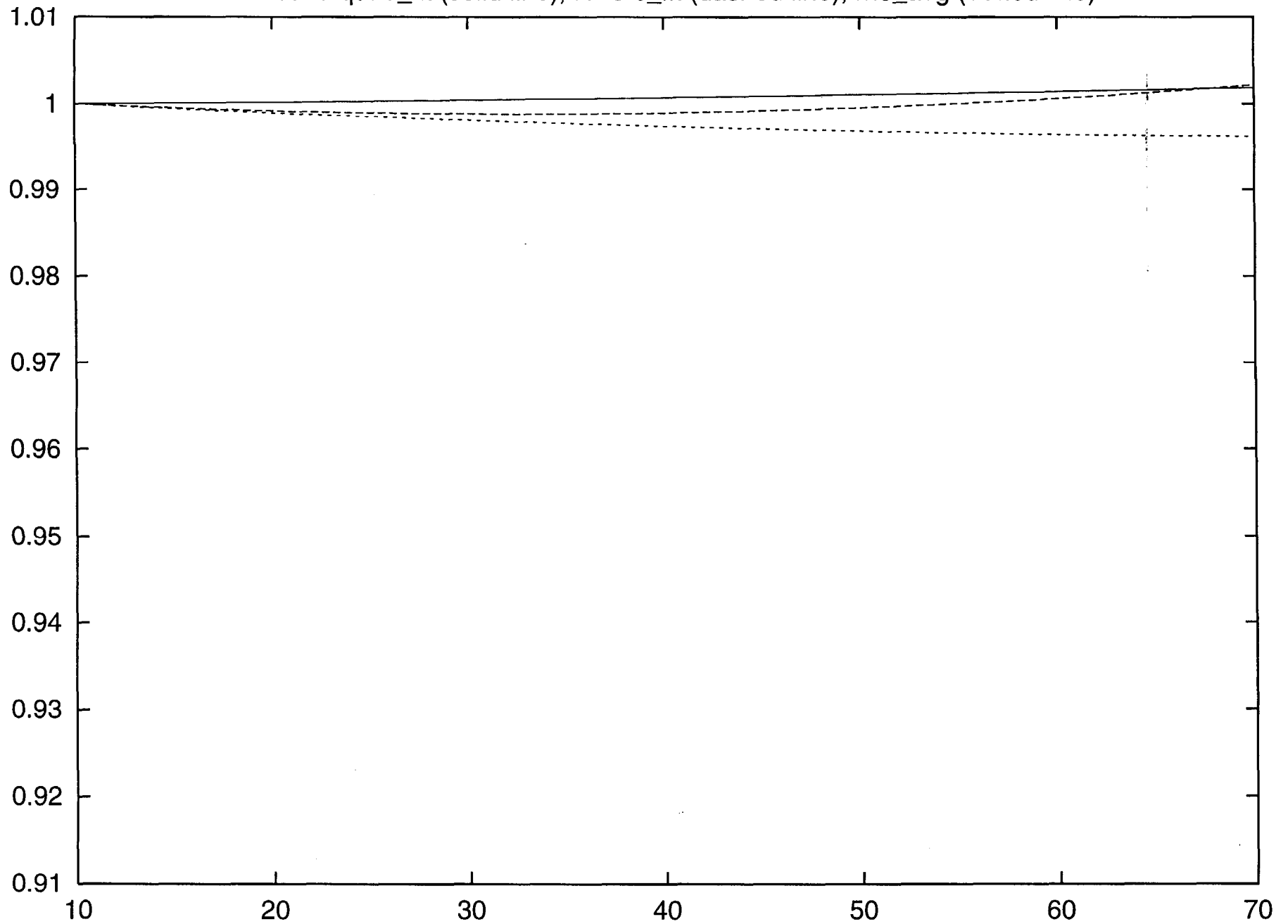
B22 RVS quad_fit (solid line), RVS c_fit (dashed line), rho_avg (dotted line)



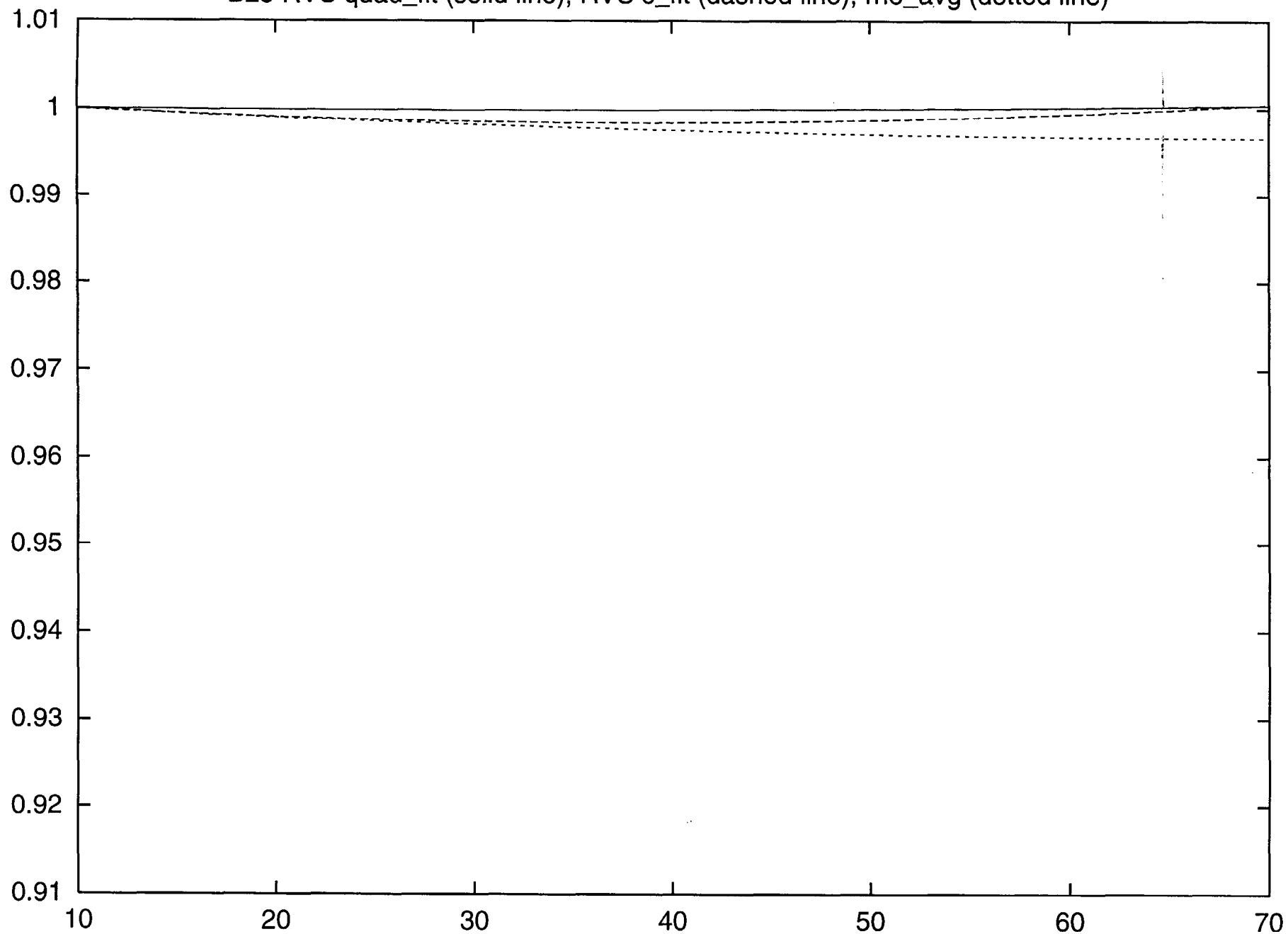
B23 RVS quad_fit (solid line), RVS c_fit (dashed line), rho_avg (dotted line)

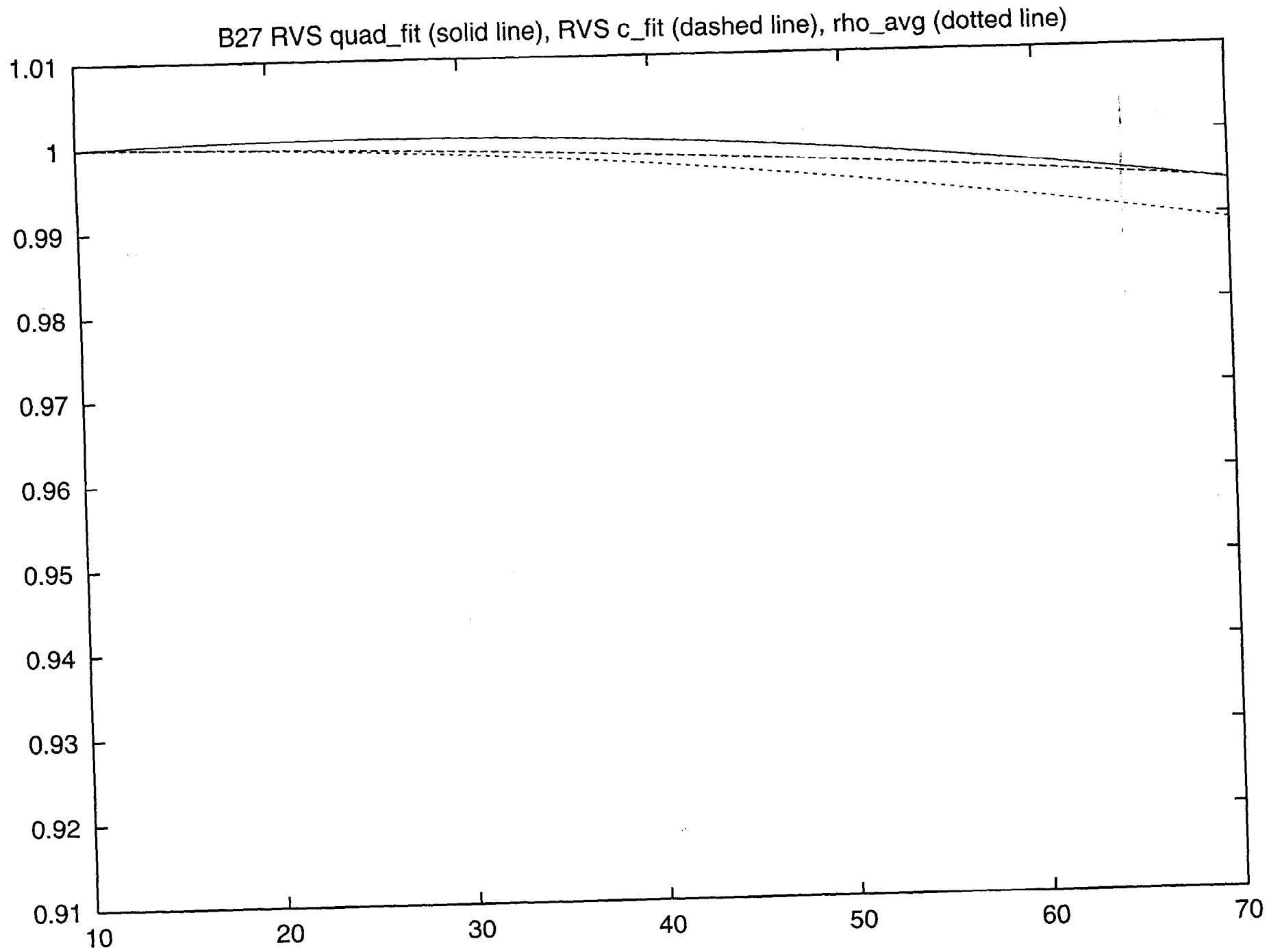


B24 RVS quad_fit (solid line), RVS c_fit (dashed line), rho_avg (dotted line)

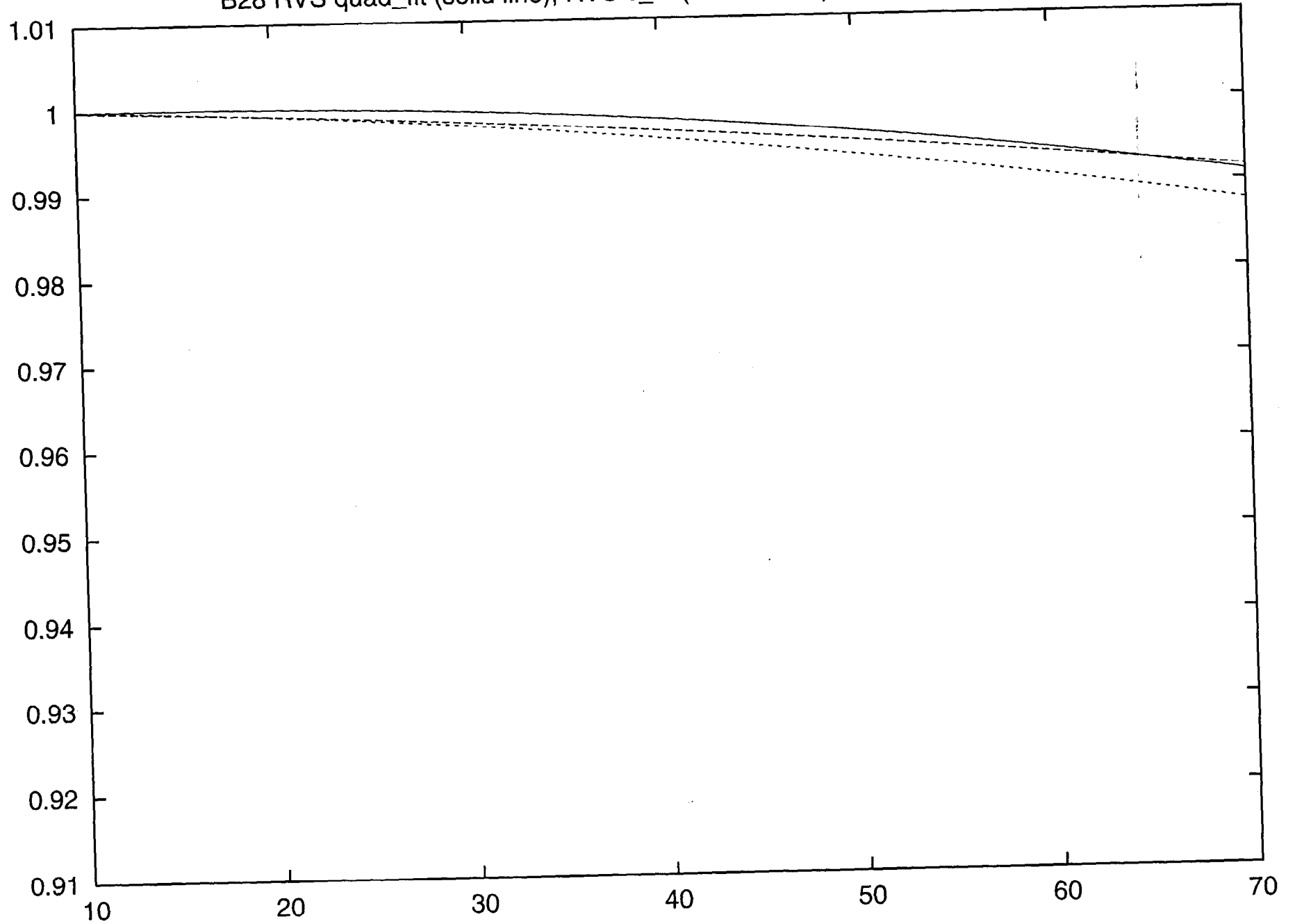


B25 RVS quad_fit (solid line), RVS c_fit (dashed line), rho_avg (dotted line)

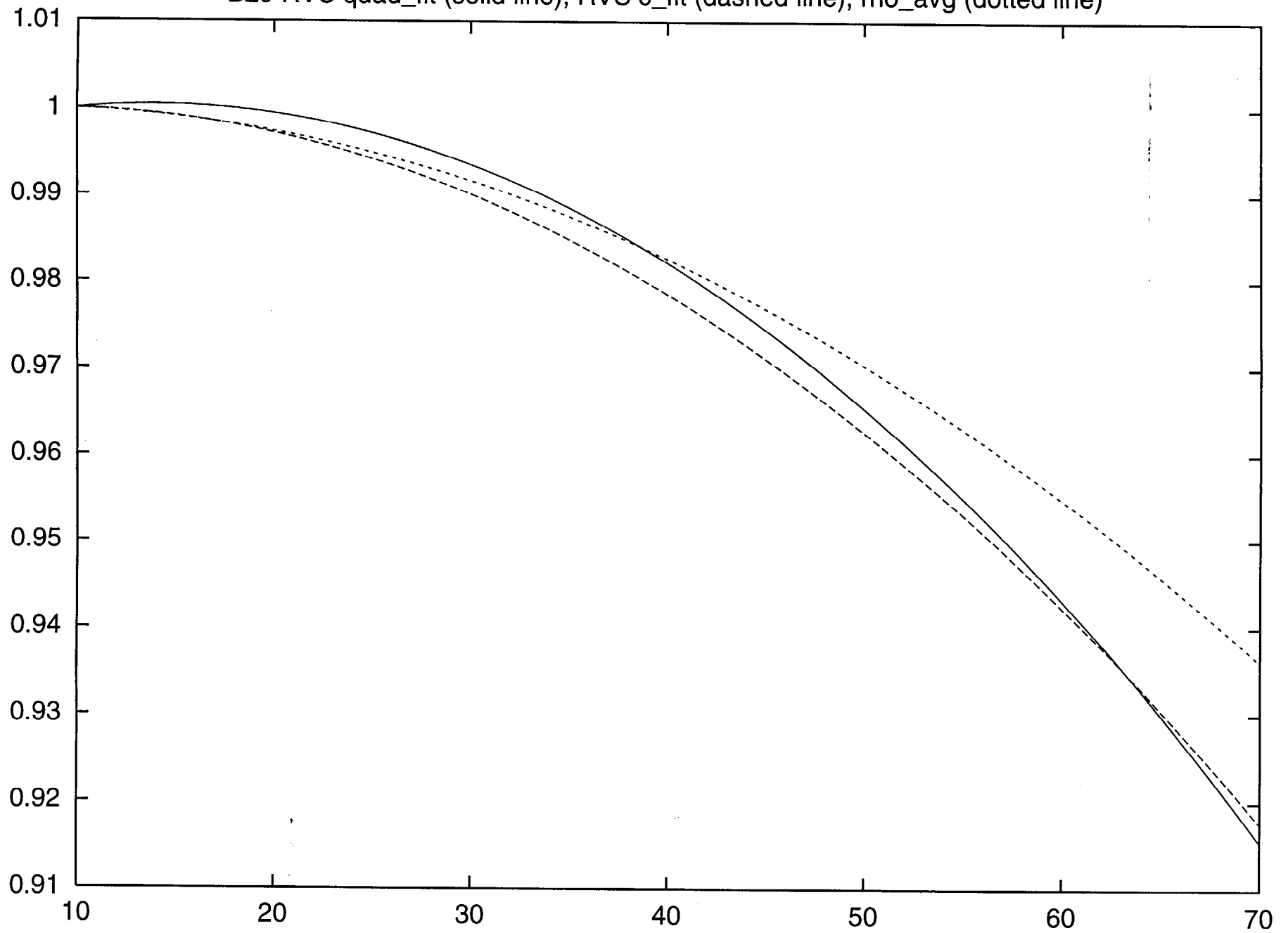




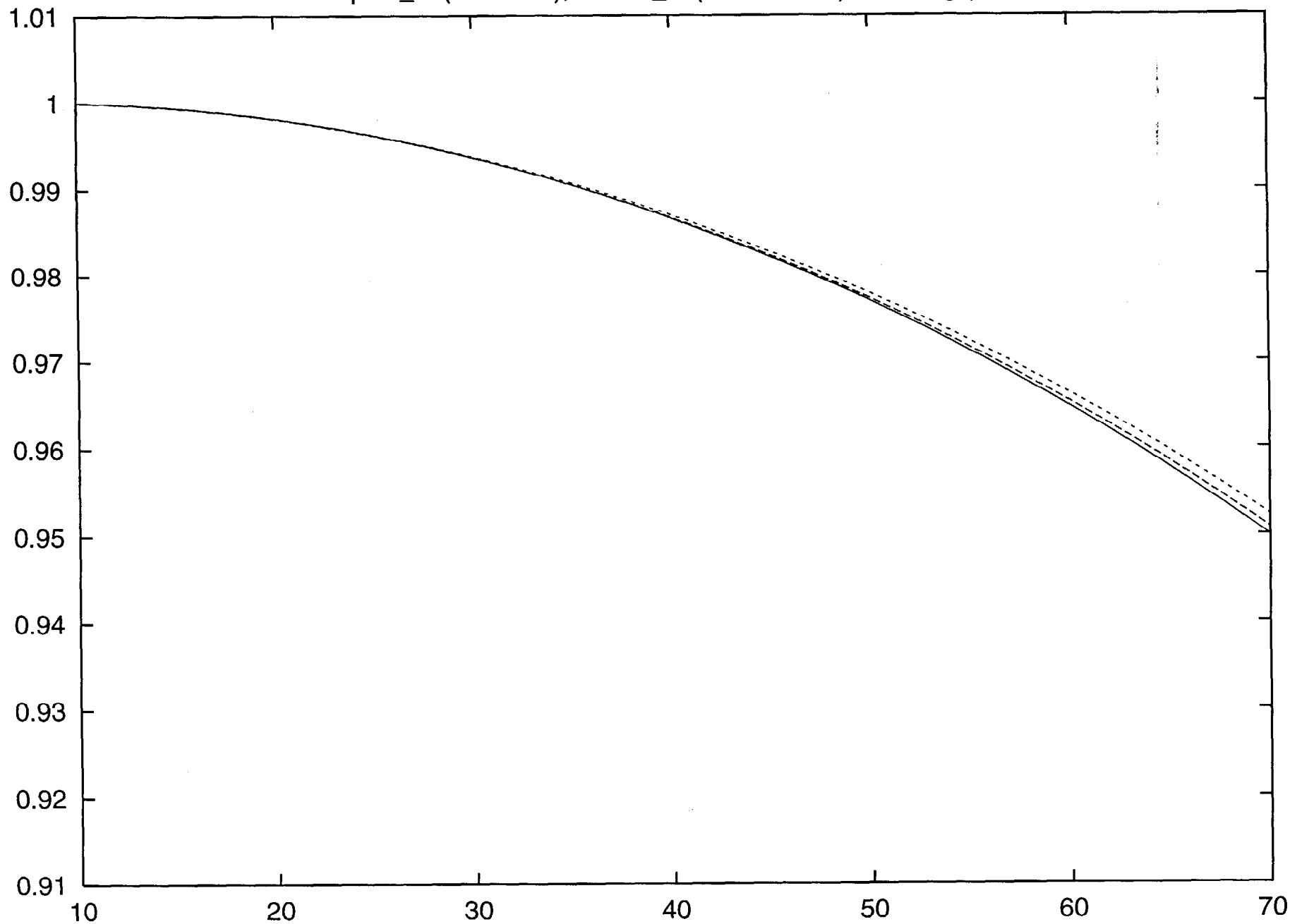
B28 RVS quad_fit (solid line), RVS c_fit (dashed line), rho_avg (dotted line)



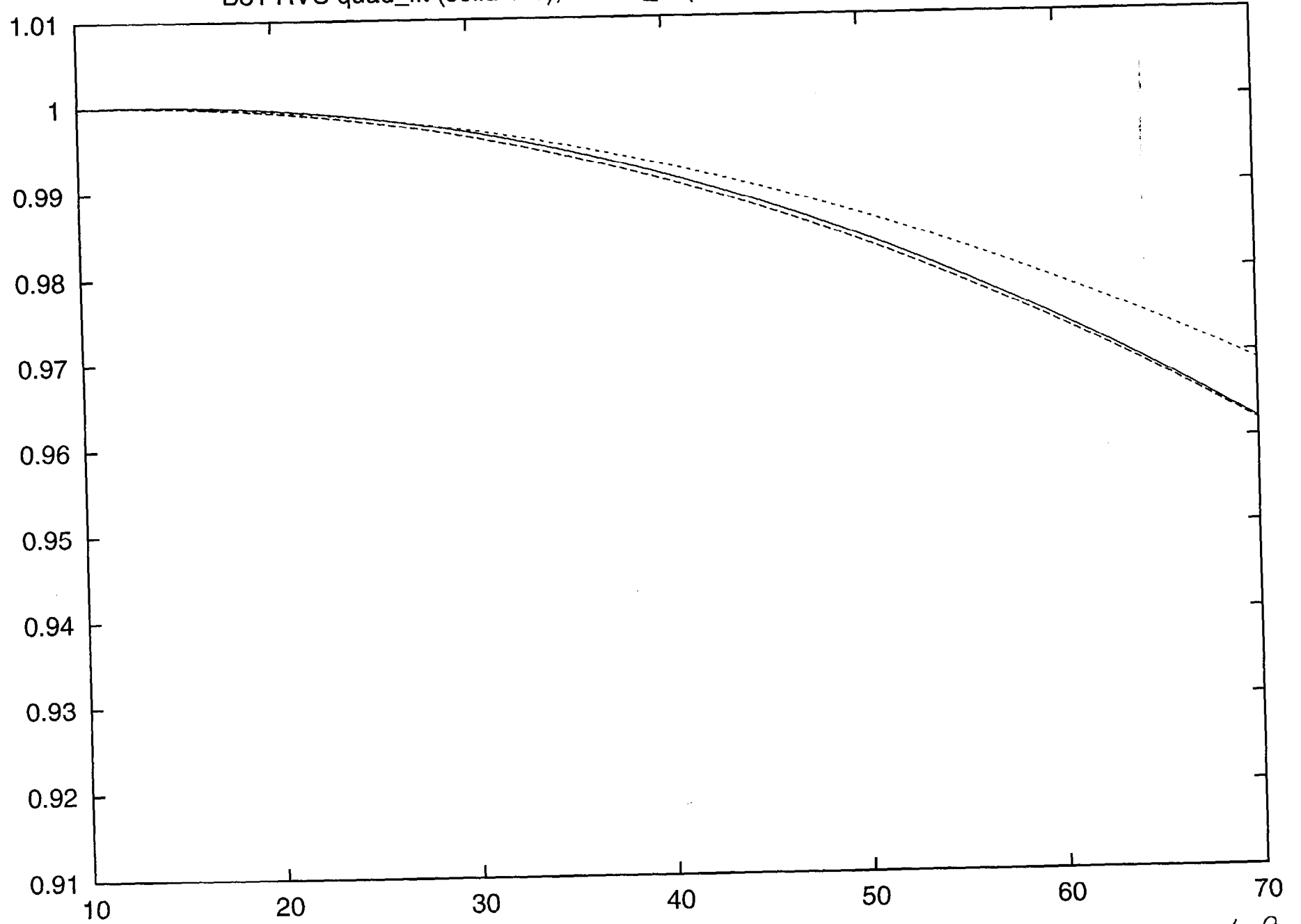
B29 RVS quad_fit (solid line), RVS c_fit (dashed line), rho_avg (dotted line)



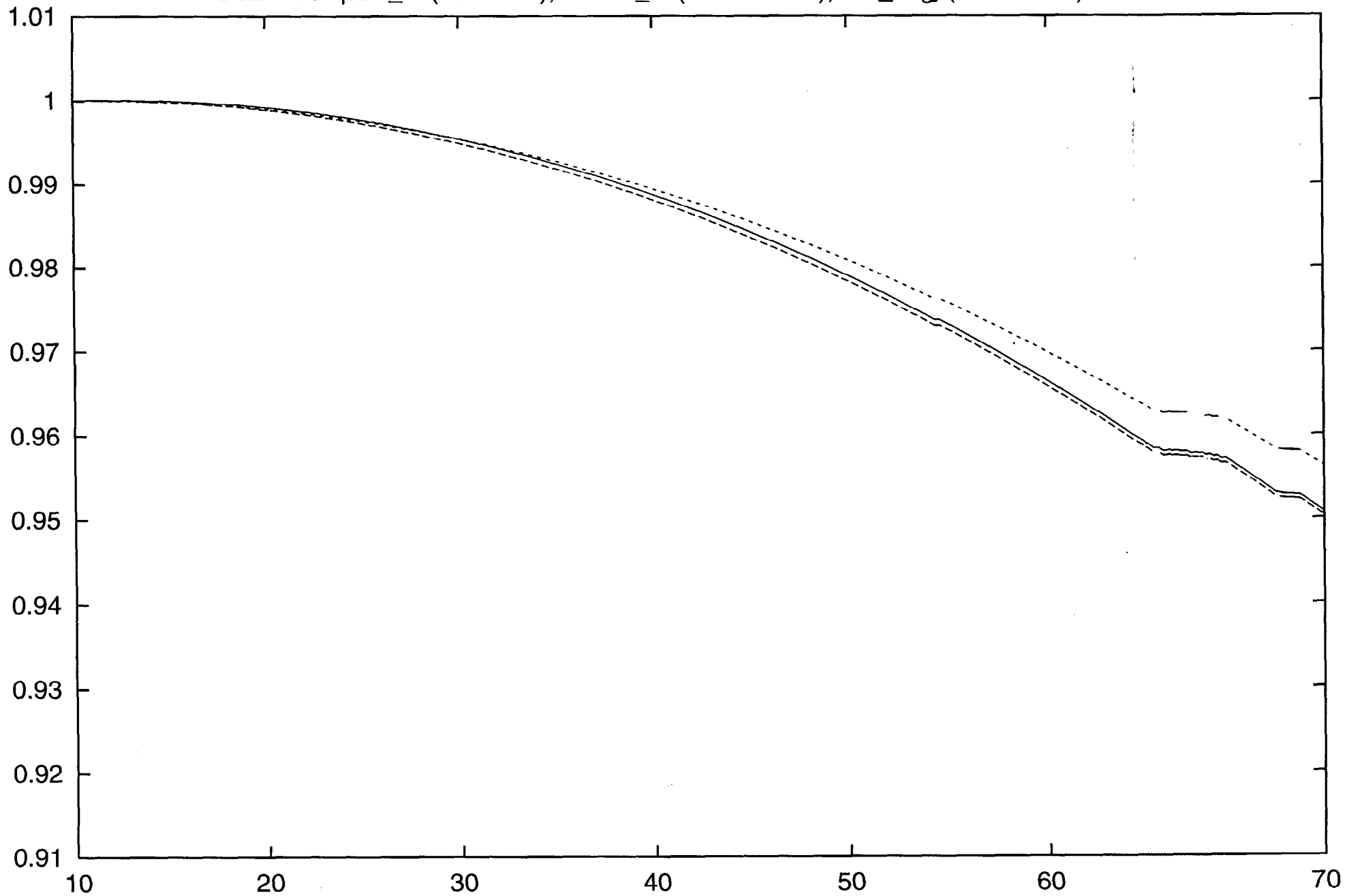
B30 RVS quad_fit (solid line), RVS c_fit (dashed line), rho_avg (dotted line)



B31 RVS quad_fit (solid line), RVS c_fit (dashed line), rho_avg (dotted line)

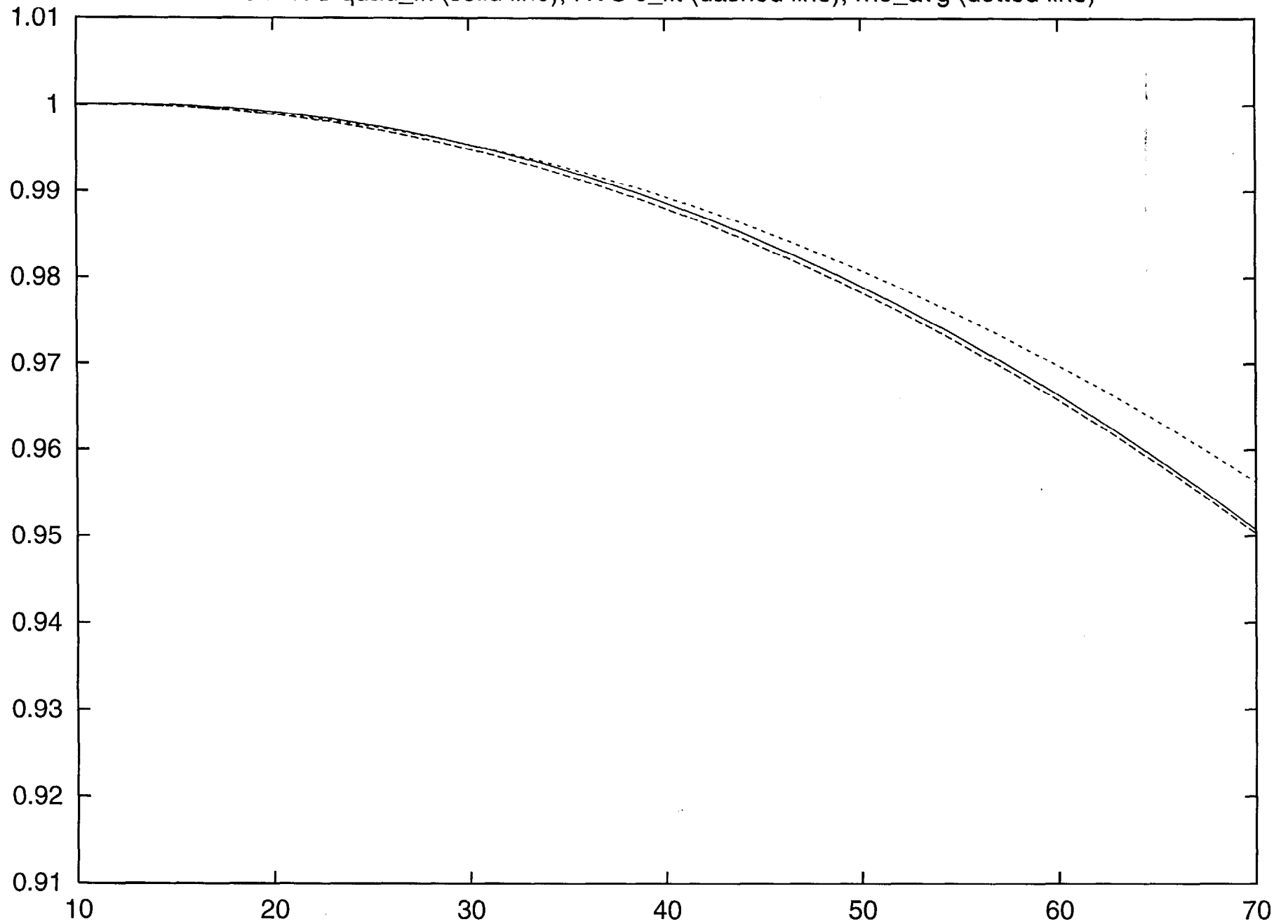


B32 RVS quad_fit (solid line), RVS c_fit (dashed line), rho_avg (dotted line)

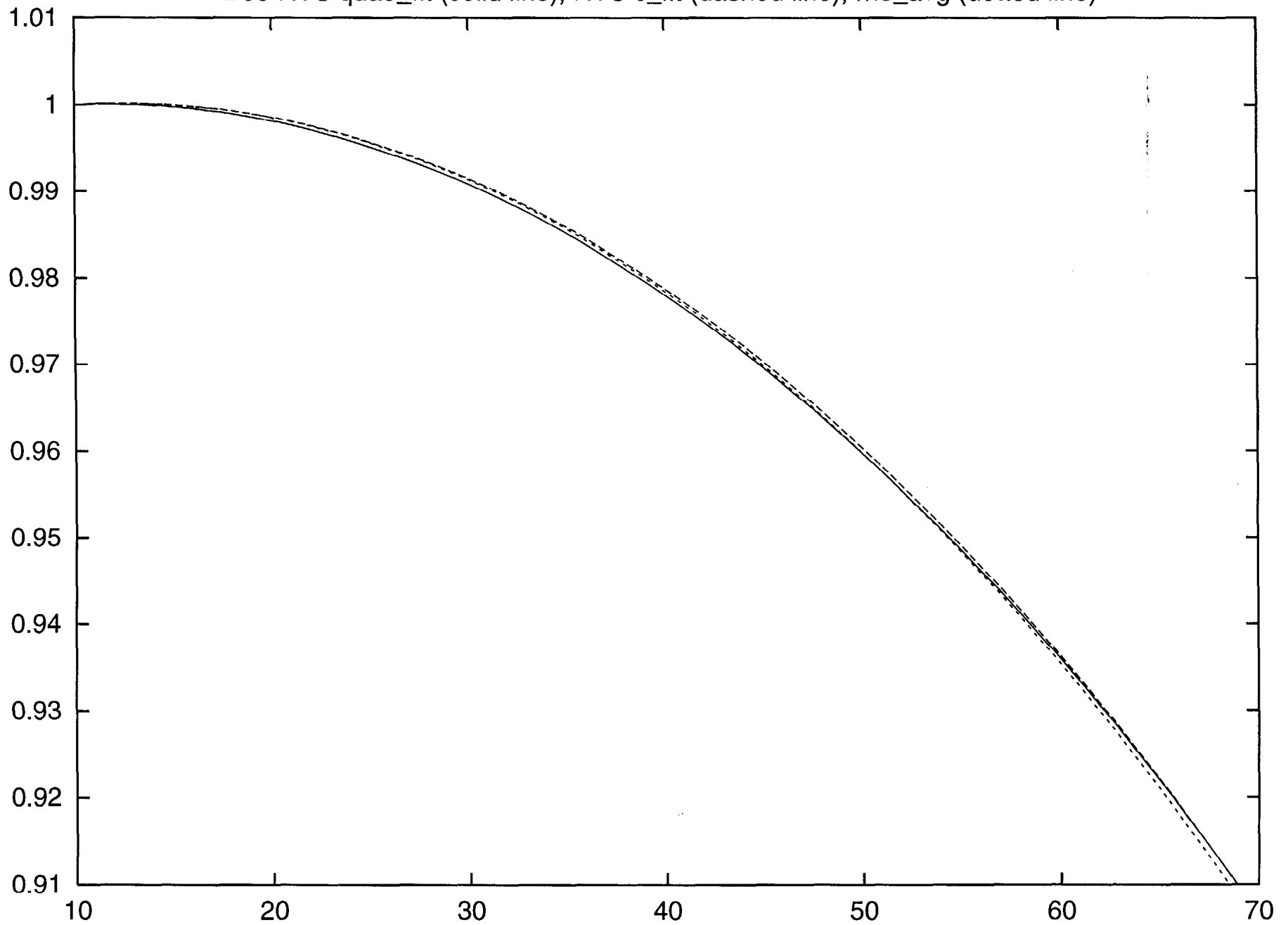


101

B32 RVS quad_fit (solid line), RVS c_fit (dashed line), rho_avg (dotted line)

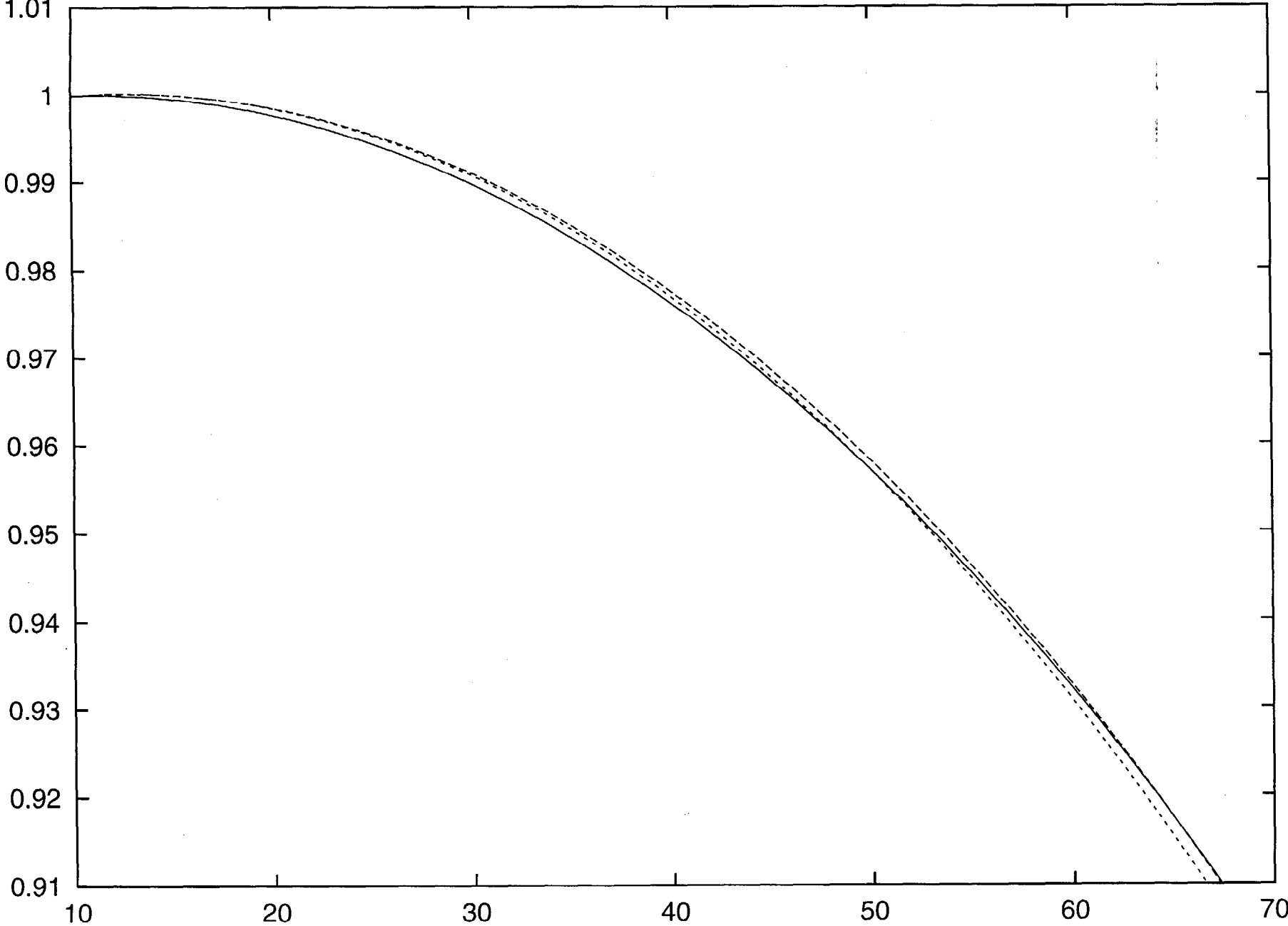


B33 RVS quad_fit (solid line), RVS c_fit (dashed line), rho_avg (dotted line)

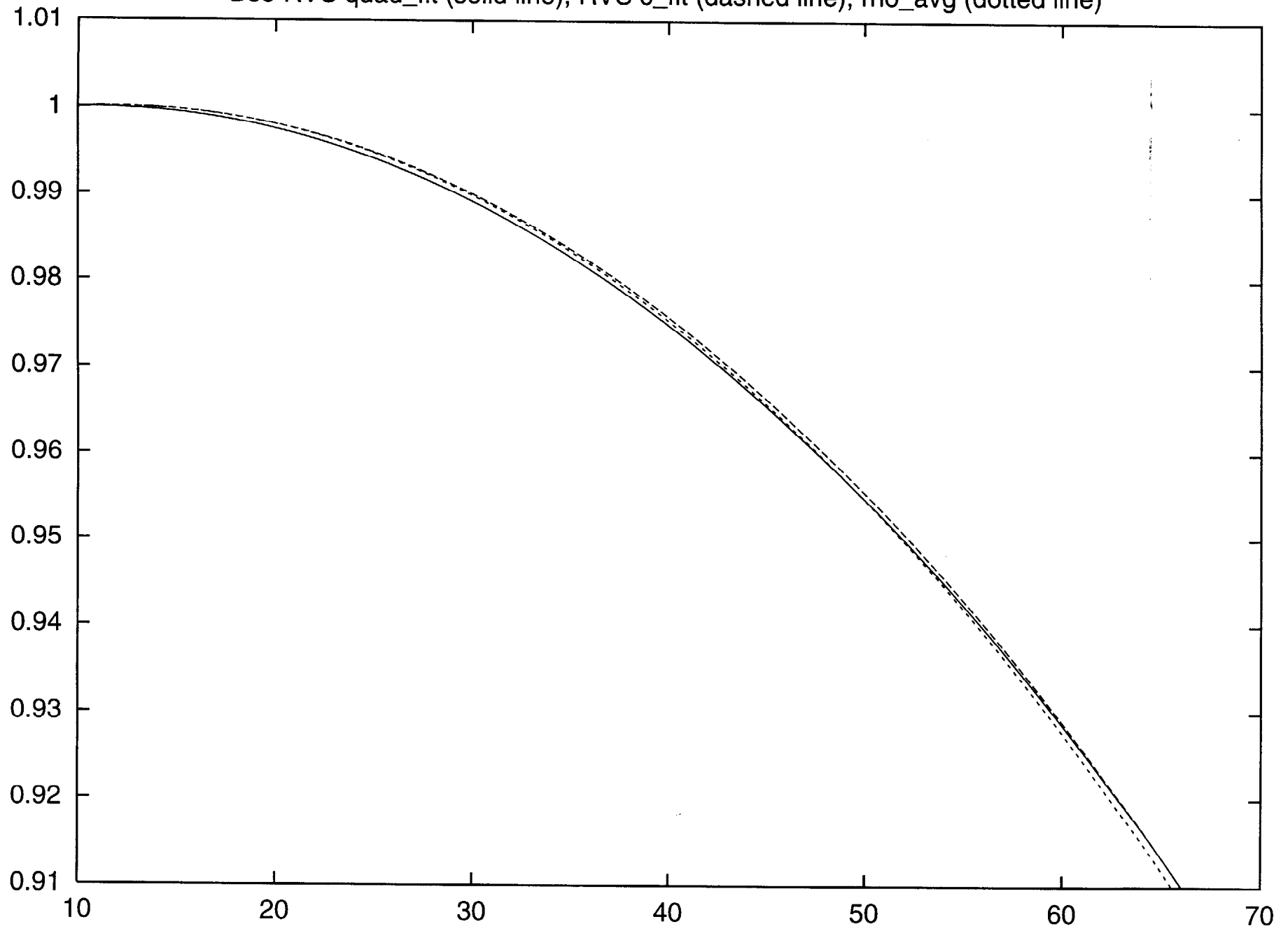


///

B34 RVS quad_fit (solid line), RVS c_fit (dashed line), rho_avg (dotted line)



B35 RVS quad_fit (solid line), RVS c_fit (dashed line), rho_avg (dotted line)



Scan Mirror brightness temperatures ($T_{sm}=270K$)

These temperatures are determined from the scan mirror absolute radiance emission, i.e., not the net radiance difference between the Earth View scan mirror emission and the Cold Space View scan mirror emission.

	AOI=10.5	15.5	20.5	25.5	30.5	35.5	40.5	45.5	50.5	55.5	60.5	65.5	
t =	203.4	203.4	203.4	203.4	203.5	203.6	203.9	204.4	205.3	206.8	208.9	211.6	20
	199.6	199.6	199.6	199.6	199.7	199.8	200.1	200.7	201.7	203.3	205.6	208.6	21
	199.8	199.8	199.8	199.9	199.9	200.1	200.4	201	202	203.6	205.9	208.8	22
	198.7	198.7	198.7	198.8	198.8	199	199.3	200	201.1	202.8	205.2	208.3	23
	193.5	193.5	193.5	193.6	193.7	194	194.6	195.5	196.9	198.8	201.2	204.1	24
	192.6	192.6	192.6	192.7	192.9	193.2	193.7	194.6	196	197.9	200.4	203.3	25
	172.9	172.9	173	173.1	173.5	174.1	175.1	176.7	178.8	181.6	184.9	188.7	27
	169	169	169	169.2	169.4	169.9	170.8	172.2	174.2	176.8	180.1	184	28
	162.8	163.5	164.7	166.7	169.4	172.7	176.5	180.7	185	189.5	194	198.4	29
	155.1	155.6	156.6	158.2	160.5	163.5	167.1	171.1	175.3	179.8	184.4	189	30
	142.6	143	143.8	145.2	147.1	149.6	152.5	155.9	159.5	163.4	167.4	171.5	31
	137.9	138.2	139	140.2	142	144.3	147.1	150.3	153.8	157.6	161.5	165.6	32
	130.3	131.6	133.7	136.5	139.9	143.8	148	152.3	156.7	161.2	165.6	170	33
	127.8	129.5	132	135.3	139.1	143.3	147.7	152.2	156.8	161.4	165.8	170.3	34
	127.9	129.5	132.1	135.3	139.1	143.3	147.7	152.2	156.8	161.4	165.9	170.4	35
	126.5	128.2	130.7	134	137.9	142.1	146.6	151.2	155.9	160.6	165.2	169.7	36

Preliminary Estimated Scan Mirror Signal-to-Noise Ratios (SNRs)

(for radiance emitted from the scan mirror for 1 minute data collect based on T/V measured SNRs; assumes T_{sm}=270K and T_{fpa} constant at 83K)

Band	20	21	22	23	24	25	27	28	29	30	31	32	33	34	35	36	AOI	
																	=	
M036 =	0	0	0	0	0	0	0	0	0	0	0	0	0	0	0	0	10.5°	
	0	0	0	0	0	0	0	0	1	0	1	0	1	1	1	0	15.5°	
	0	0	0	0	0	0	0	0	0	3	1	2	1	2	2	2	1	20.5°
	0	0	0	0	0	0	0	0	0	7	3	3	3	3	3	3	2	25.5°
	0	0	0	0	0	0	0	0	1	13	5	6	5	6	5	5	3	30.5°
	0	0	0	0	0	0	1	1	1	21	9	10	9	8	7	7	5	35.5°
	1	0	1	1	1	1	2	2	2	32	13	16	13	12	11	10	7	40.5°
	1	0	1	1	1	1	3	4	4	45	19	23	20	17	14	14	10	45.5°
	1	0	1	1	2	2	6	8	8	60	27	32	27	22	19	18	12	50.5°
	1	0	1	2	3	2	9	13	13	78	37	43	37	28	24	23	16	55.5°
	2	1	2	3	4	4	13	20	20	99	47	56	48	35	29	28	20	60.5°
3	1	3	4	6	5	19	28	28	124	60	71	61	42	35	34	24	65.5°	

Highbay Response vs Scan Angle (RVS)

(Test Results, PFM Retrieval Methodology and On-orbit Validation Issues)

Presented to MODIS Science Team

December 14, 1998

Outline

- 1) Introduction
- 2) Highbay RVS measurement approach
- 3) Scan mirror witness sample polarized reflectance measurements
- 4) Unpolarized equations used for test data processing results
- 5) Raw data analysis, corrections and fitting results
- 6) Summary of SBRS Highbay RVS results
- 7) Summary of polarized equations used for test data processing
- 8) Polarized response fitting results
- 9) RVS Uncertainty Approach and Analysis
- 10) On-orbit RVS Determination via S/C Maneuver Issues
- 11) Discussion of phenomenological based RVS retrieval approaches
- 12) Discussion

Outline

- 1) Introduction
- 2) Highbay RVS measurement approach
- 3) Scan mirror witness sample polarized reflectance measurements
- 4) Unpolarized equations used for test data processing results
- 5) Raw data analysis, corrections and fitting results
- 6) Summary of SBRS Highbay RVS results
- 7) Summary of polarized equations used for test data processing
- 8) Polarized response fitting results
- 9) RVS Uncertainty Approach and Analysis
- 10) On-orbit RVS Determination via S/C Maneuver Issues
- 11) Discussion of phenomenological based RVS retrieval approaches
- 12) Discussion

Data Analysis Contributors

- Kwo Fu “Vincent” Chiang
- Tim Dorman
- Gerry Godden
- Shi-Yue Qiu
- Xindong Wang
- Jack Xiong

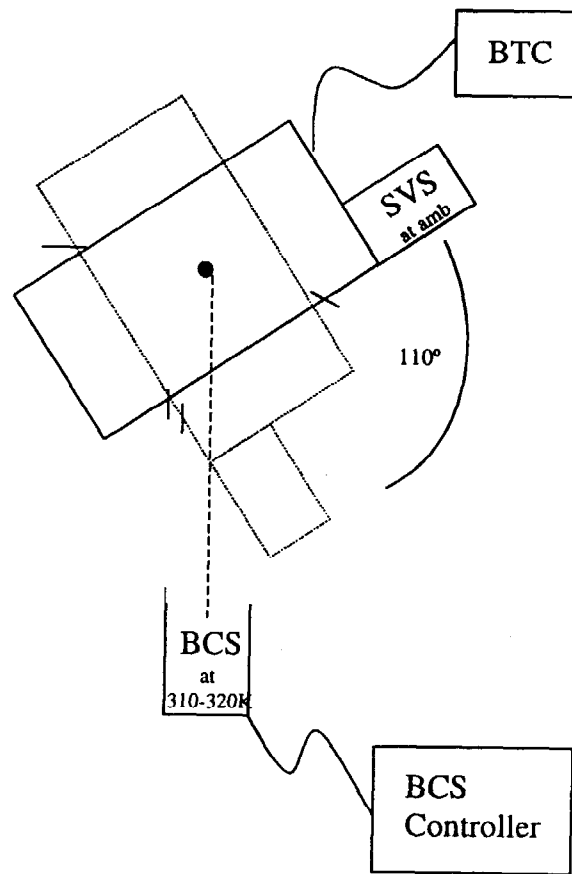
- SBRS Systems Engineering and Test Staffs

Overview of Highbay RVS Measurement Approach

Highbay RVS Test Key Features

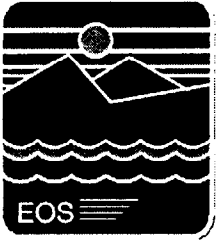
- Test configuration:
 - MODIS aligned on rotary table (ROTAB)
 - Cold FPAs cooled with BTC
 - OBC Blackbody maintained at 310K
 - MWIR and LWIR PV detectors operated with “optimum CSUB” setting (not applicable for PC detectors)
 - SVS positioned at SVP; operated at ambient temperature
 - BCS aligned and operated at one of two temperature settings (310K and 320K)
- 3 data collects taken (310K_1, 320K_2, and 320K_3)
 - Data collects spanned 8 to 10 hours, each

FM1 Highbay RVS Test Configuration

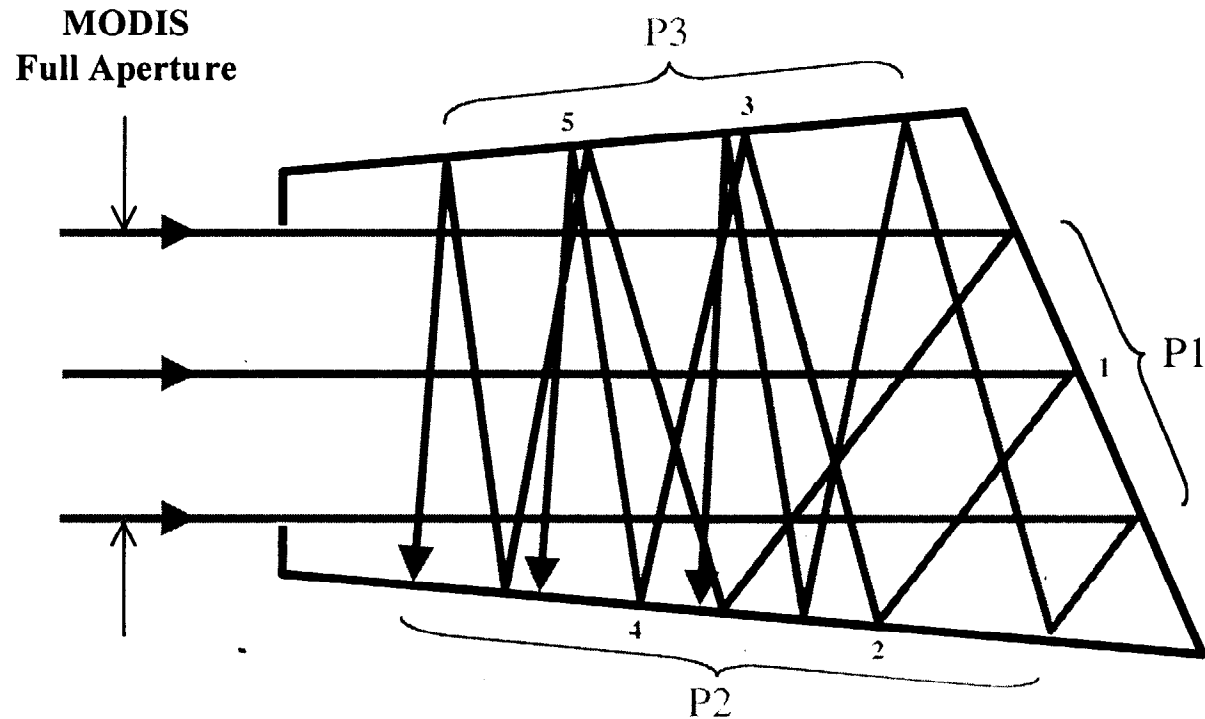


Summary of FM1 Highbay RVS Measurement Angles for 320K_3 Data Set

Collect #	Scan Angle (Degrees)	AOI (Degrees)
18	-53.62	11.19
1	-53.21	11.39
2	-53.01	11.50
3	-44.88	15.56
5	-23.50	26.25
10	-10.41	32.80
6	-0.41	37.80
7	9.59	42.80
8	25.61	50.80
9	37.64	56.82
11	37.64	56.82
12	44.63	60.32
16	44.63	60.32
13	52.11	64.06
14	53.33	64.67
15	53.33	64.67
17	53.33	64.67



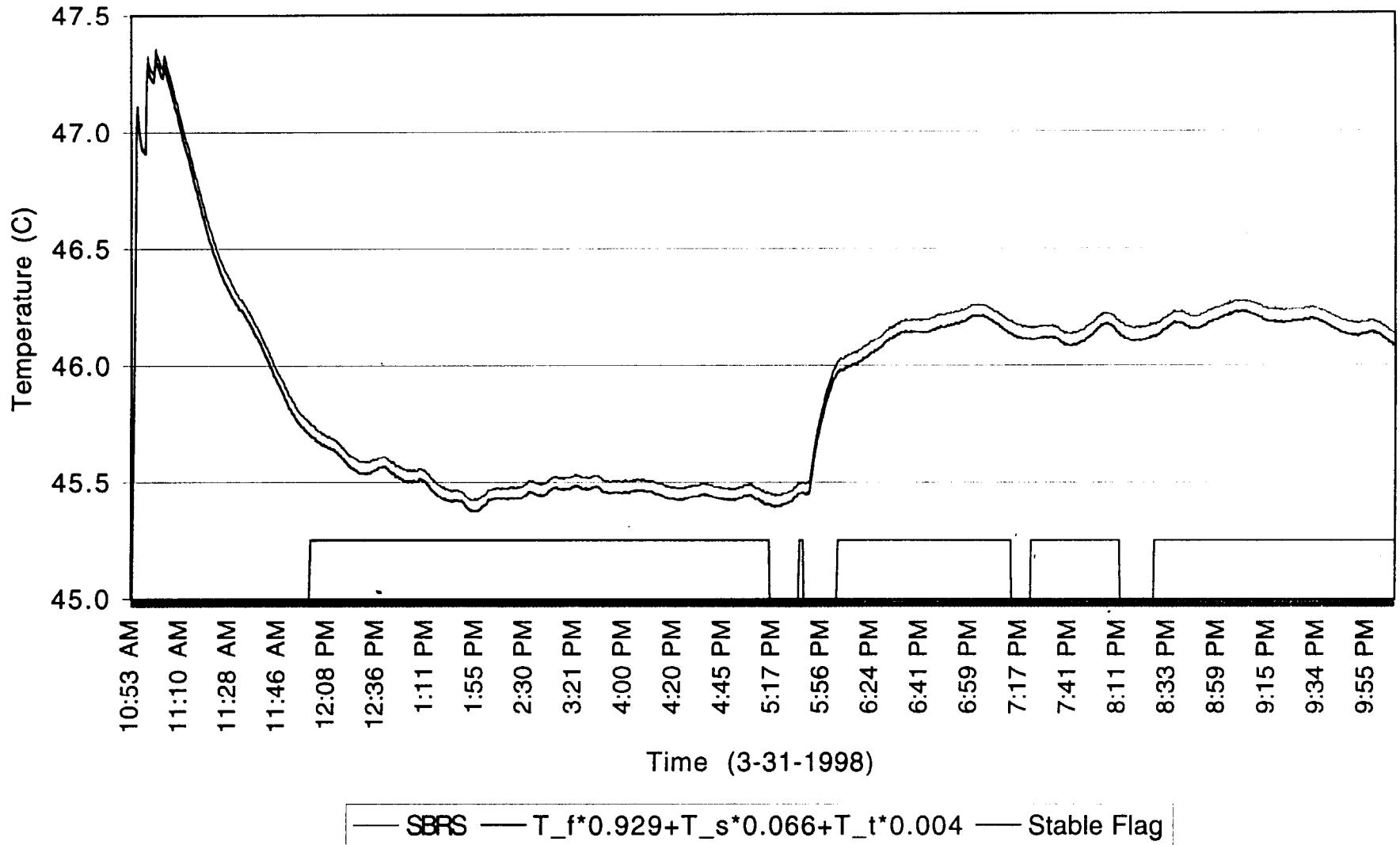
Blackbody Calibration Source (BCS)



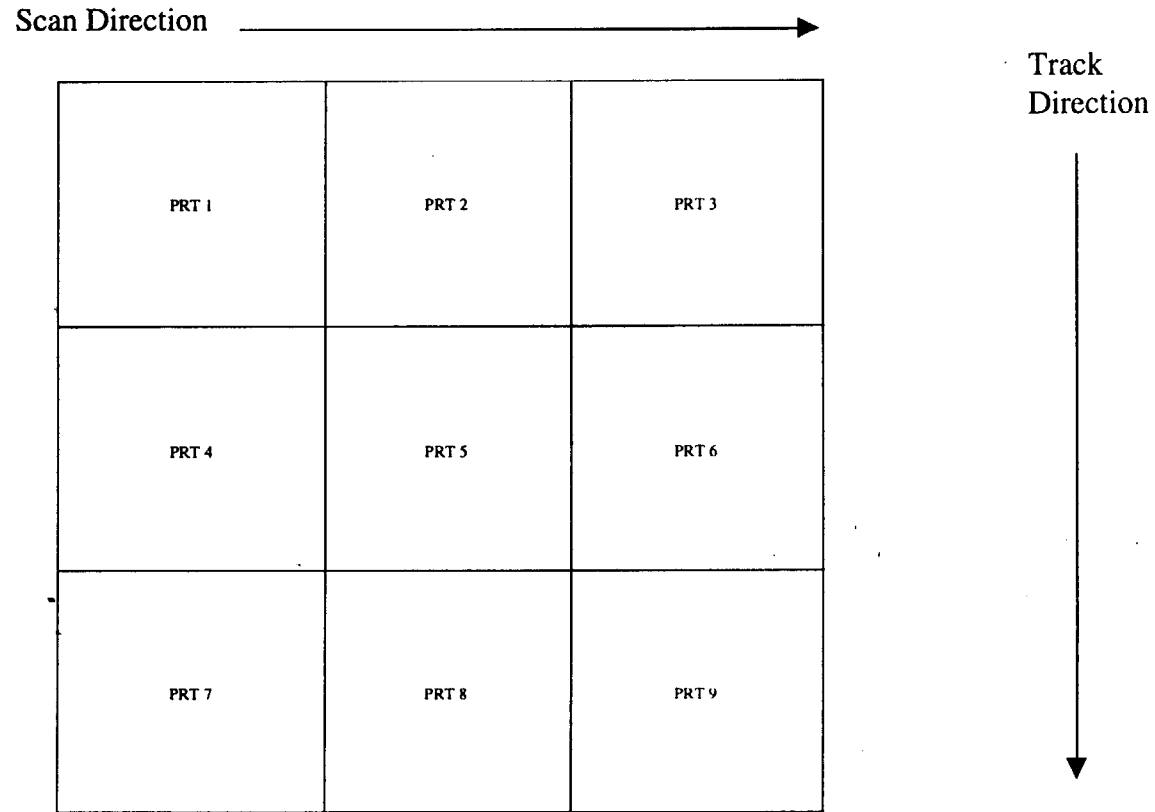
$$L_{BCS} = W_{P1} \cdot L(\lambda, T_{P1}) + W_{P2} \cdot L(\lambda, T_{P2}) + W_{P3} \cdot L(\lambda, T_{P3})$$

BCS Trapezoid Configuration Achieves > 0.998 Emissivity (From SBRS)

RVS [320_3] BCS Effective Temperature; from PRT#1-15; BDATB93.OUT

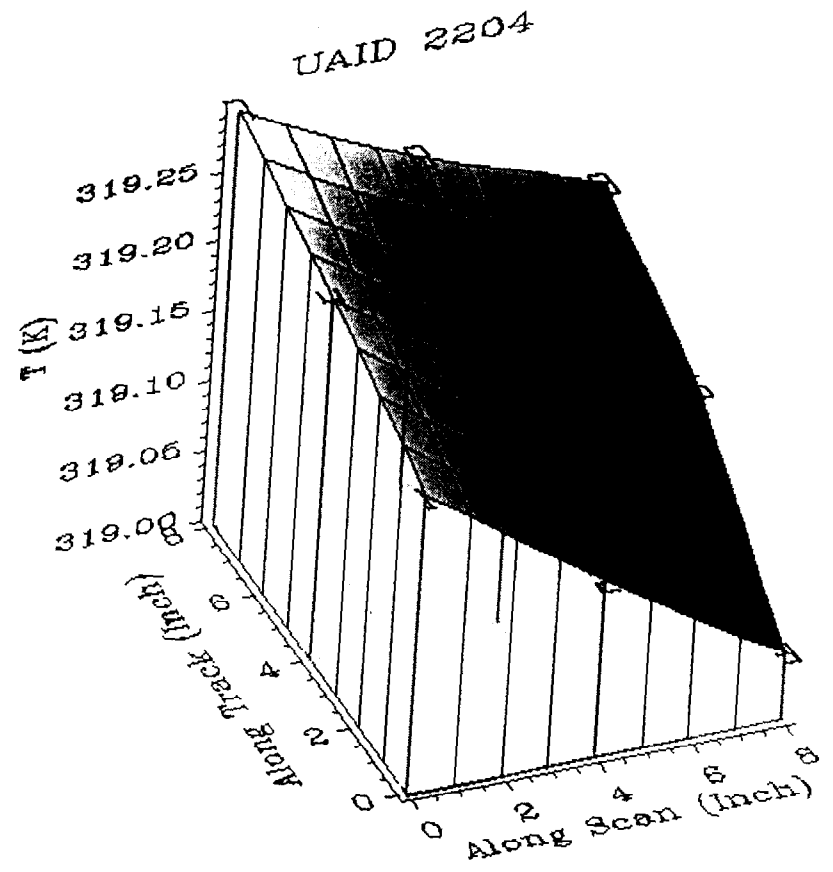
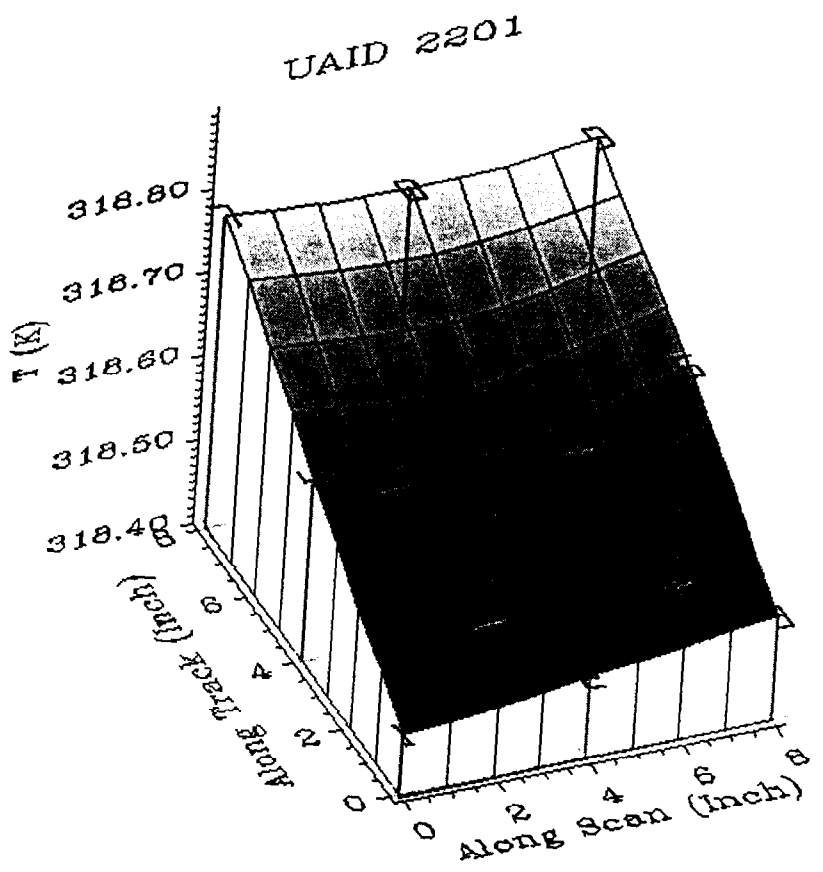


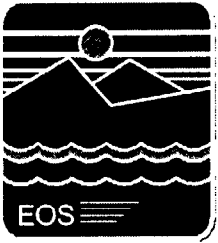
BCS First Bounce Plate Temperature Sensor Arrangement



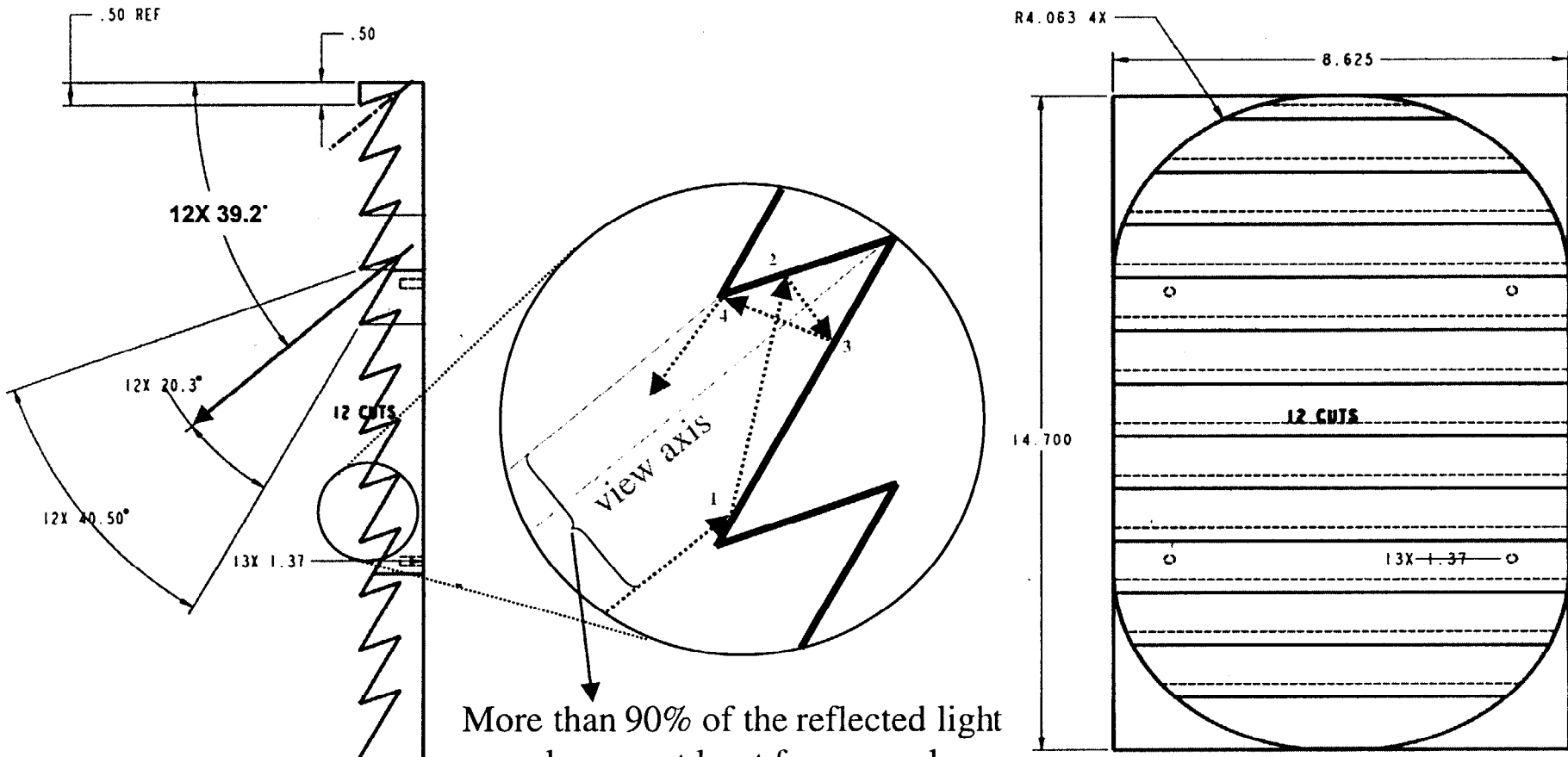
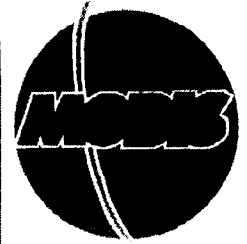
View is back of BCS

BCS First Bounce Plate 9 PRTs Interpolated Temperature Gradients
(Before and After 18:00 Hrs for 320K_3 Collect)





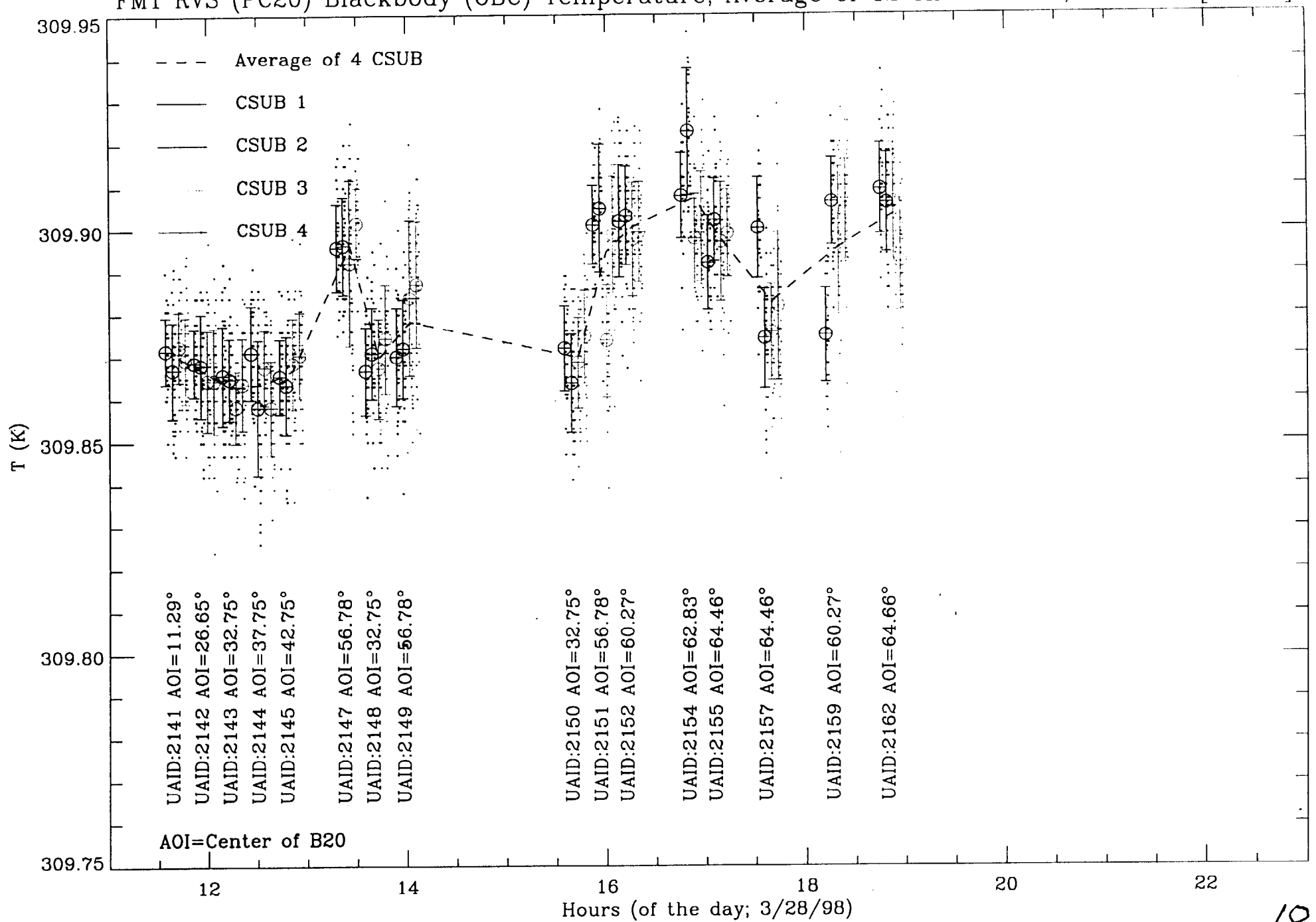
The MODIS On-Board Calibrator (OBC) Blackbody



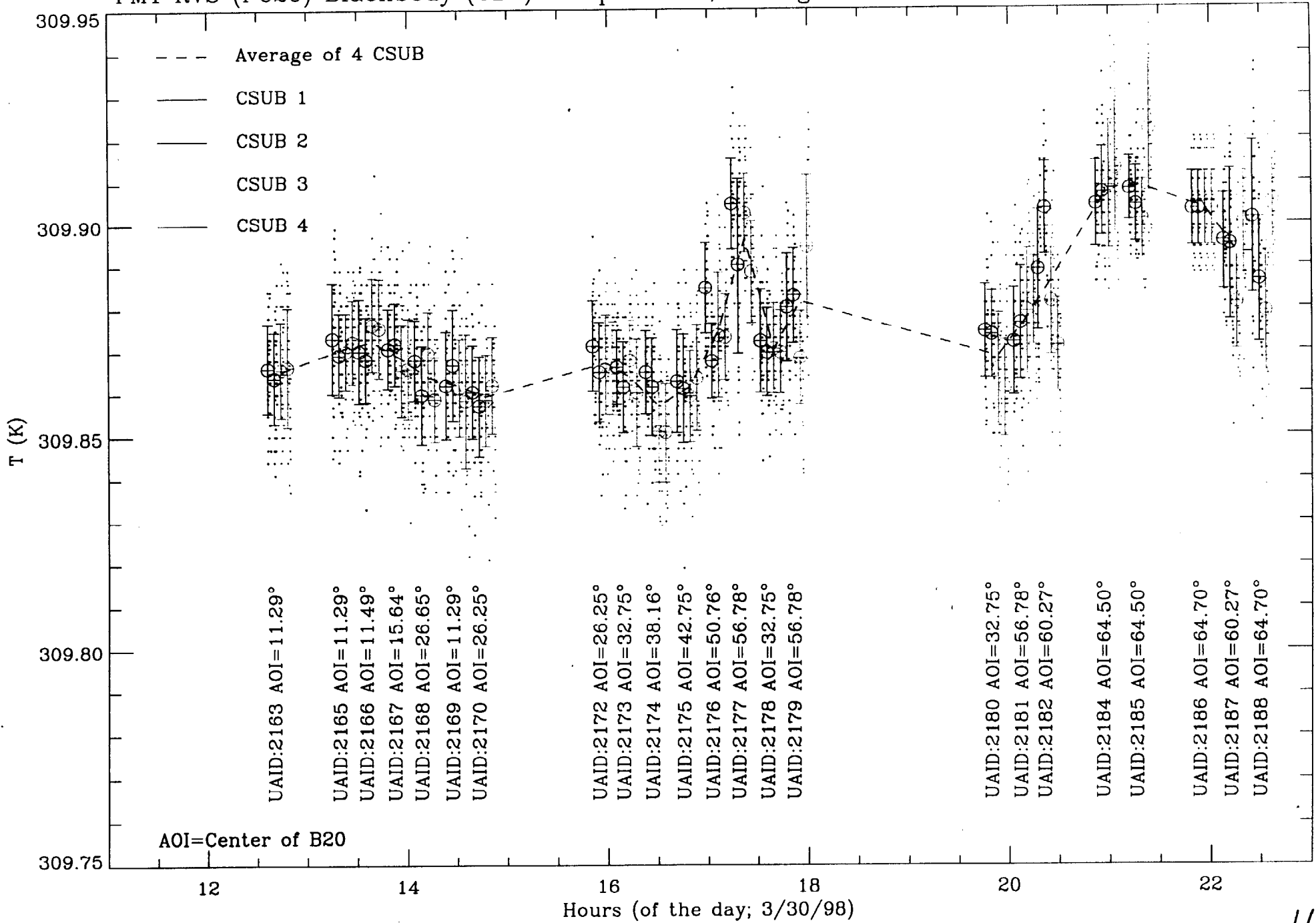
More than 90% of the reflected light
undergoes at least four specular
reflections to achieve > 0.992 emissivity

Dimensions: Inches

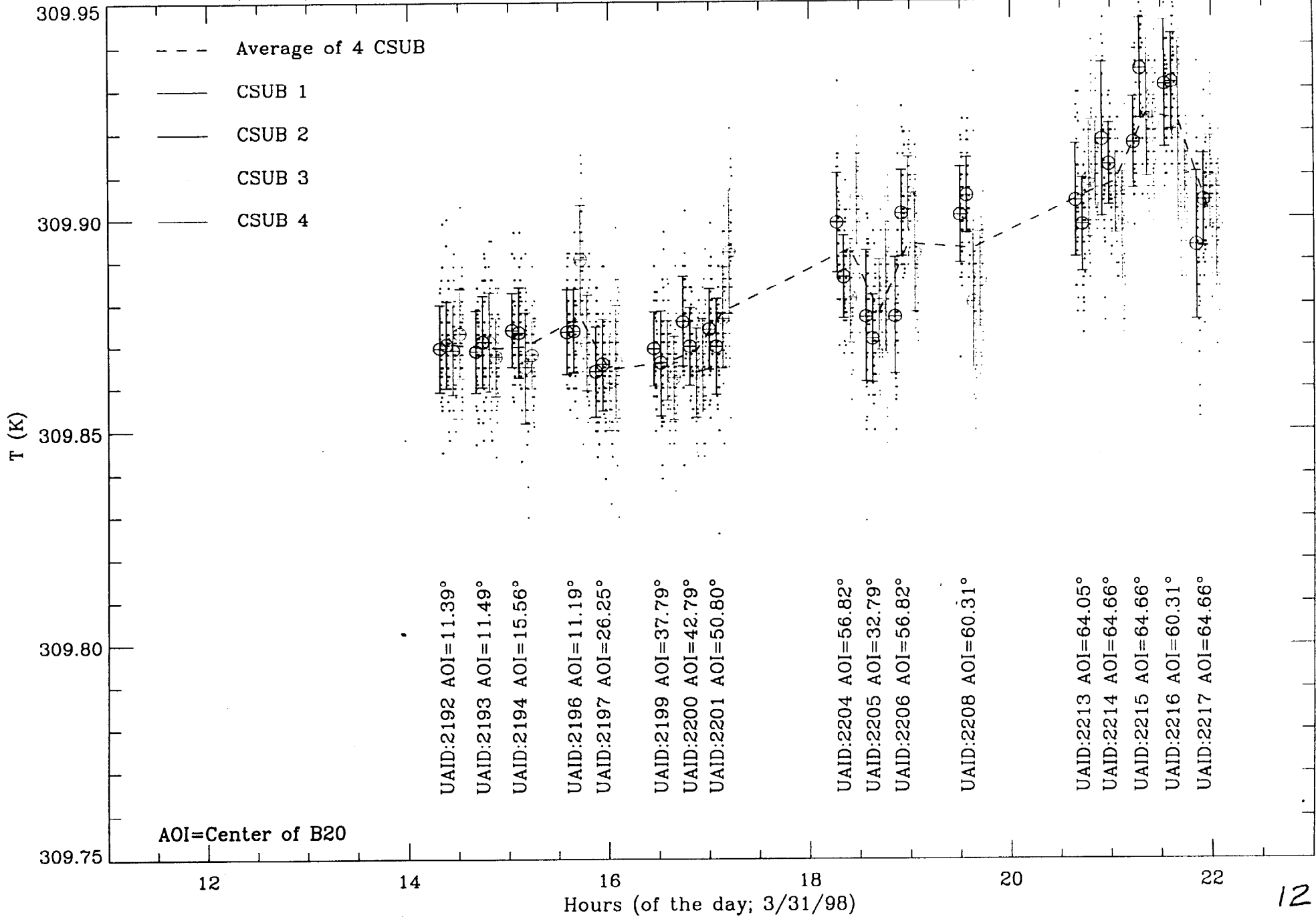
FM1 RVS (PC20) Blackbody (OBC) Temperature; Average of 12 Thermistors; Data set [310_1]



FM1 RVS (PC20) Blackbody (OBC) Temperature; Average of 12 Thermistors; Data set [320_2]

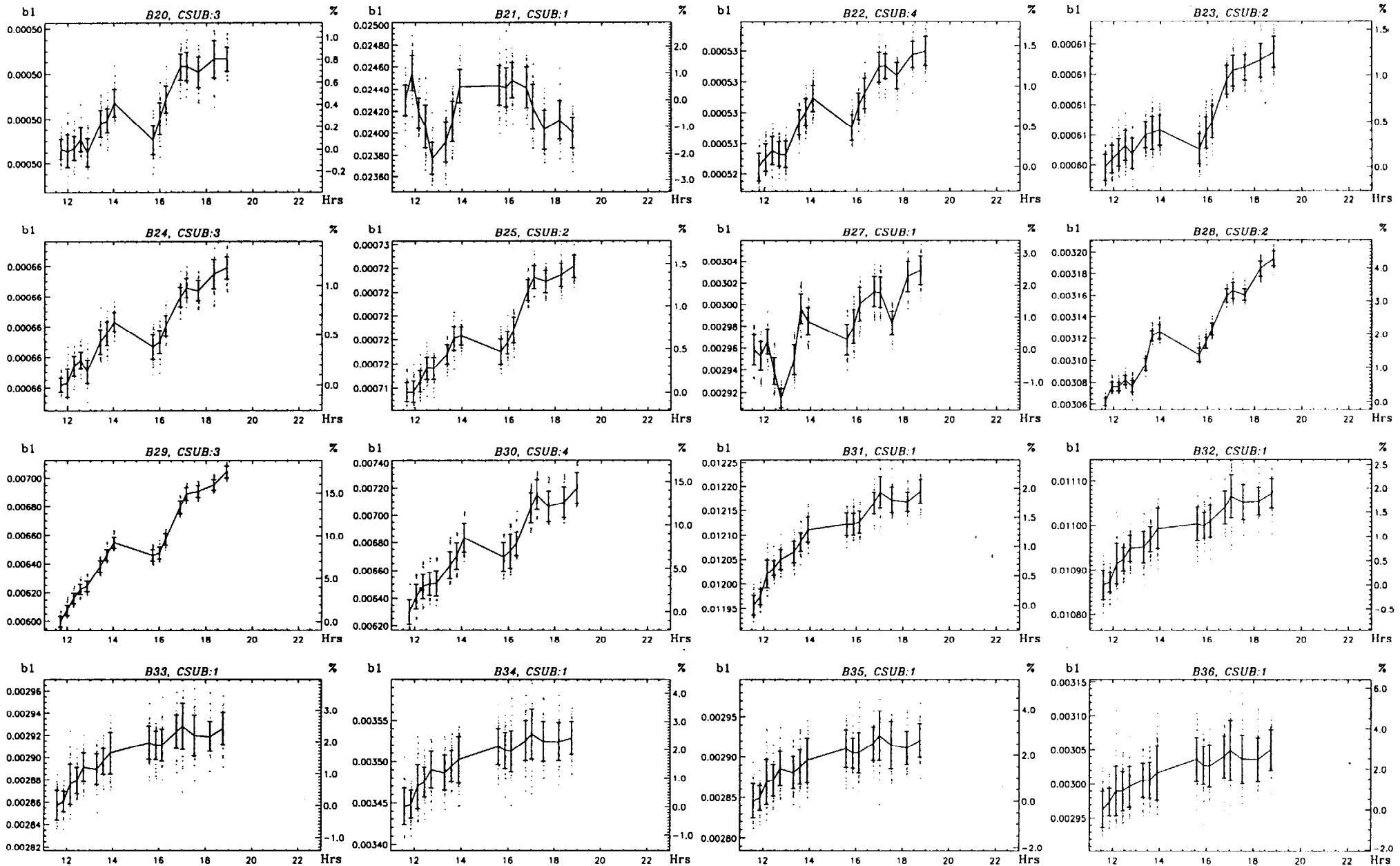


FM1 RVS (PC20) Blackbody (OBC) Temperature; Average of 12 Thermistors; Data set [320_3]



Channel 5 Linear Gain $\langle b1_{OBC} \rangle_{50 \text{ frames}}$ for 40 Scans vs Experiment Time (Hours)

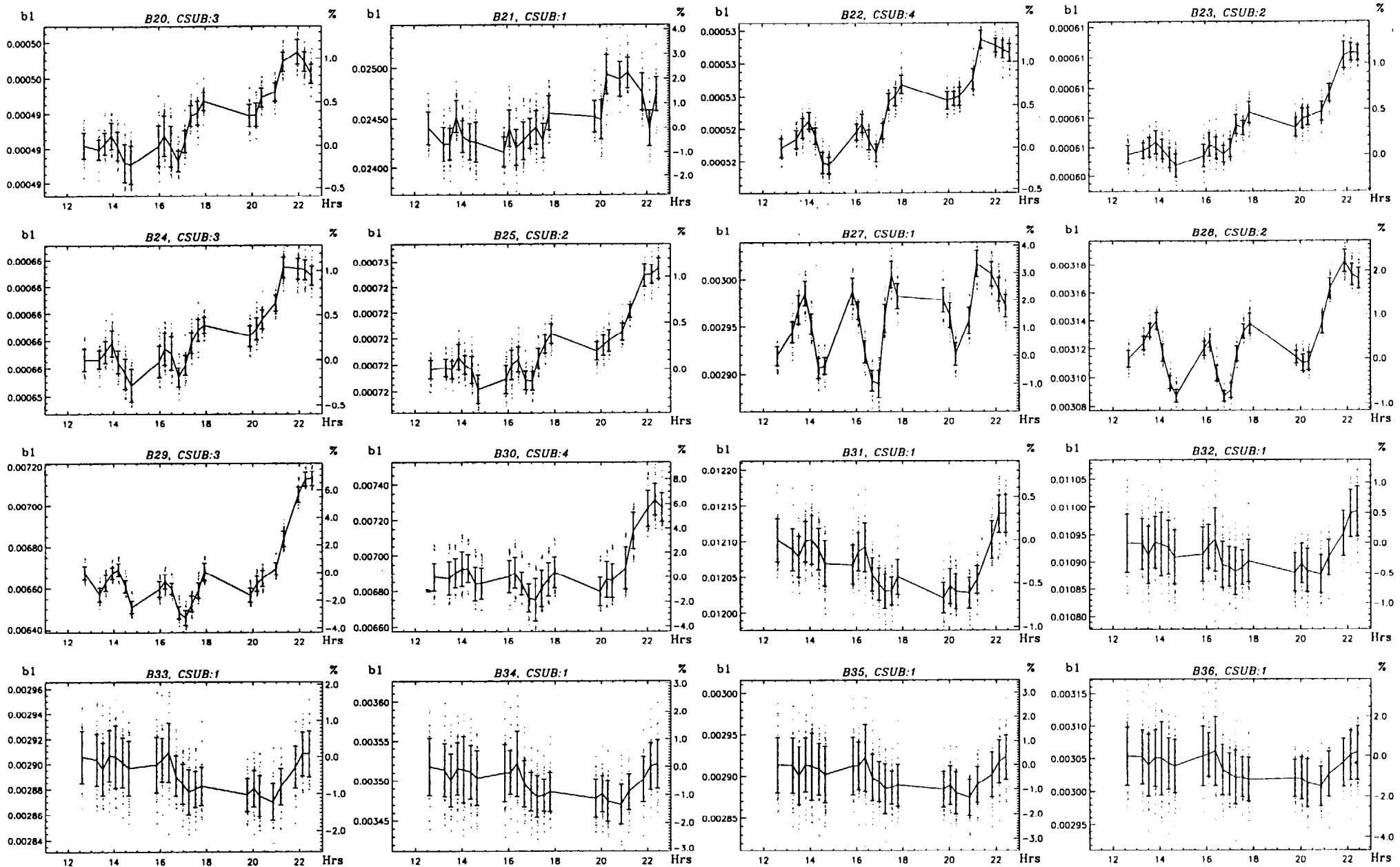
(310K_1 Data Set; Mirror A; w/50frame×40scan Average and 1- σ Error Bars; % Change from 1st Average Noted on Right Axis)



Note: $b1 = (L_{OBC} - L_{SVS}) / dn_{OBC}$

Channel 5 Linear Gain $\langle b1_{OBC} \rangle_{50 \text{ frames}}$ for 40 Scans vs Experiment Time (Hours)

(320K_2 Data Set; Mirror A; w/50frame×40scan Average and 1- σ Error Bars; % Change from 1st Average Noted on Right Axis)

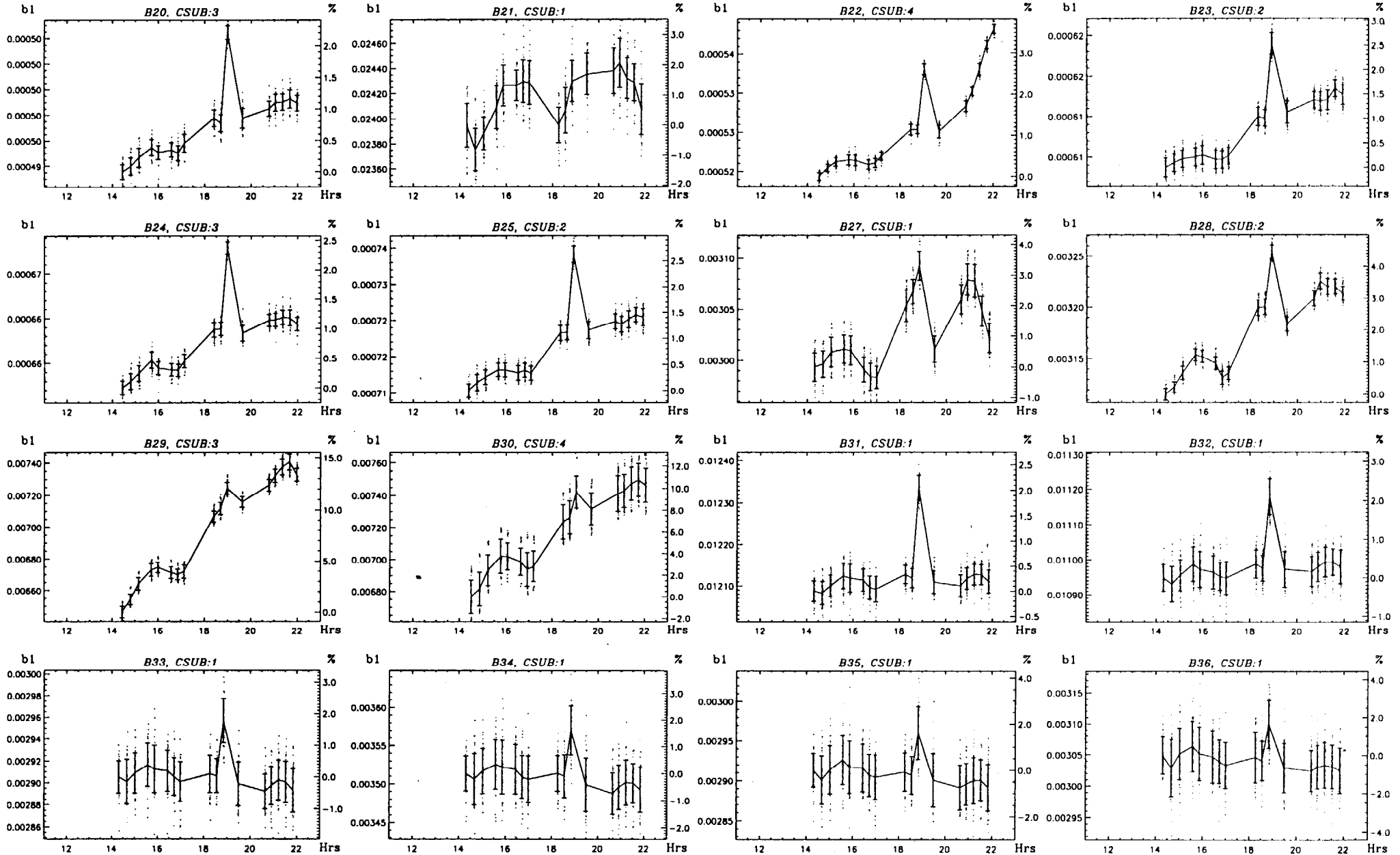


14

Note: $b1 = (L_{OBC} - L_{SVS}) / dn_{OBC}$

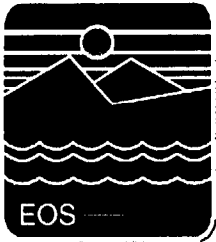
Channel 5 Linear Gain $\langle b1_{OBC} \rangle_{50 \text{ frames}}$ for 40 Scans vs Experiment Time (Hours)

(320K_3 Data Set; Mirror A; w/50frame×40scan Average and 1- σ Error Bars; % Change from 1st Average Noted on Right Axis)

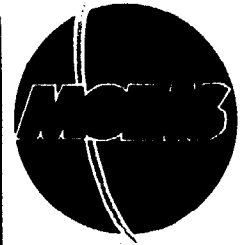


Note: $b1 = (L_{OBC} - L_{SVS}) / dn_{OBC}$

Unpolarized Equations
Used for Analysis of Highbay
RVS Test Data



RVS Equations



Relationship between the BCS path radiance and the detector's response

$$RVS_{\theta} \cdot L_{BCS(\theta)} + (\tau - RVS_{\theta}) \cdot L_{SM} + L_{BKG} = DN_{BCS}^o + b_1 \cdot DN_{BCS}^s \quad (1)$$

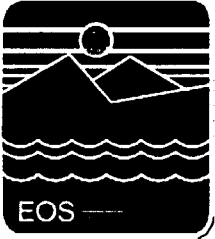
RVS_{θ} - RVS at AOI = θ

$L_{BCS(\theta)}$, L_{SM} , L_{BKG} - Radiance of BCS, Scan Mirror, and Background

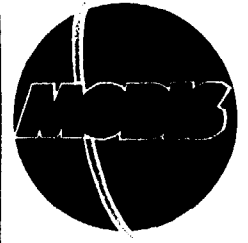
τ - system effective transmittance

b_1 - detector linear response

DN - instrument digital number $DN = DN^o + DN^s$ (offset term + signal term)



RVS Equations (cont'd)



Relationship between the BCS path radiance and the detector's response

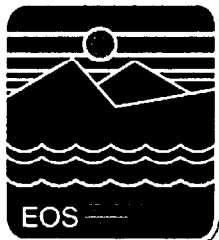
$$RVS_{\theta} \cdot L_{SVS(\theta)} + (\tau - RVS_{\theta}) \cdot L_{SM} + L_{BKG} = DN_{SVS}^0 + b_1 \cdot DN_{SVS}^s \quad (2)$$

From Equations (1) and (2)

$$RVS_{BCS(\theta)} \cdot (L_{BCS(\theta)} - L_{SM}) = b_1 \cdot (DN_{BCS} - DN_{SVS}) + RVS_{SVS} \cdot (L_{SVS} - L_{SM}) \quad (3)$$

For highbay test $T_{SM} \approx T_{SVS}$. For $T_{BCS} = 320K$, the second term on the RHS of Equation (3) is $\sim 0.1\%$, then

$$RVS_{BCS(\theta)} = b_1 \cdot \frac{DN_{BCS} - DN_{SVS}}{L_{BCS(\theta)} - L_{SVS}} \quad (4)$$



RVS Equations (cont'd)

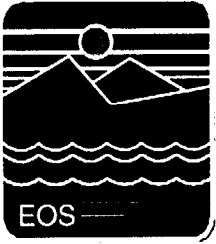


Using the On Board Calibrator (OBC) to correct detector's scan to scan response fluctuation, Equation (4) becomes

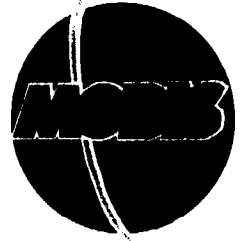
$$RVS_{BCS(\theta)} = RVS_{OBC} \cdot \underbrace{\frac{L_{OBC} - L_{SVS}}{DN_{OBC} - DN_{SVS}}}_{b_1} \cdot \frac{DN_{BCS} - DN_{SVS}}{L_{BCS(\theta)} - L_{SVS}} \quad (5)$$

The normalized RVS (to AOI = 10.75°)

$$RVS^{\text{Norm}}(\theta) = \frac{RVS_{BCS(\theta)}}{RVS_{BCS(\theta=10.75^\circ)}} = f(DN_S, \lambda, T_S, \epsilon_{OBC}, \theta) \quad (6)$$



RVS Uncertainty



Approach 1

$$RVS^{\text{Norm}}(\theta) = \frac{f(DN_S, \lambda, T_S, \epsilon_{\text{OBC}}, \theta)}{f(DN_S, \lambda, T_S, \epsilon_{\text{OBC}}, \theta = 10.75^\circ)} = \frac{f(x_i, \theta)}{f(y_i, \theta = 10.75^\circ)} \quad (7)$$

$$\frac{\Delta RVS^{\text{Norm}}(\theta)}{RVS^{\text{Norm}}(\theta)} = \sqrt{\sum \left(\frac{\partial f(x_i, \theta)}{\partial x_i} \cdot \frac{\Delta x_i}{f(x_i, \theta)} \right)^2} \quad (8)$$

Approach 2

Computer $RVS^{\text{Norm}}(\theta)_i$ for Measurement i ($=1, 2, 3$)
(frame, scan, channel average)

$$\Delta RVS^{\text{Norm}}(\theta) = \text{stdev}\{RVS^{\text{Norm}}(\theta)_1, RVS^{\text{Norm}}(\theta)_2, RVS^{\text{Norm}}(\theta)_3\} \quad (9)$$

Scan Mirror Witness Sample Reflectance Measurements

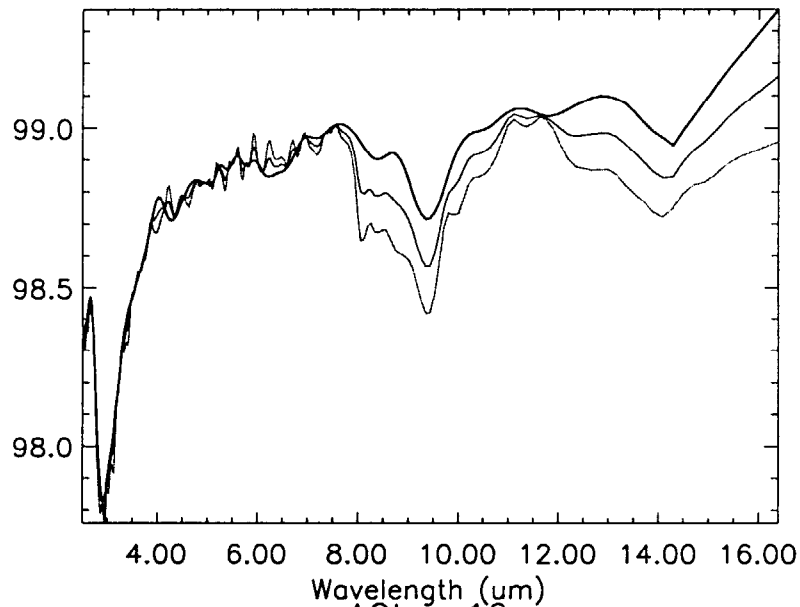
Summary of NPL Scan Mirror Witness Sample Polarized Reflectance Measurements

- 2 witness samples from PFM scan mirror (SN03 and SN04), and 2 witness samples from FM1 scan mirror (SN08 and SN16)
 - SN03 and SN04 samples previously measured by Lincoln Laboratory on two separate occasions
- Measured s and p polarization reflectance of 4 witness samples over 2.50 to 15.15 micron wavelength region, in 10 cm^{-1} increments, for 10° , 26.7° , 38.0° , 50.0° and 65.5° Angles-of-Incidence (AOIs).
- NPL estimated 95% confidence level uncertainties quoted at:
 - $\pm 0.4\%$ for s-polarization for 2.5 to 12.5 microns range, rising to $\pm 0.4\%$ to $\pm 0.7\%$ between 12.5 and 15.15 microns. Except $\pm 0.3\%$ for 10° AOI over the whole wavelength range.
 - $\pm 0.3\%$ for p-polarization
- Average reflectance results compare to within $\pm 1\%$ with Lincoln Laboratory measurements for SN03 and SN04 samples
- Significant differences between PFM and FM1 samples exist

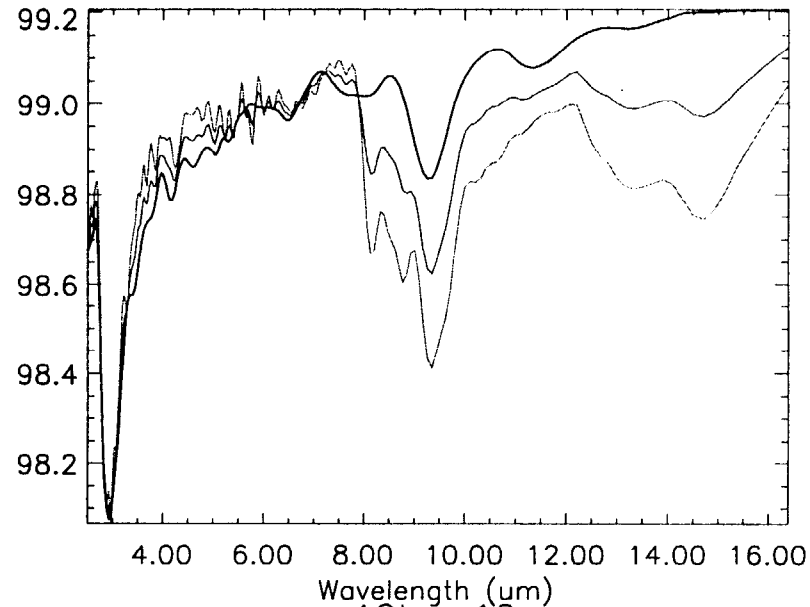
Summary of Scan Mirror Witness Sample Polarized Reflectance Measurements

- Graph Summaries Provided for:
 - NPL S, P and Average reflectances for SN03, SN04, SN08 and SN16 samples at 6 AOIs
 - Comparisons of LL and NPL SN03 and SN04 measurements
 - Sample-to-sample variations for PFM SN03/SN04 and FM1 SN08/SN16 samples
 - FM1 and PFM Average Reflectances versus wavelength
 - FM1 and PFM Polarization Factors versus wavelength
 - FM1 Band-weighted Average Reflectances versus AOI
- Table of FM1 Band's Band-weighted S, P and Average Reflectances for 6 AOIs

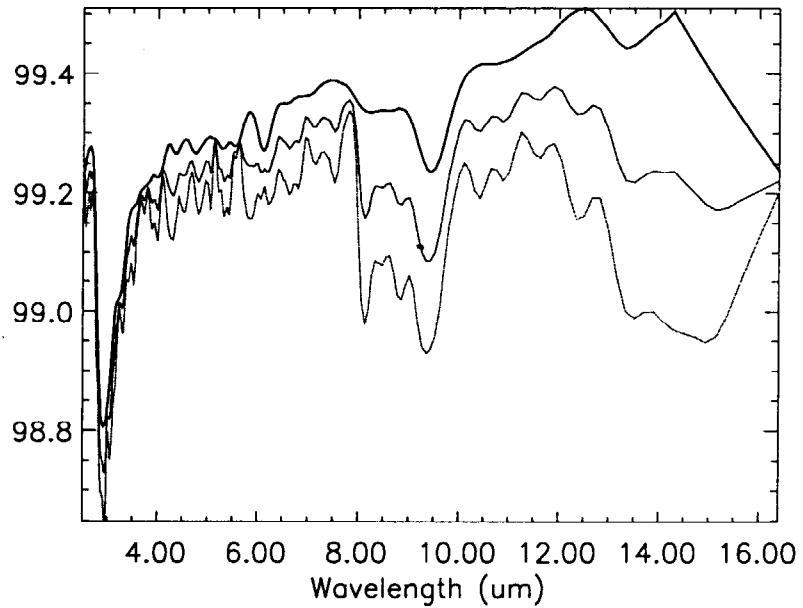
AOI = 10
SN03 S,P and (S+P)/2 Reflectances



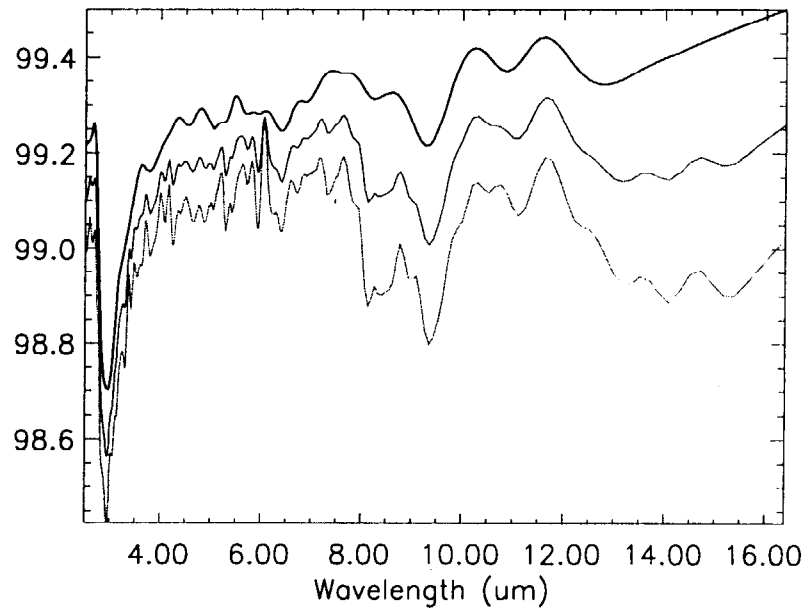
AOI = 10
SN04 S,P and (S+P)/2 Reflectances

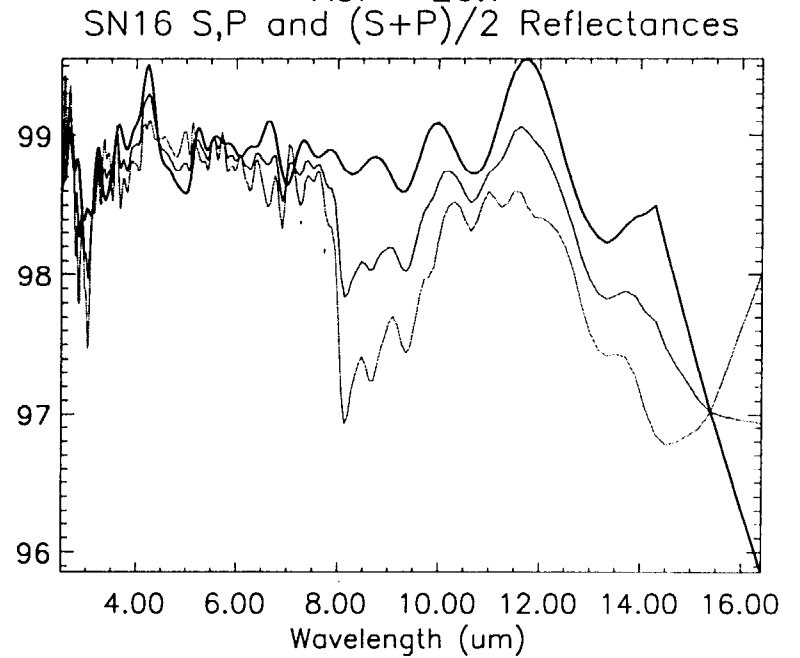
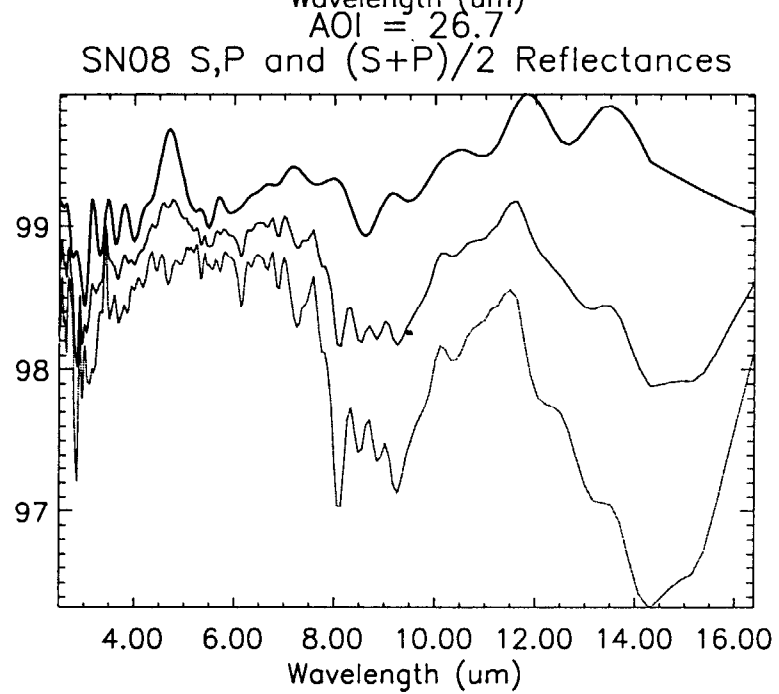
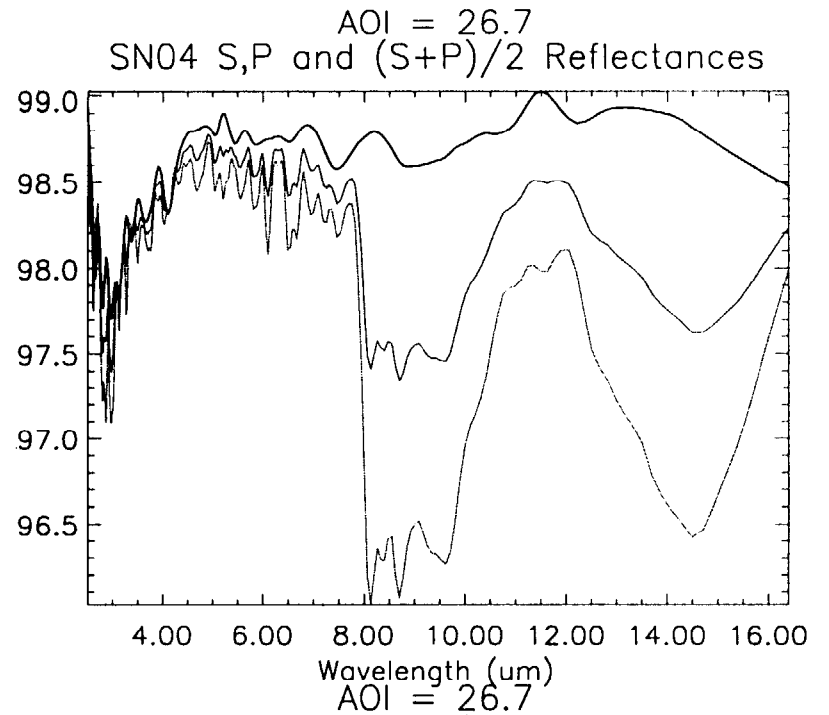
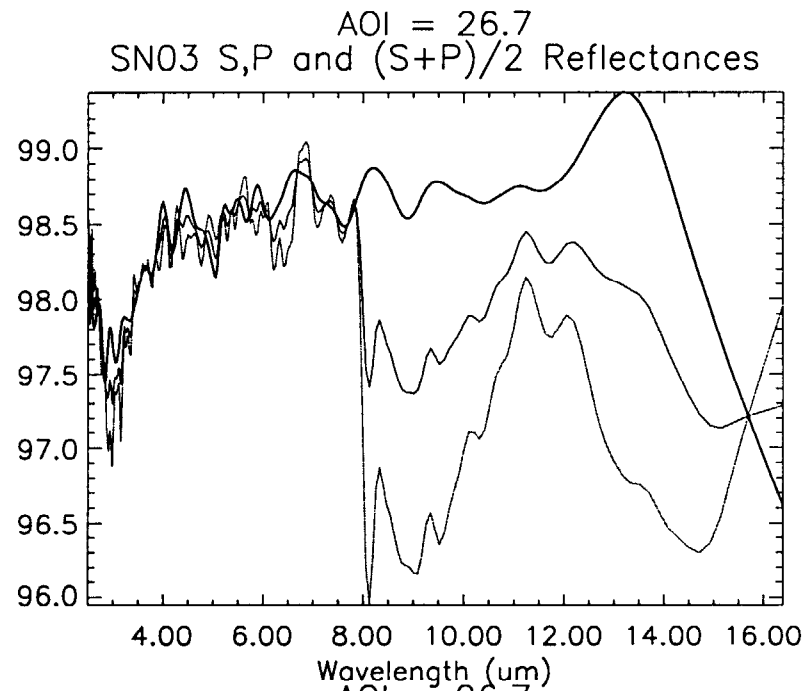


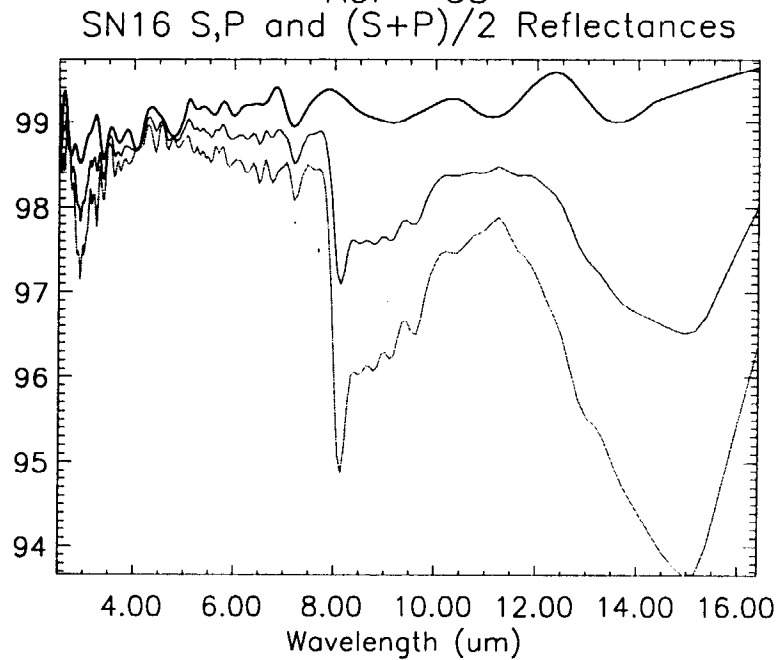
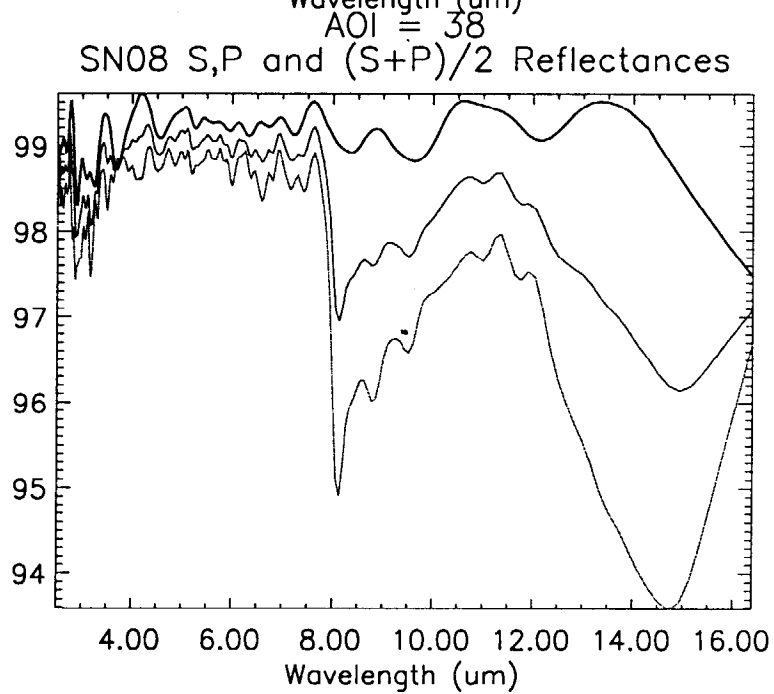
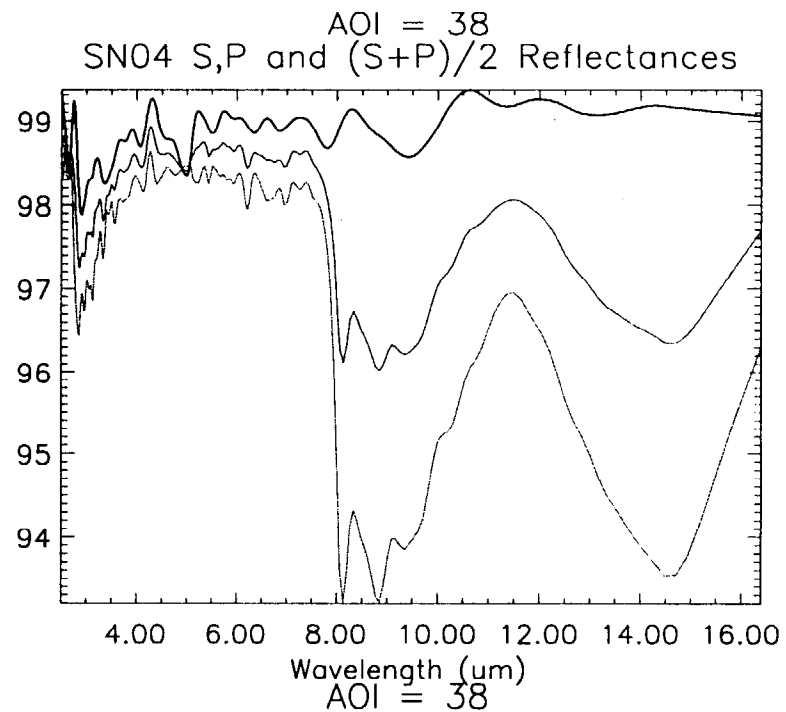
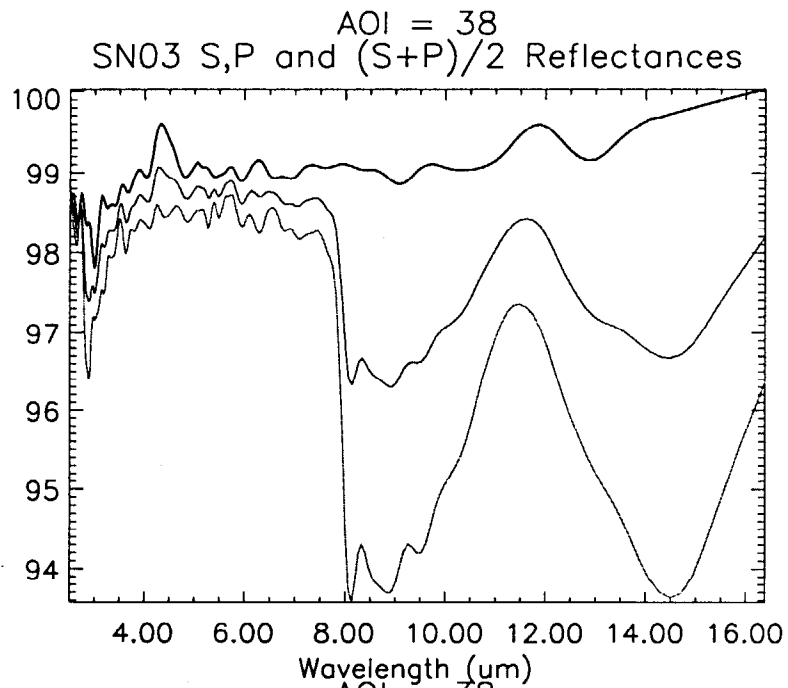
AOI = 10
SN08 S,P and (S+P)/2 Reflectances



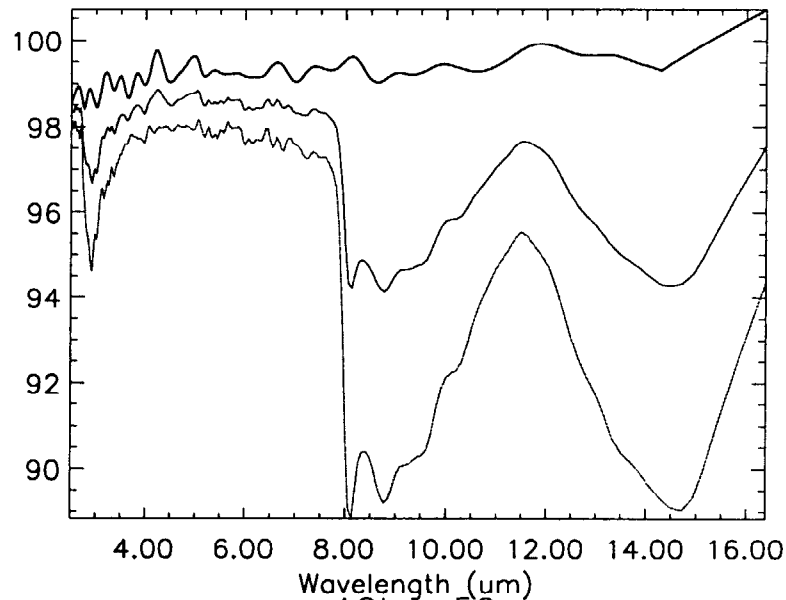
AOI = 10
SN16 S,P and (S+P)/2 Reflectances



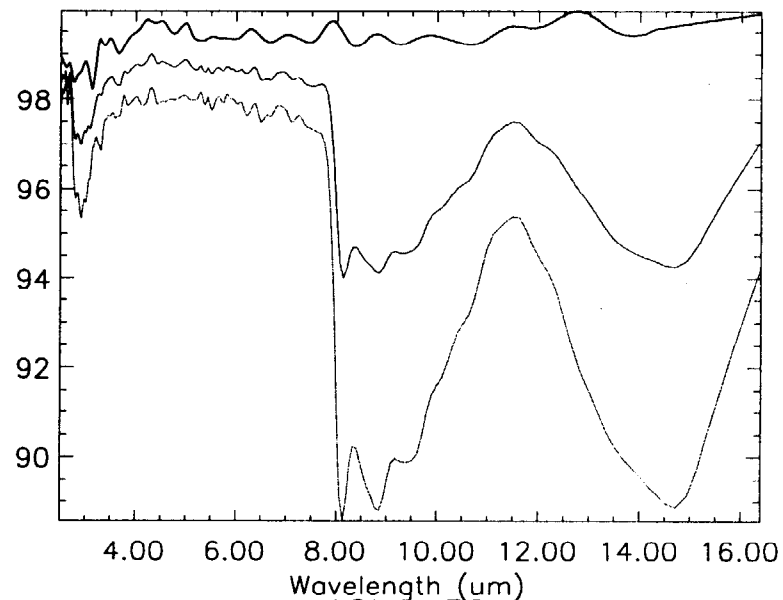




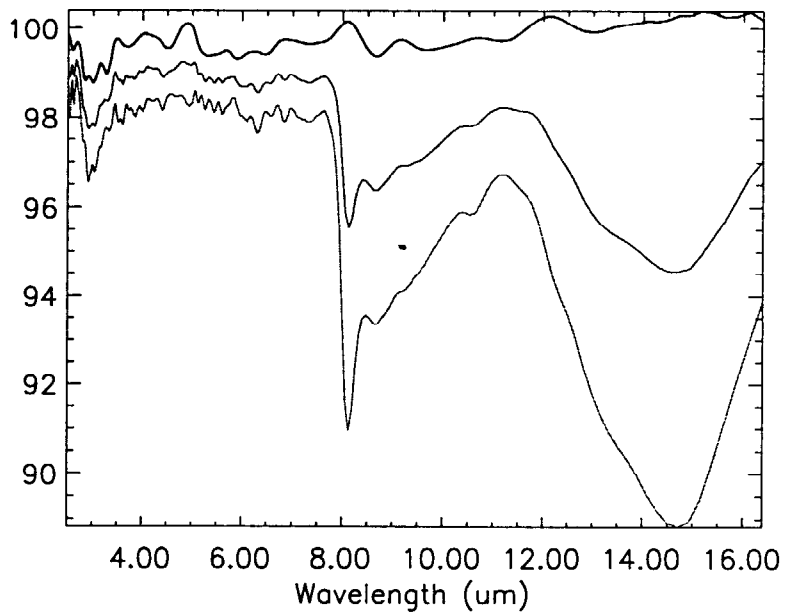
AOI = 50
SN03 S,P and (S+P)/2 Reflectances



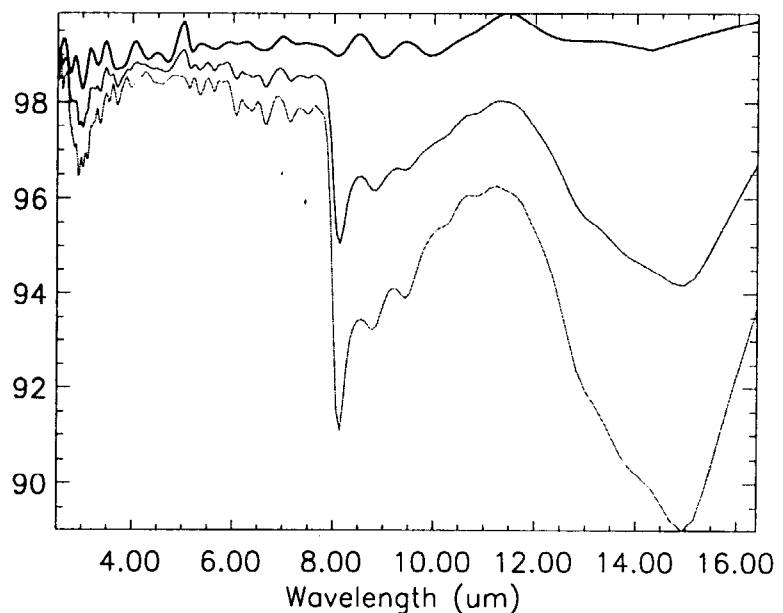
AOI = 50
SN04 S,P and (S+P)/2 Reflectances

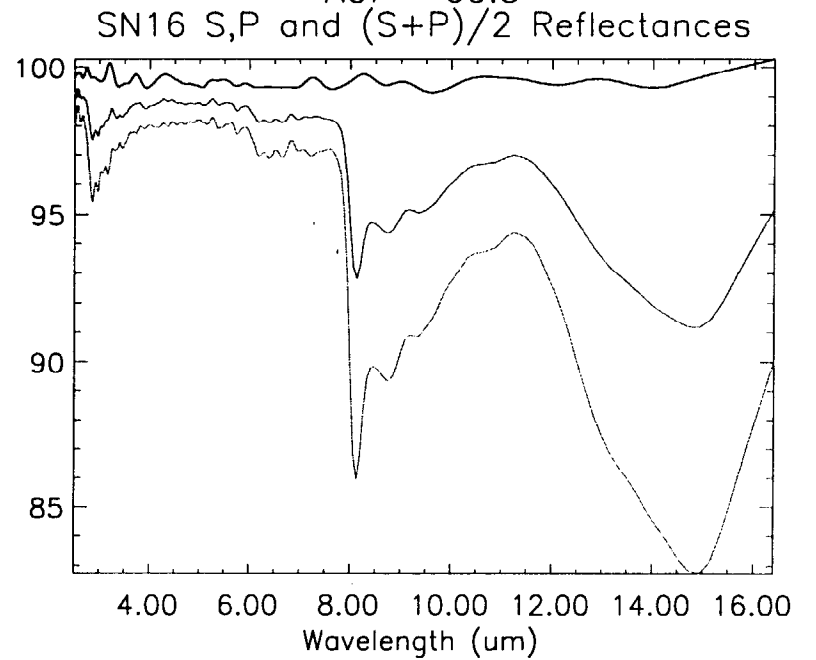
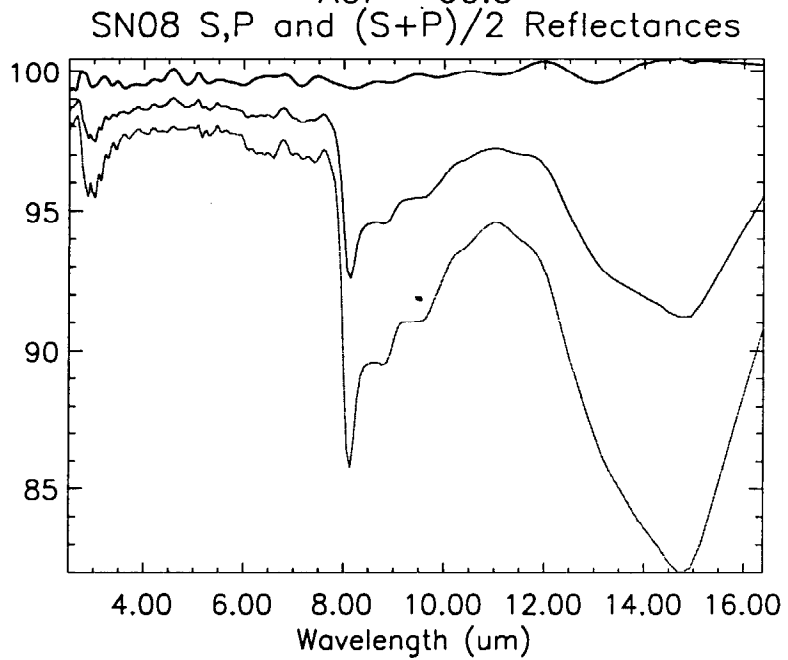
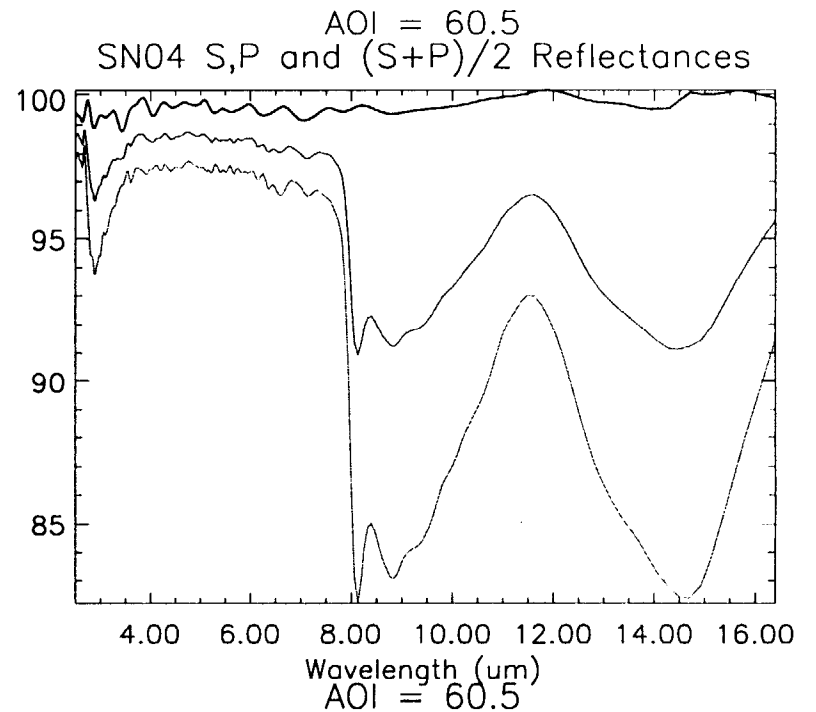
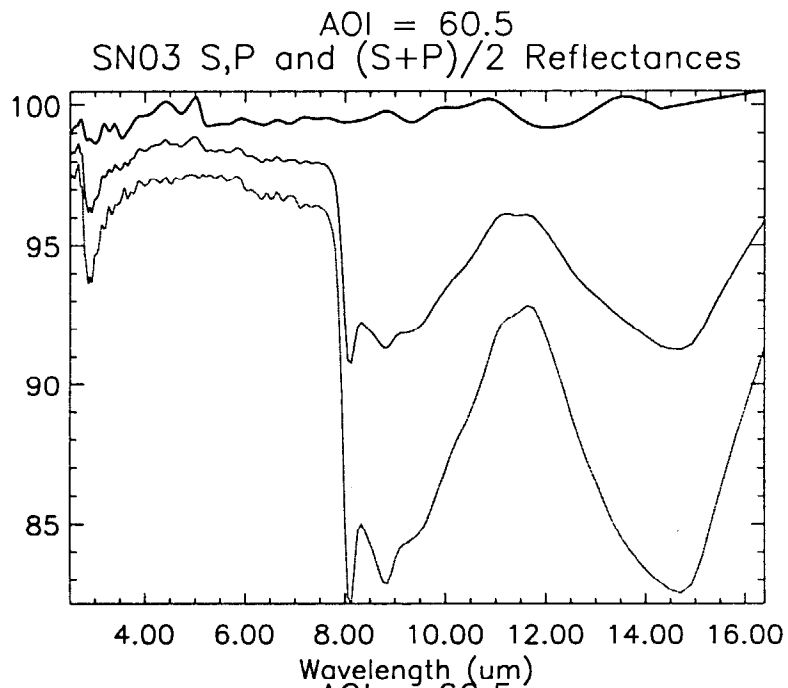


AOI = 50
SN08 S,P and (S+P)/2 Reflectances

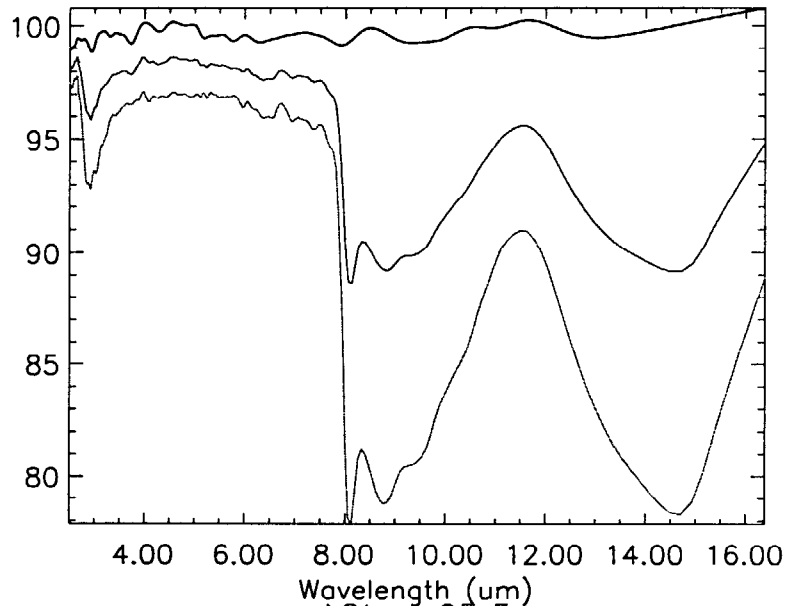


AOI = 50
SN16 S,P and (S+P)/2 Reflectances

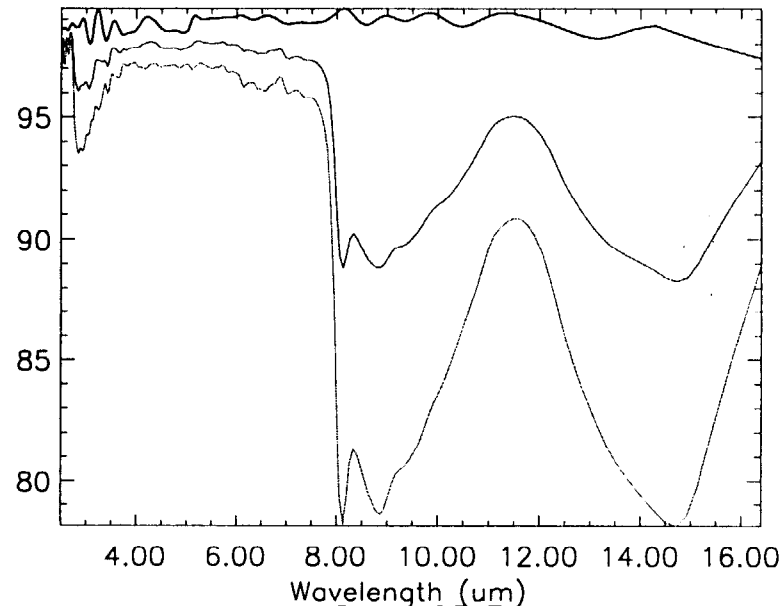




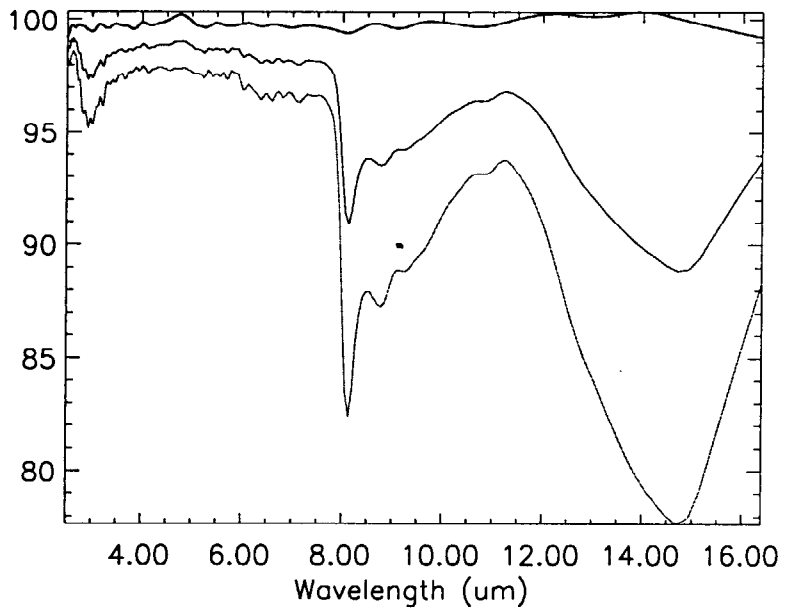
AOI = 65.5
SN03 S,P and (S+P)/2 Reflectances



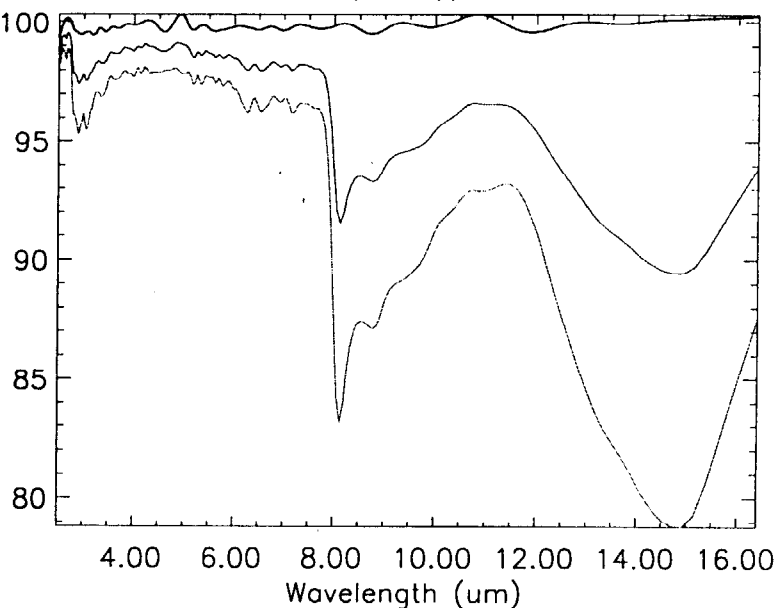
AOI = 65.5
SN04 S,P and (S+P)/2 Reflectances



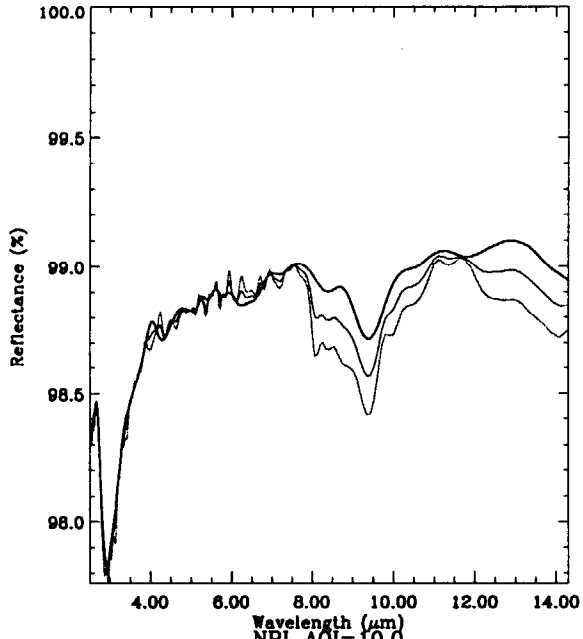
AOI = 65.5
SN08 S,P and (S+P)/2 Reflectances



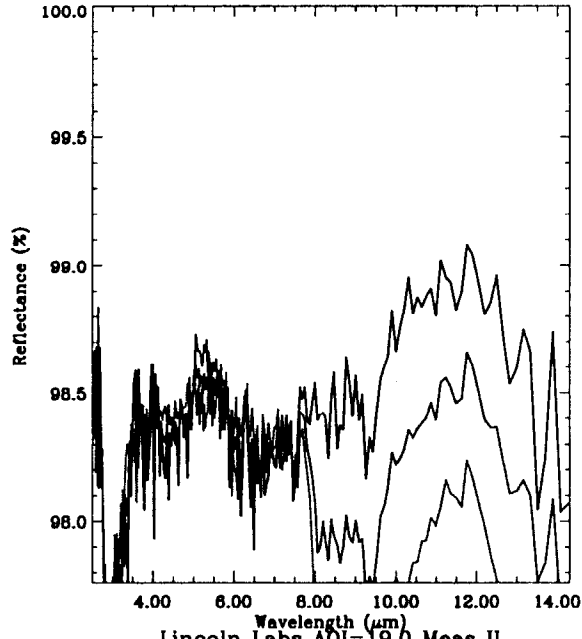
AOI = 65.5
SN16 S,P and (S+P)/2 Reflectances



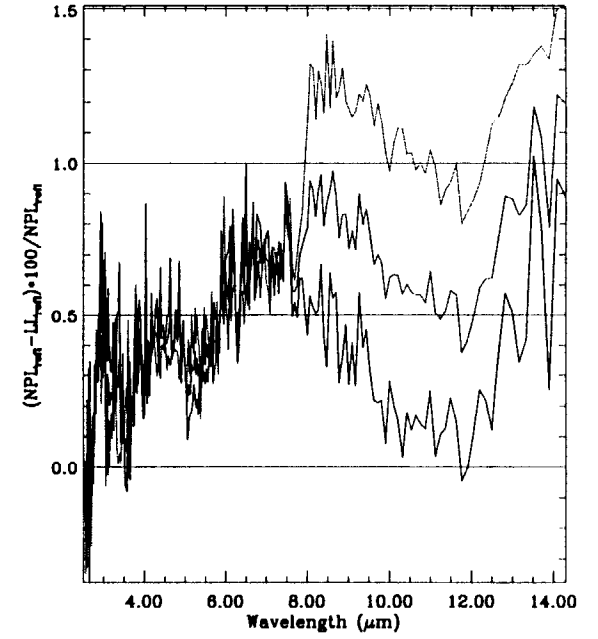
NPL AOI=10.0
SN03 S,P and (S+P)/2 Reflectances



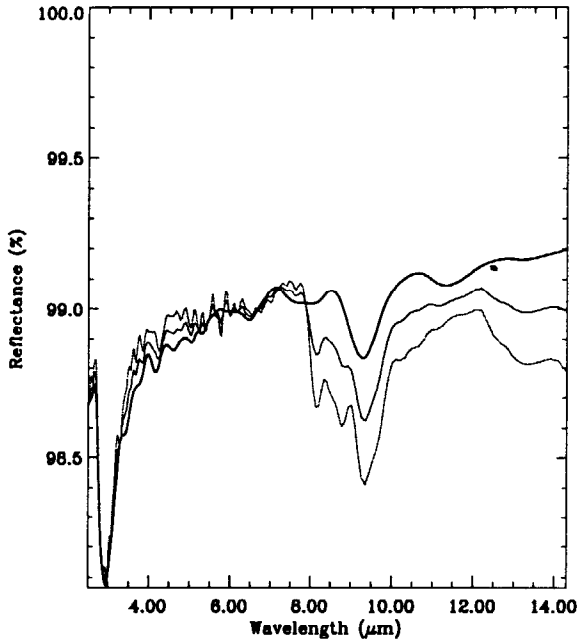
Lincoln Labs AOI=19.0 Meas II
SN03 S,P and (S+P)/2 Reflectances



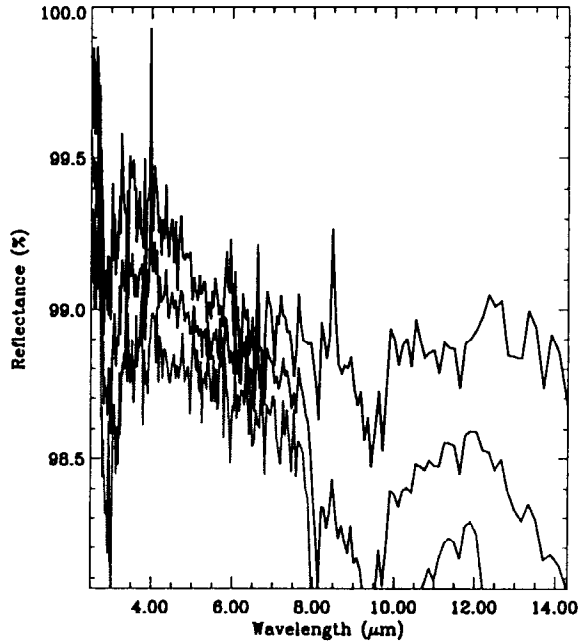
Percent Difference of LL and NPL Ave Reflectances



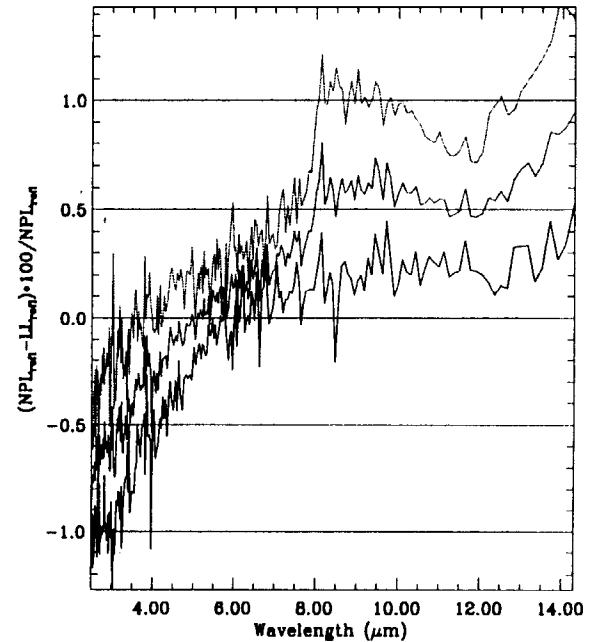
NPL AOI=10.0
SN04 S,P and (S+P)/2 Reflectances

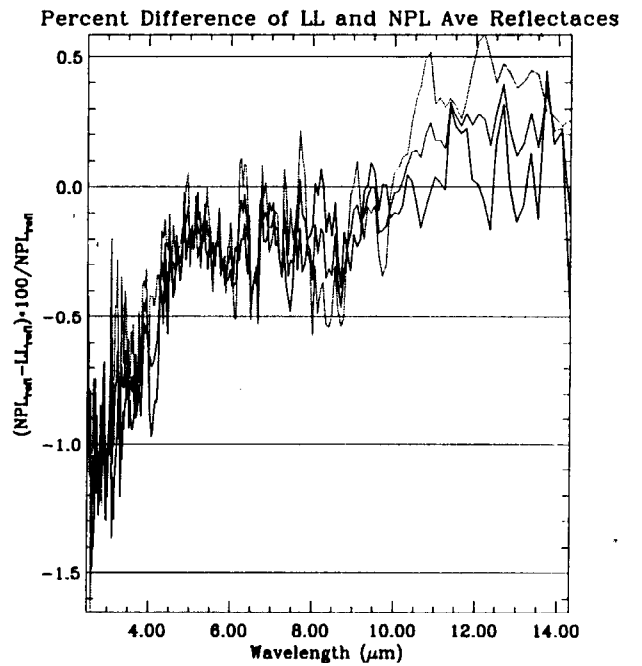
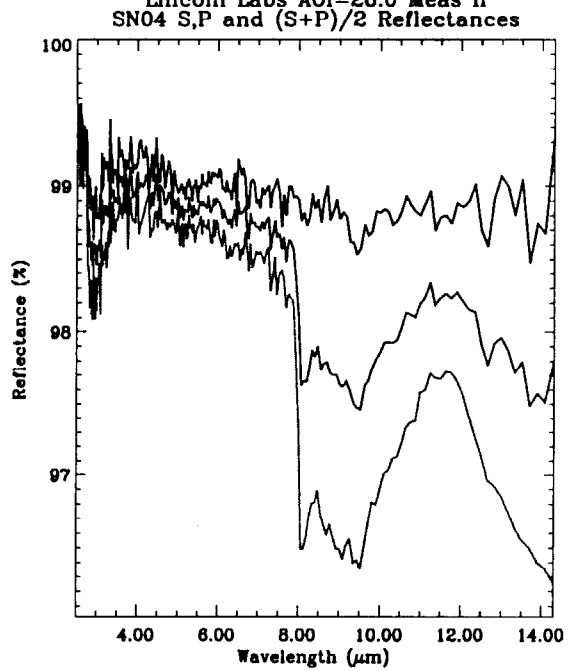
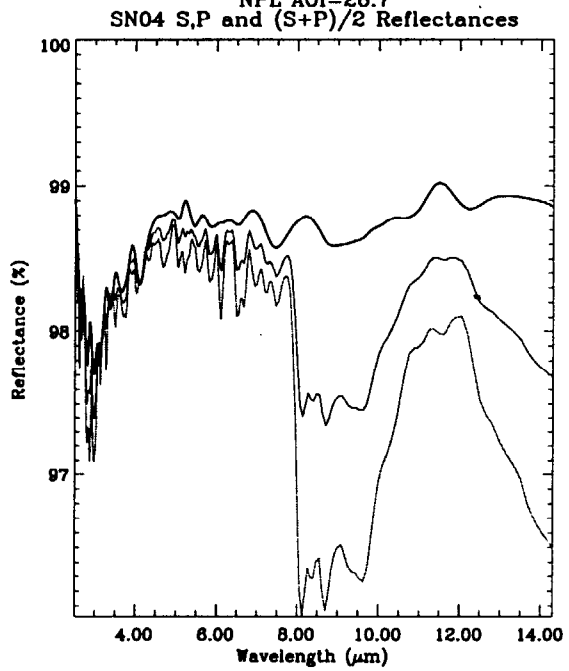
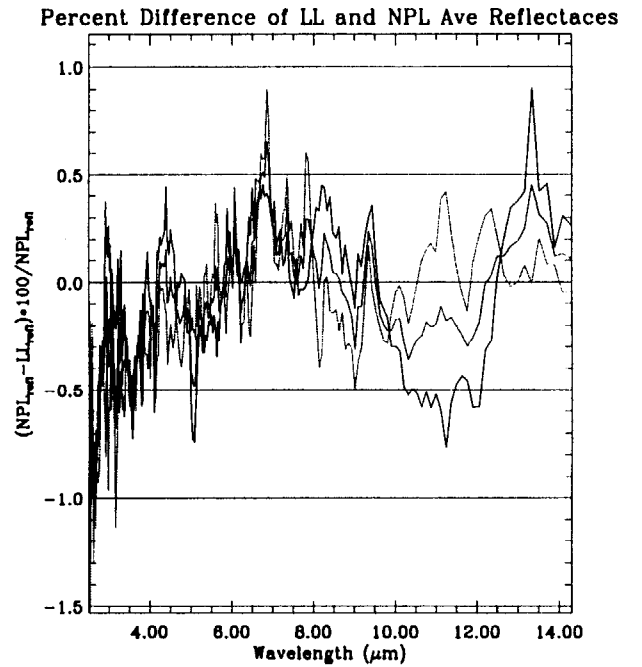
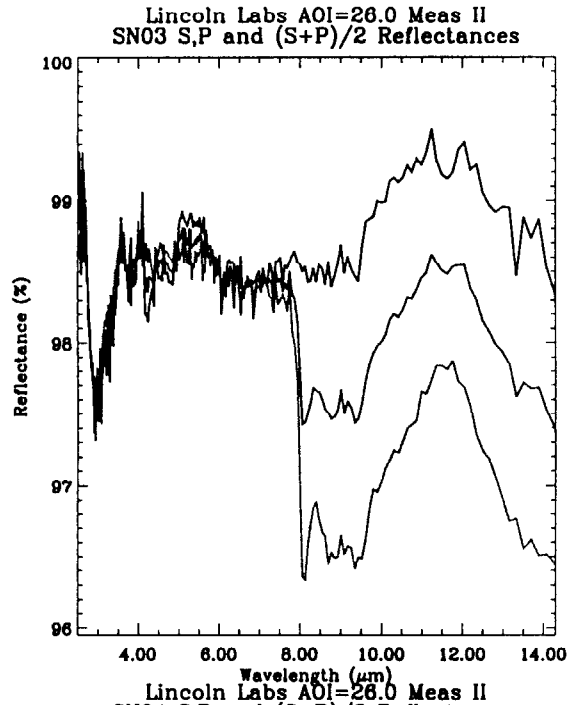
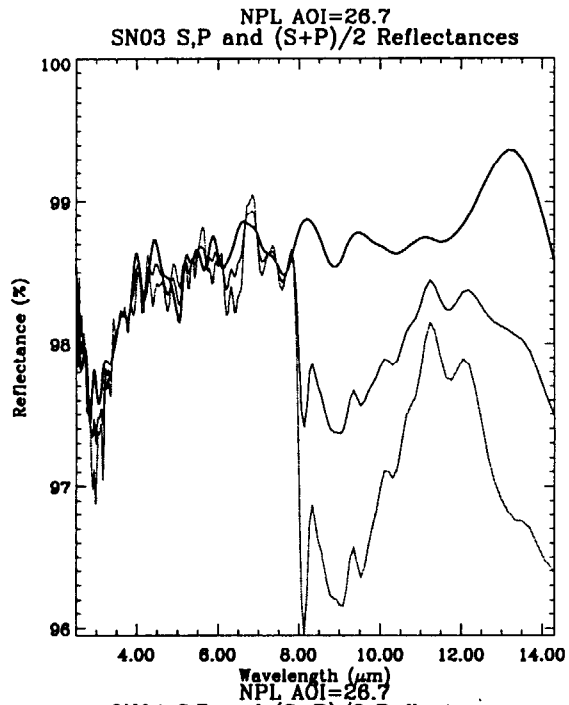


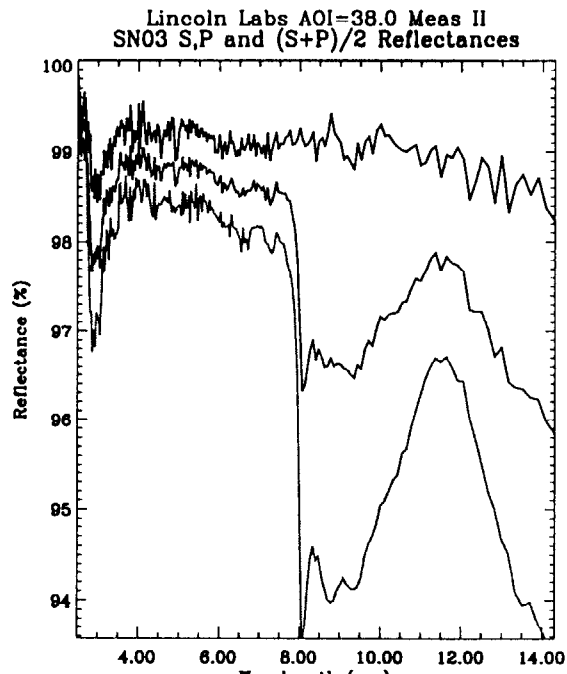
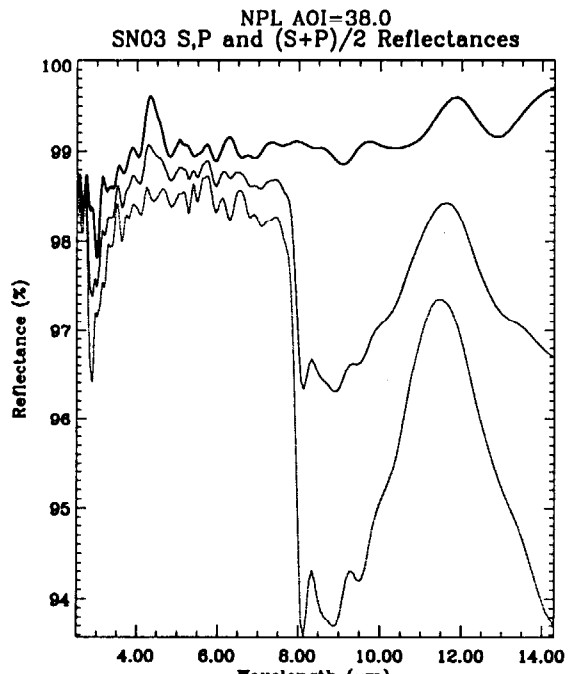
Lincoln Labs AOI=19.0 Meas II
SN04 S,P and (S+P)/2 Reflectances



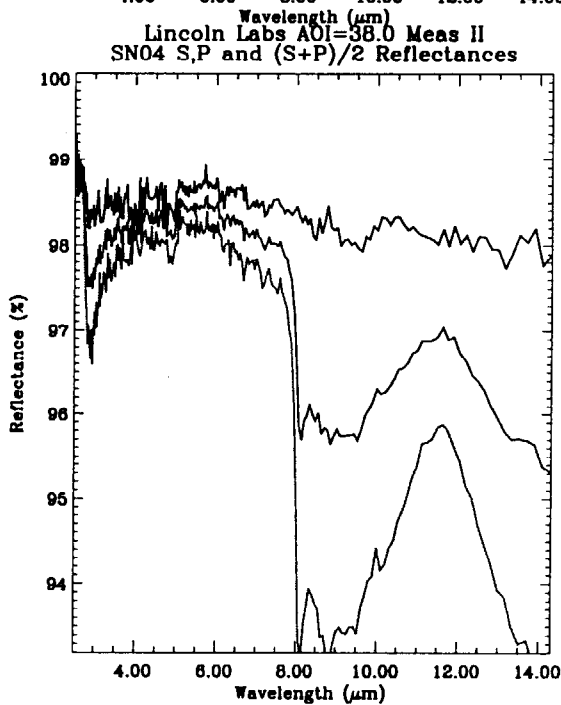
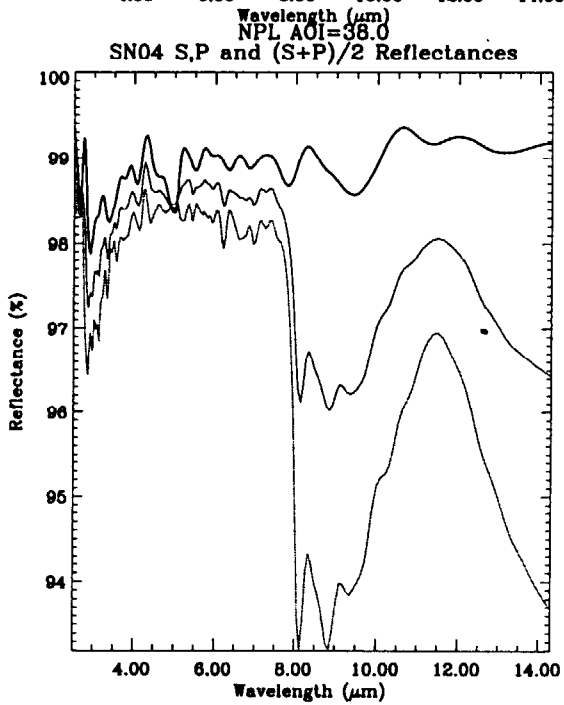
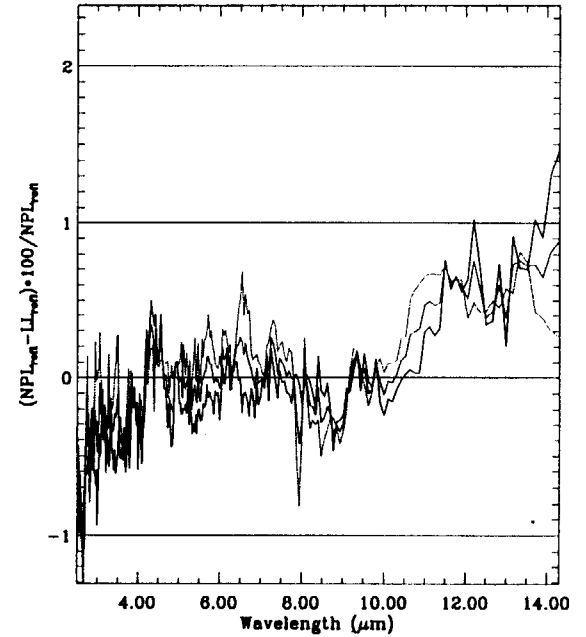
Percent Difference of LL and NPL Ave Reflectances



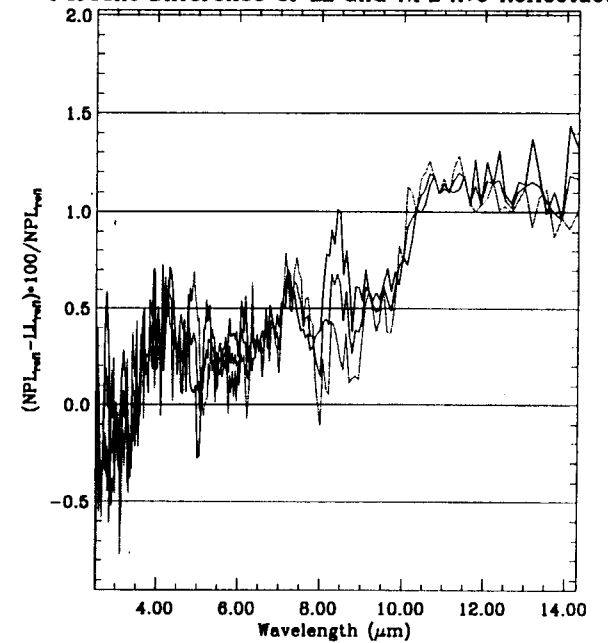


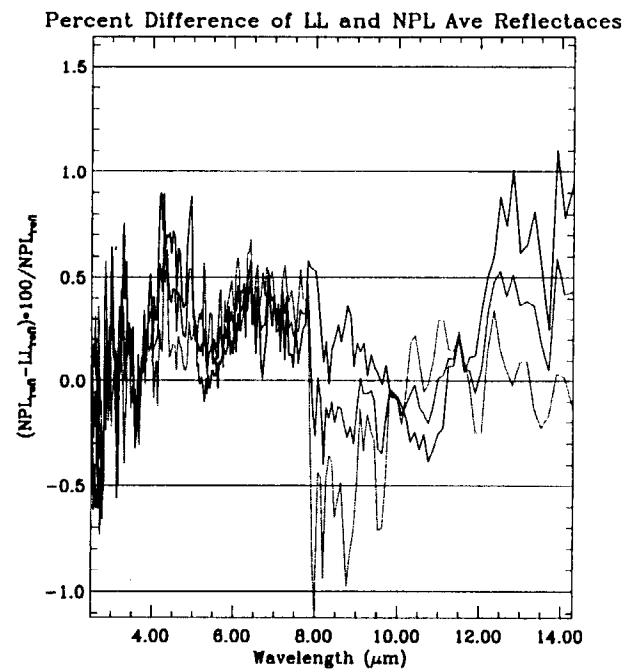
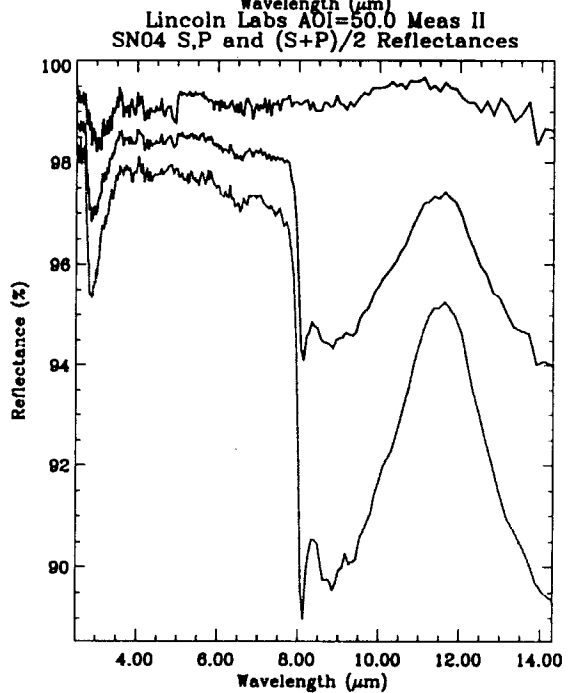
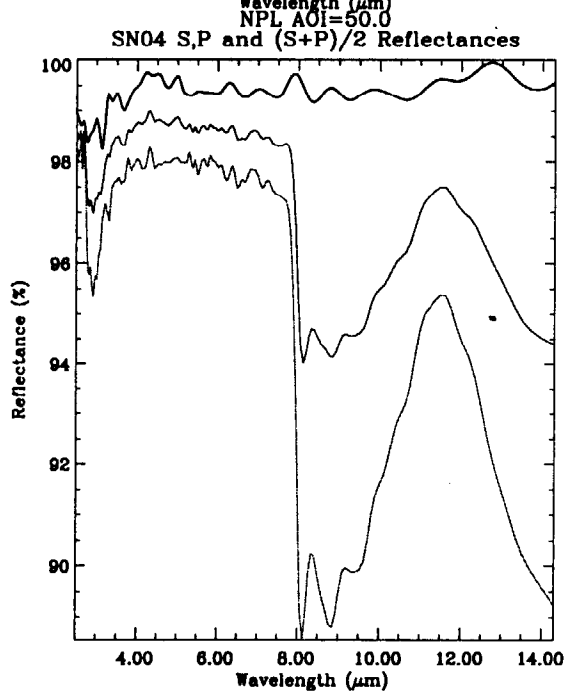
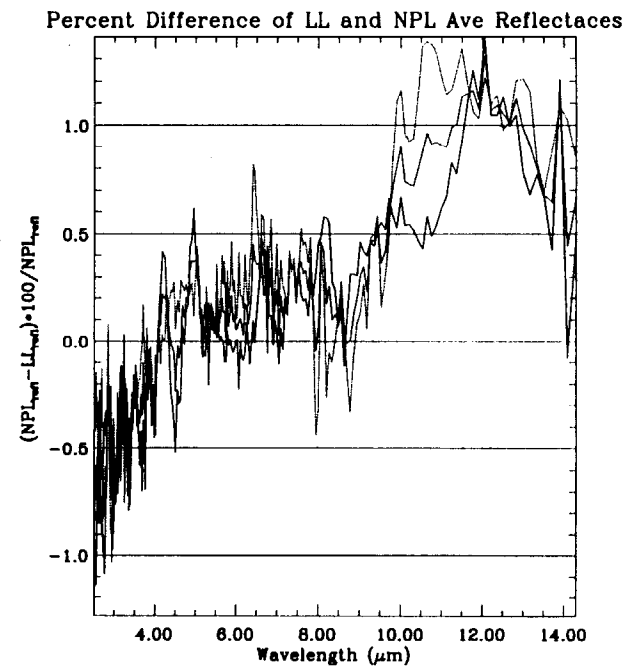
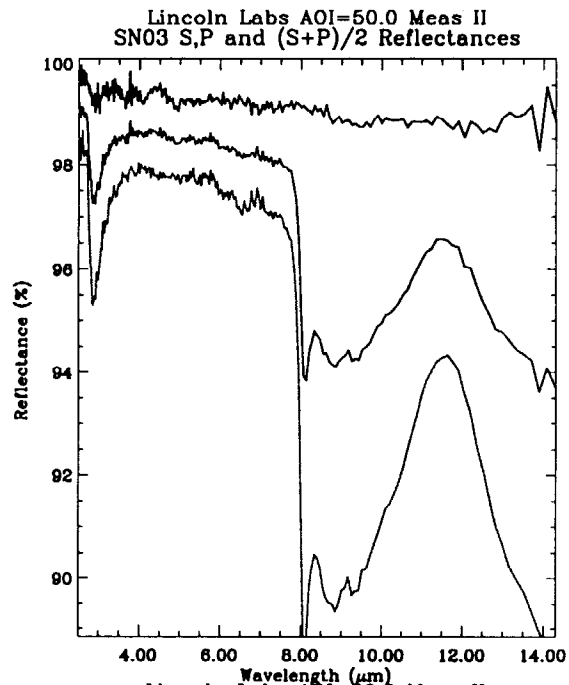
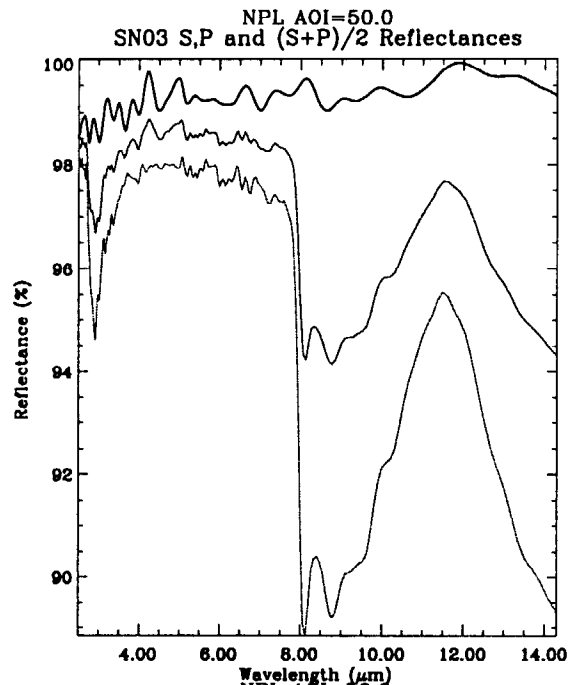


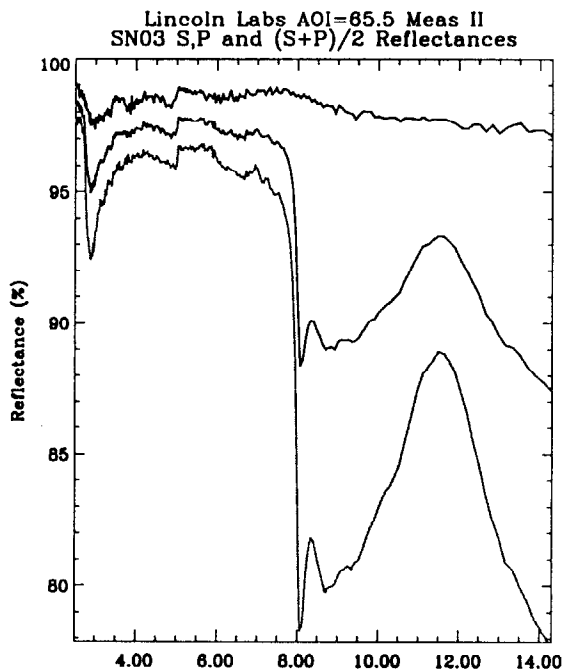
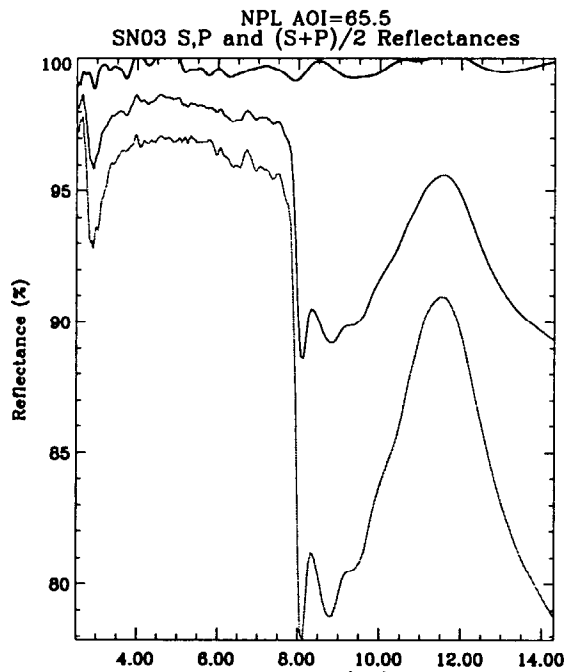
Percent Difference of LL and NPL Ave Reflectances



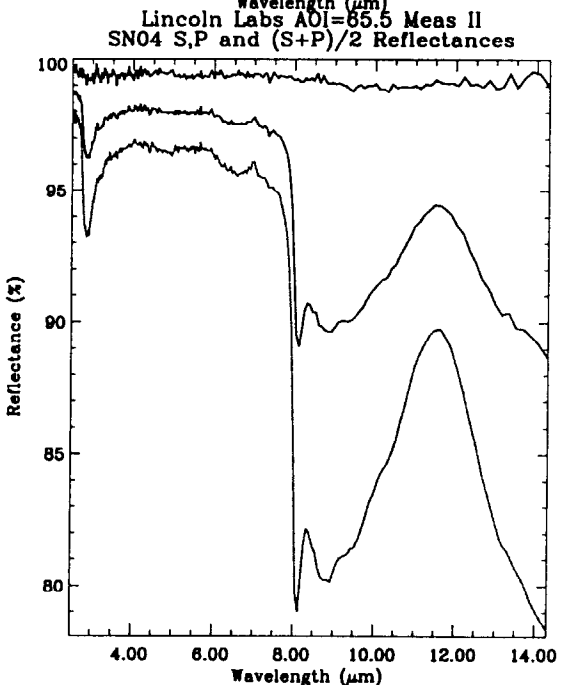
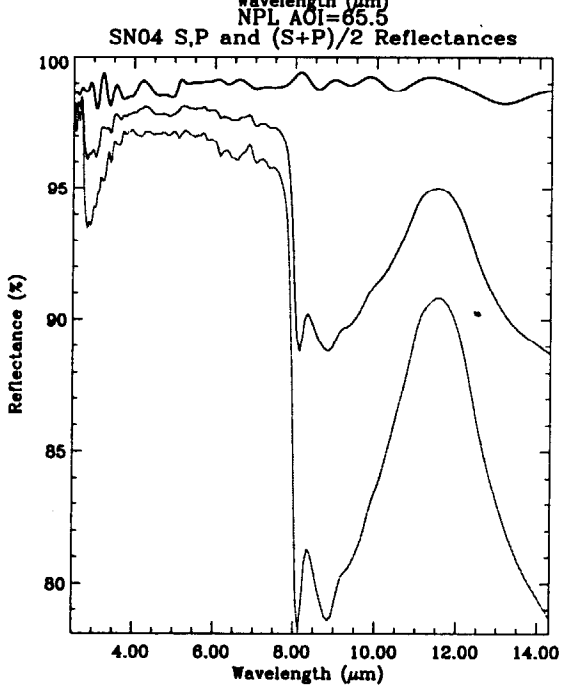
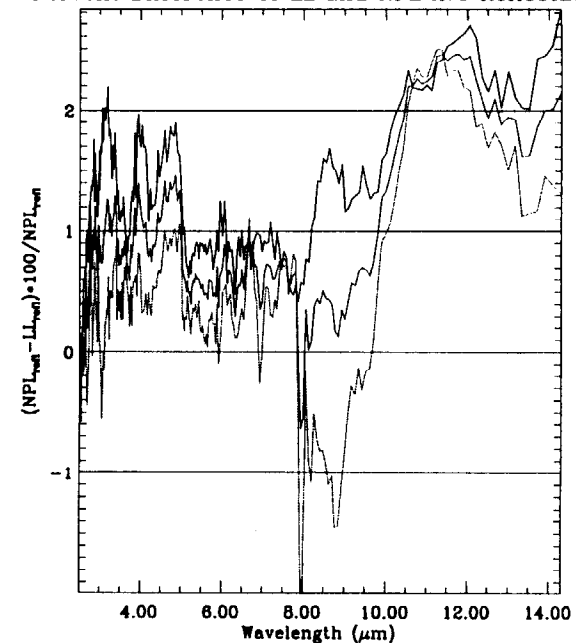
Percent Difference of LL and NPL Ave Reflectances



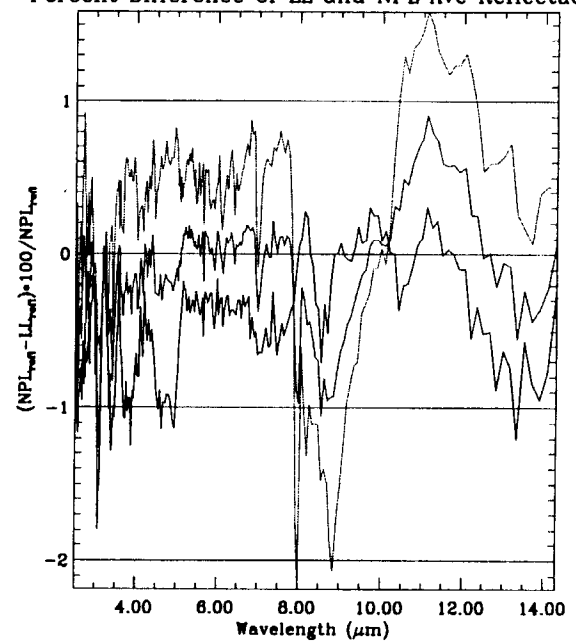


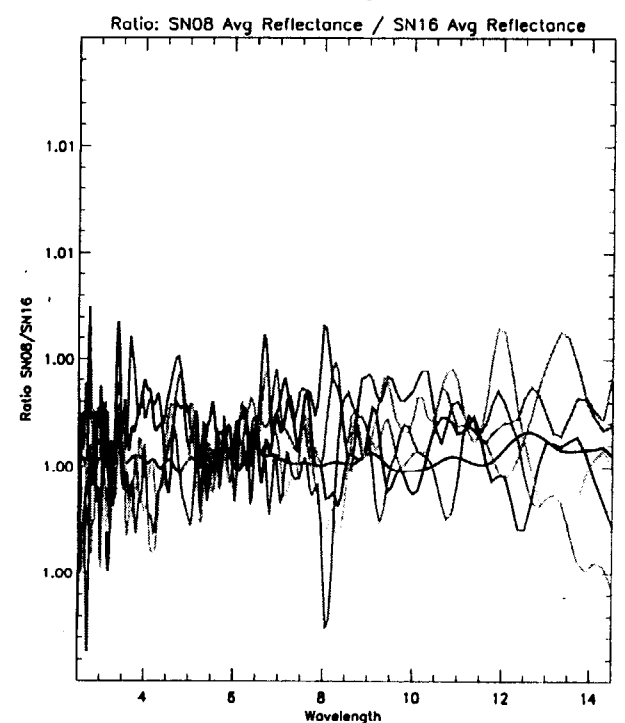
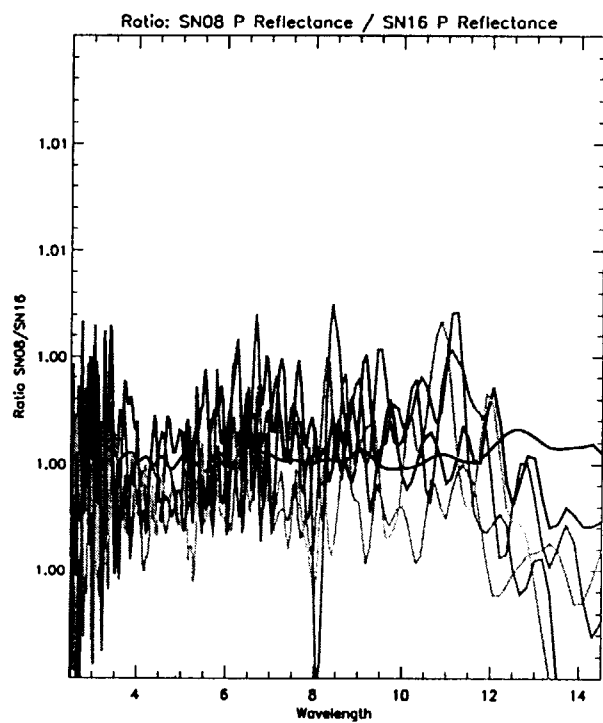
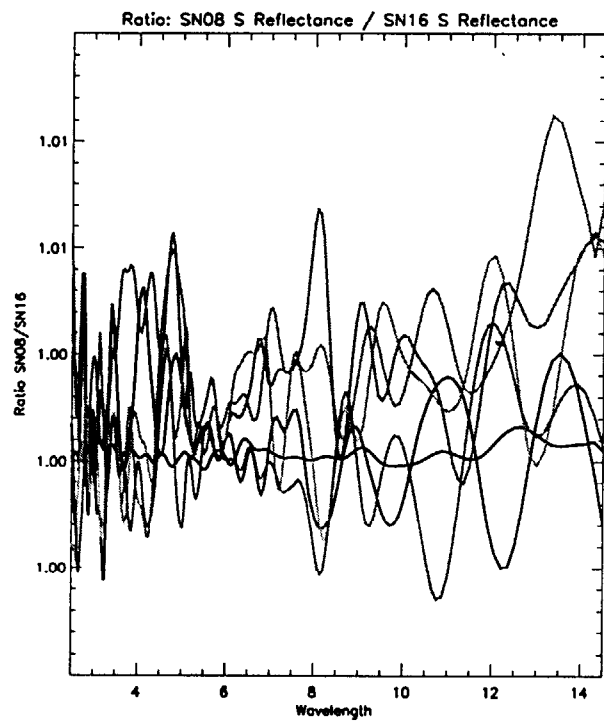
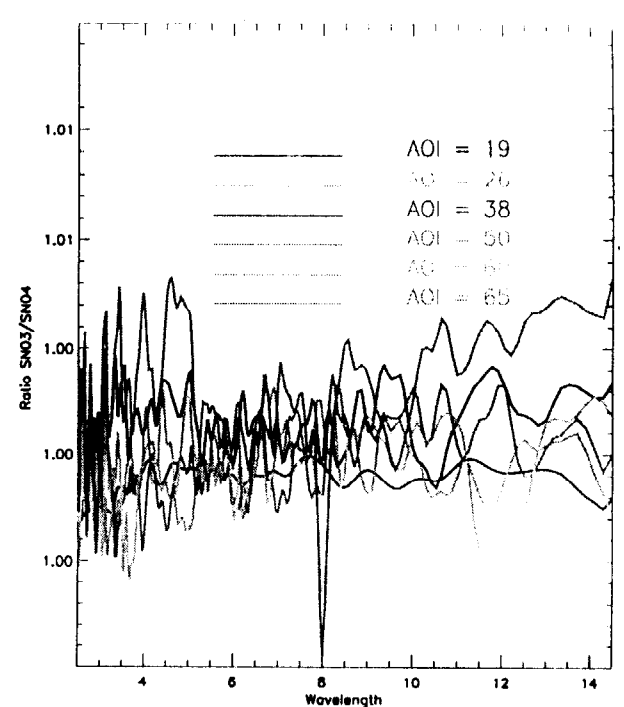
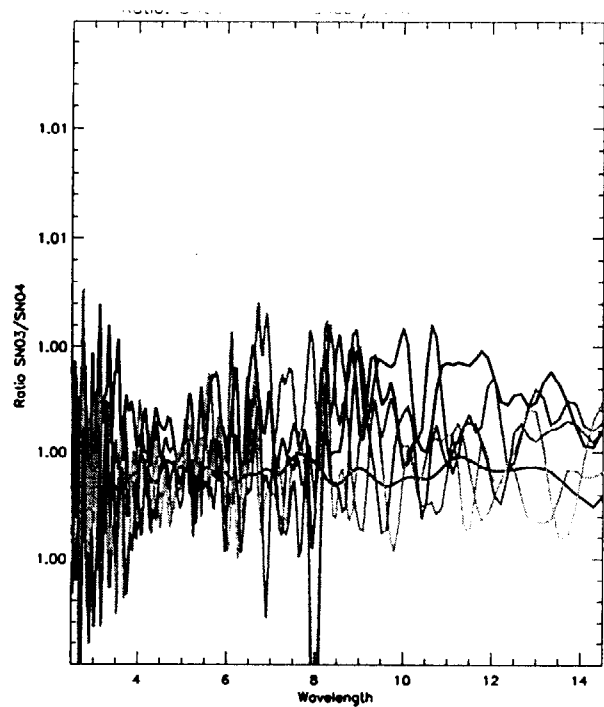
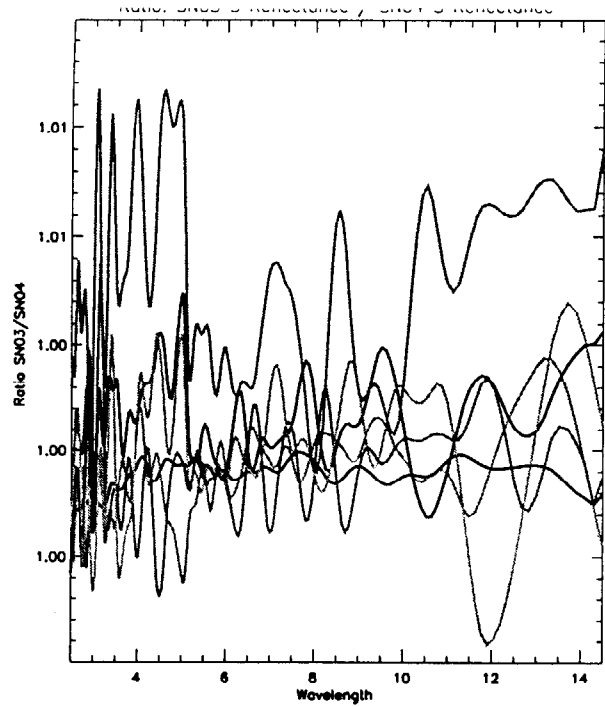


Percent Difference of LL and NPL Ave Reflectances

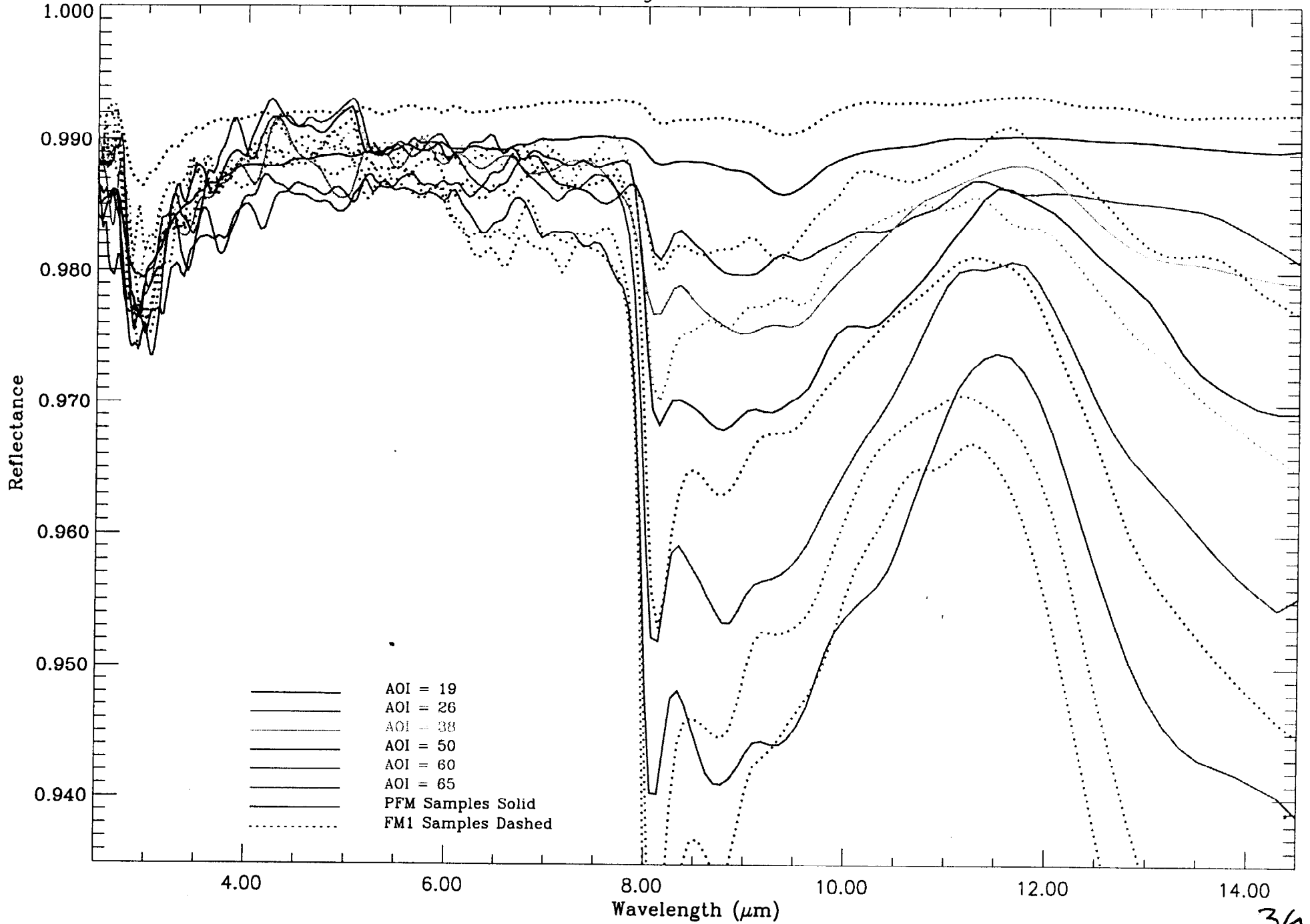


Percent Difference of LL and NPL Ave Reflectances

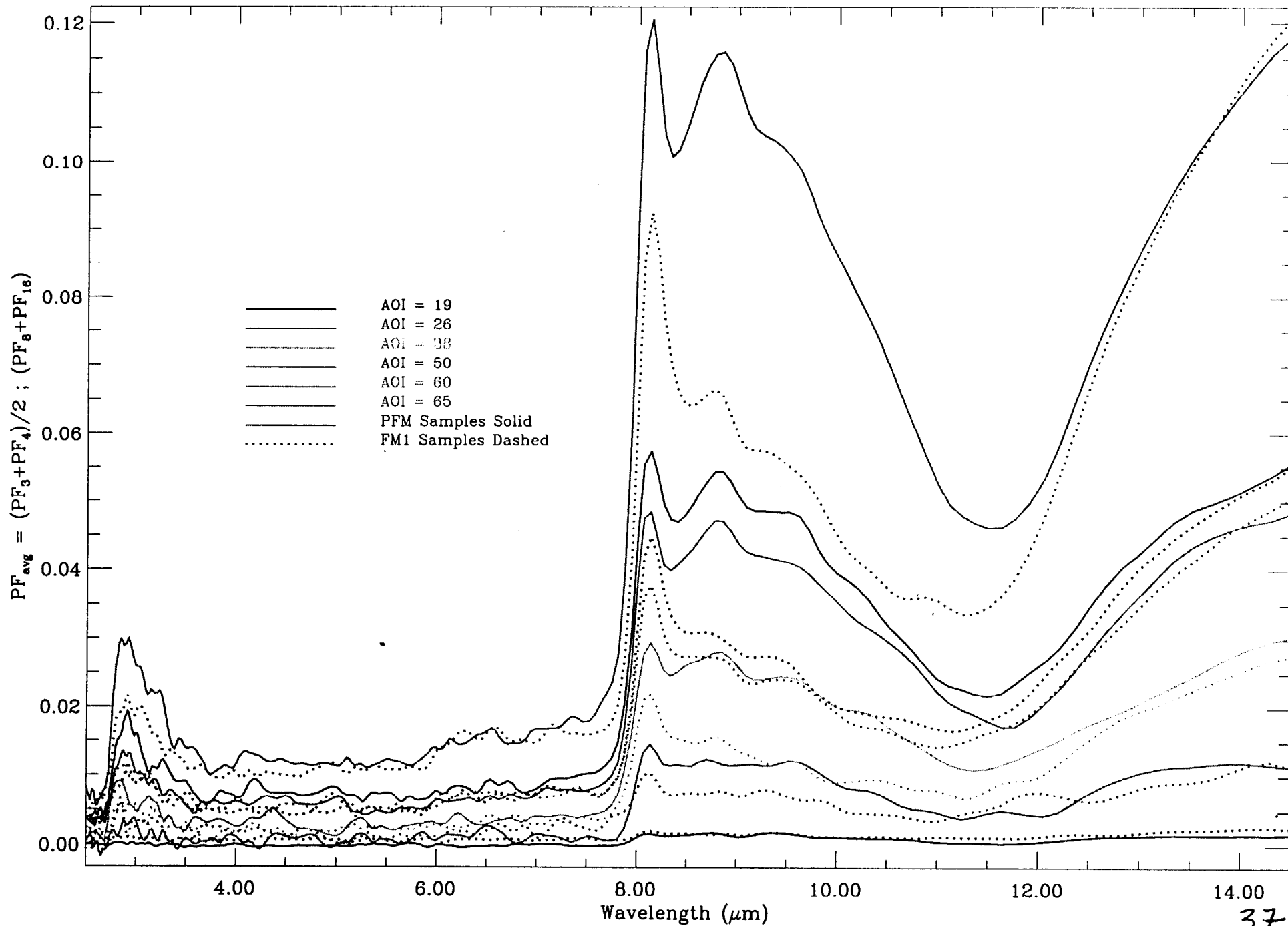




NPL Average Reflectance Data

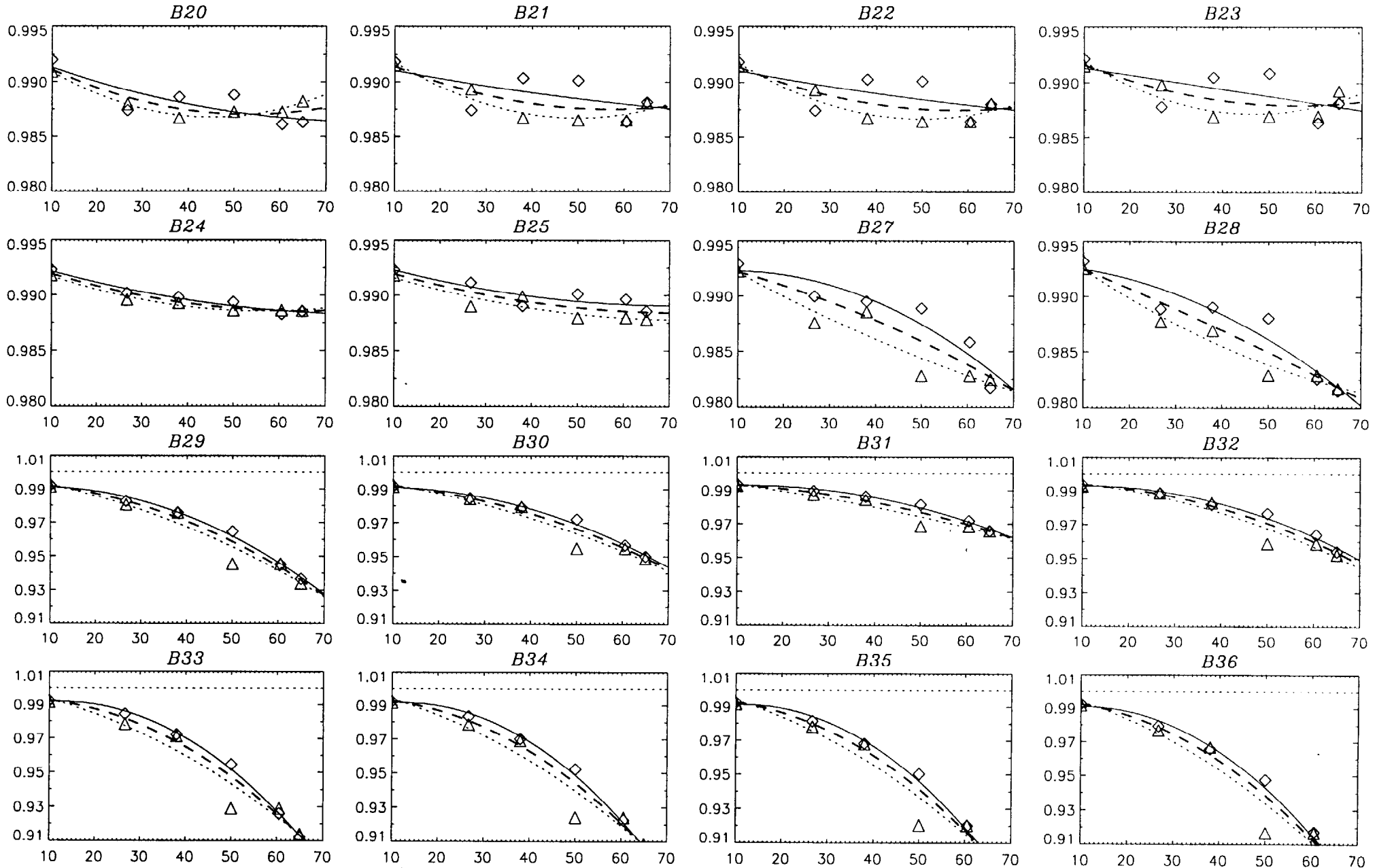


FM1 and PFM Scan Mirror Witness Sample Average
Polarization Factors from NPL Measurements



FM1 Scan Mirror Witness Sample Average Polarization Reflectances vs AOI
 (NPL Measurements of Witness Samples SN08 and SN16 with Quadratic Fit)

◇——◇ SN08 △·····△ SN16 - - - - - Average of Two



Summary of Highbay RVS Measurements

Summary of Data Analysis

- Raw (not-normalized) RVS data results
 - 16 bands, 10 channels*, 3 RVS data collects (310K_1, 320K_2, and 320K_3)
 - data points averaged over 40 scans and ~50 frames†, with 1-sigma error bars
 - data collected at 10 AOIs; repeated measurements at 4 AOIs
 - corrected for drift (via b1 changes), and $T_{svs} \neq T_{sm}$ effect
- Normalized RVS fitted results
 - raw RVS data averaged over: 40 scans; 50 BCS frames† (with a few exceptions regarding # of frames to assure all data in BCS sweet spot)
 - averaged data preliminarily fitted to a Normalized Best-Fit Quadratic (NBFQ) function on channel-by-channel basis
 - RVS data normalized to average response (40 scans; 50 BCS frames†) at BCS AOI=10.75°

* B22, channels 1-7, and B36, Channel 6 deleted due to obvious saturation/noise problems

† some exceptions to 50 BCS frames depending on location of BCS sweet spot on band-by-band basis

Summary of Data Analysis

(continued)

- Normalized Best Fit Quadratic chart series provided:
 - 1) Normalized RVS vs AOI - channel dependent (averaged over 40 scans and 50 BCS frames[†]; for 16 bands and 3 data collects)
 - 2) Normalized RVS vs AOI - data collect dependent (averaged over 40 scans, 50 BCS frames[†] and 10 channels^{*}; for 16 bands)
 - 3) Normalized RVS vs AOI - grand average (averaged over 40 scans, 50 BCS frames[†], 10 channels^{*} and 3 datasets; for 16 bands)

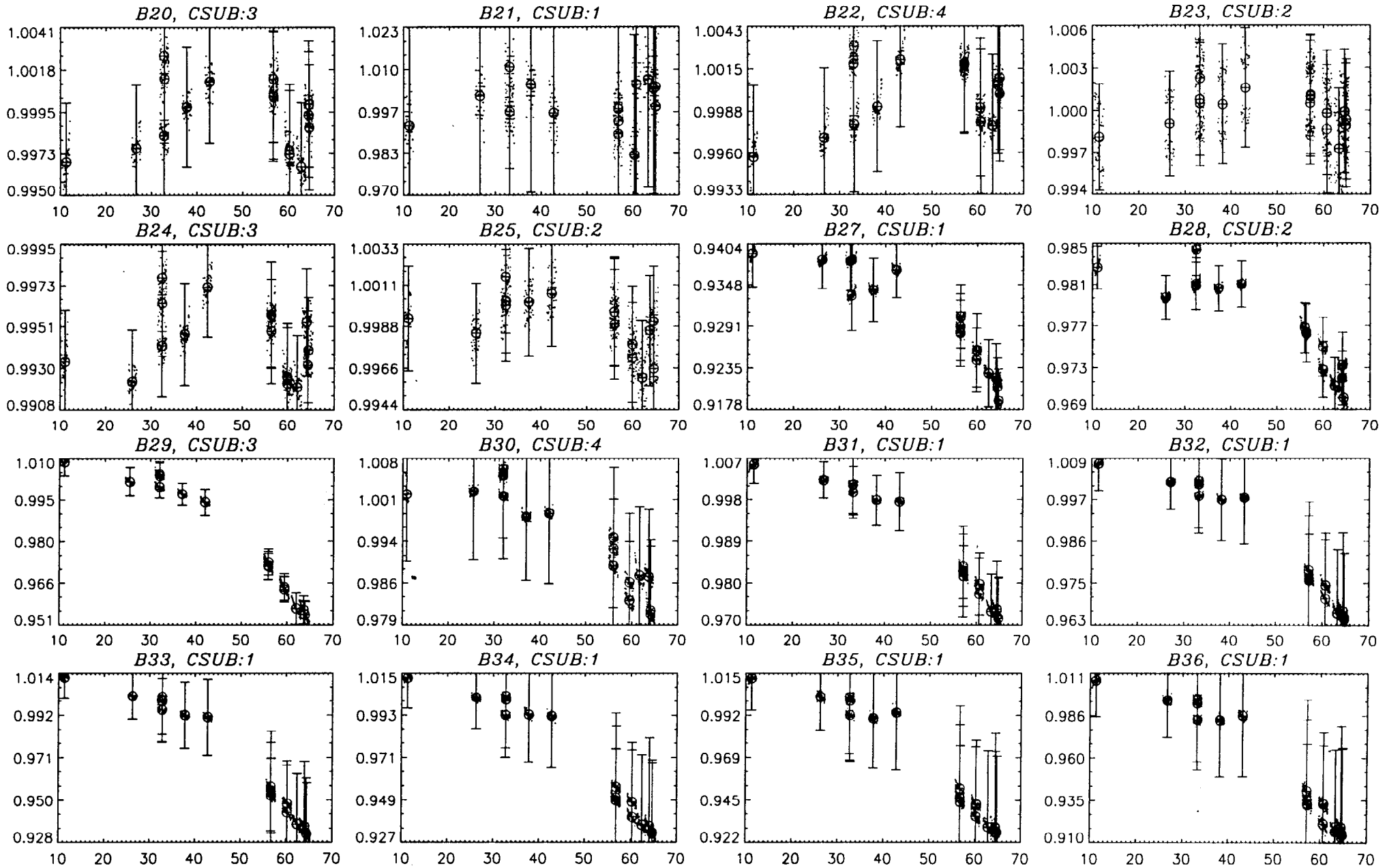
Channel-by-Channel Highbay RVS Raw Data Results

(after correction for drift via reference to OBC blackbody)

- Channel 8 charts processed w/ $T_{sm}=T_{svs}$
- Channel 8 chart for 320K_3 w/ $T_{sm}\neq T_{svs}$
- Channel 8 chart comparing $T_{sm}=T_{svs}$ results with $T_{sm}\neq T_{svs}$ correction

Channel 8 Raw $\langle RVS \rangle_{40 \text{ scans}}$ vs AOI for 50 BCS Frames

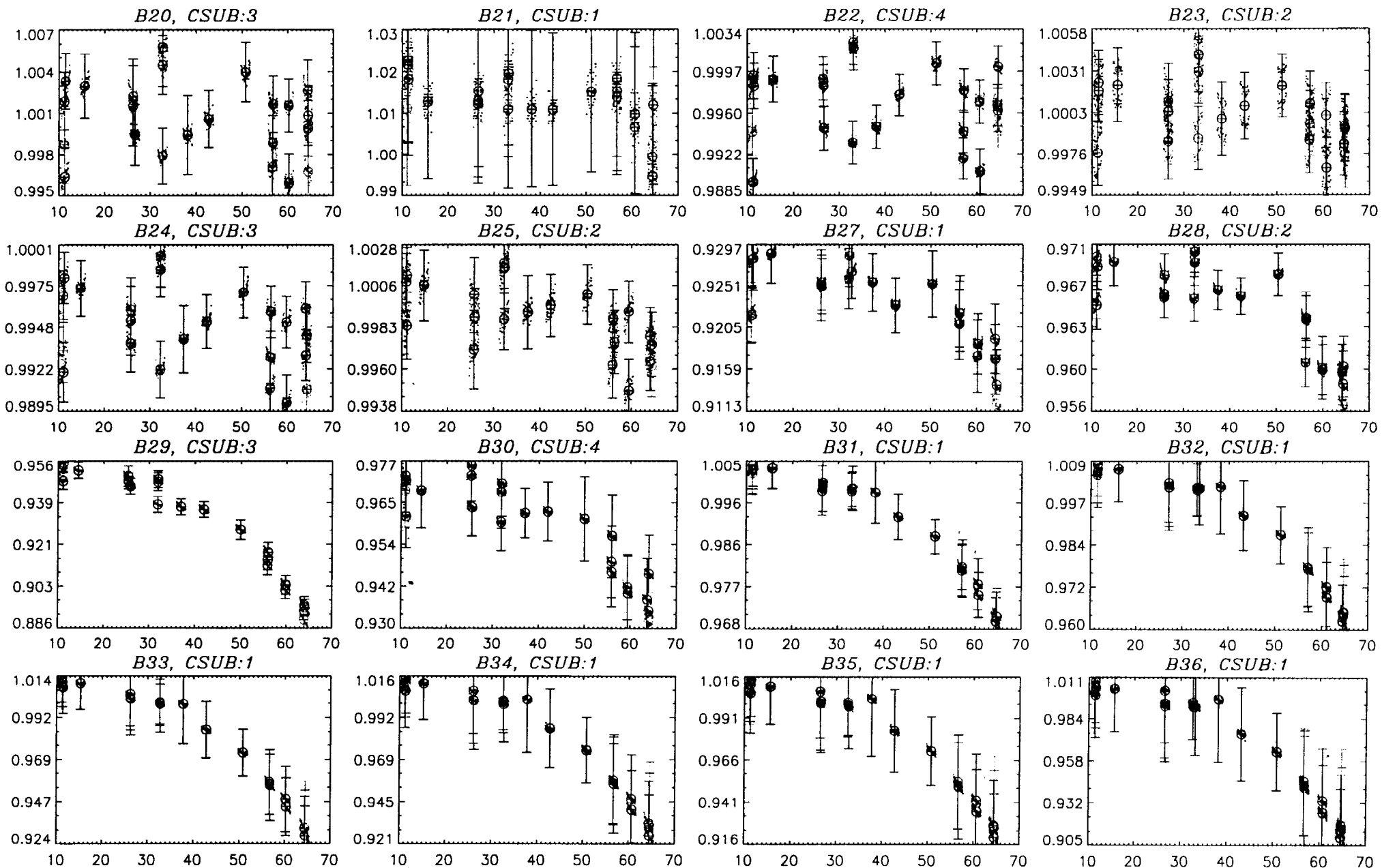
(310K_1 Data Set; Mirror A; w/50frame \times 40scan Average and 1- σ Error Bars; Optimum CSUB; Repeat AOIs in Color)



Instrument & Source Drift Corrected via OBC b1 (1st order); $T_{SM} \neq T_{SVS}$ Term Excluded)

Channel 8 Raw $\langle RVS \rangle_{40 \text{ scans}}$ vs AOI for 50 BCS Frames

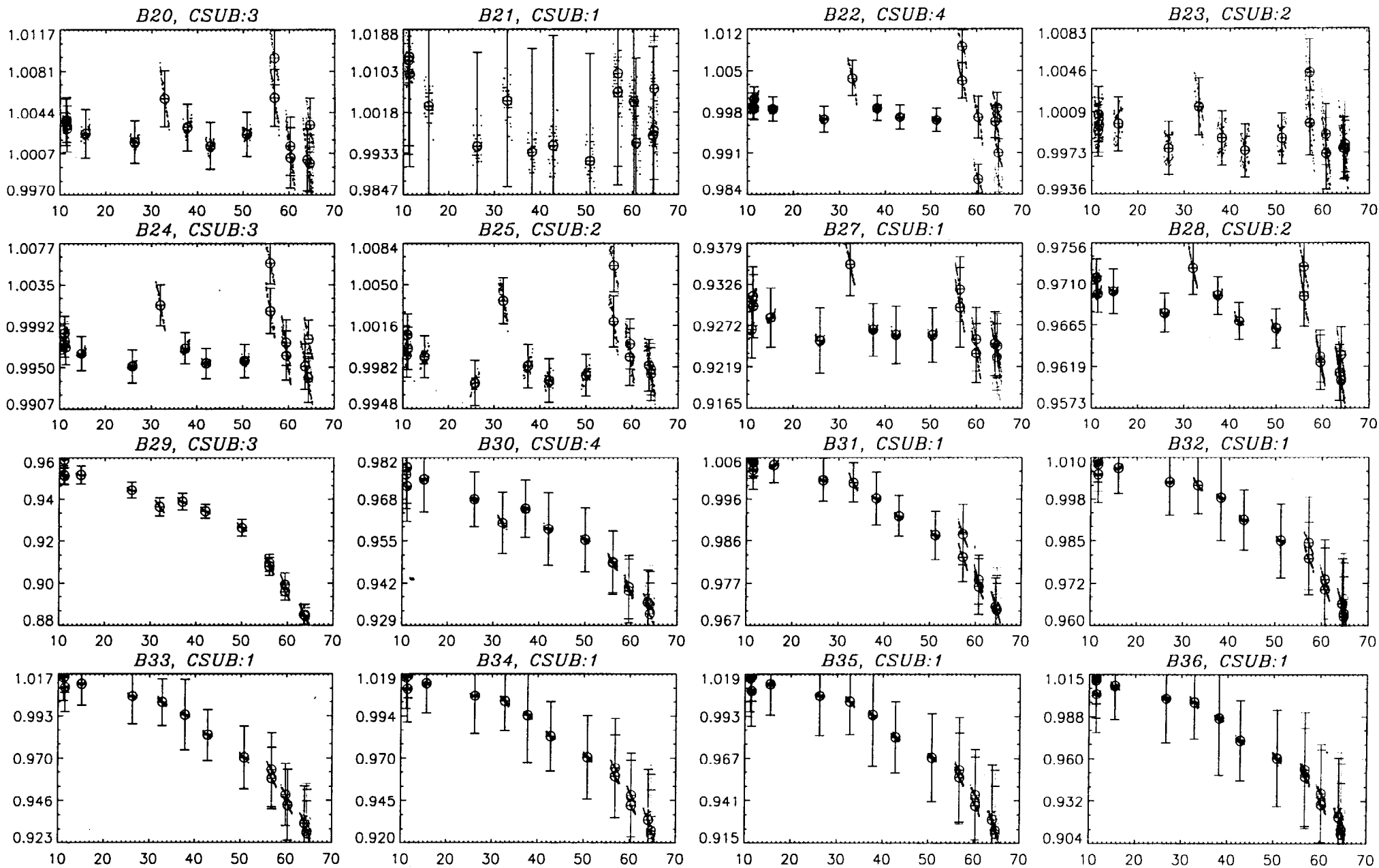
(320K_2 Data Set; Mirror A; w/50frame \times 40scan Average and $1-\sigma$ Error Bars; Optimum CSUB; Repeat AOIs in Color)



Instrument & Source Drift Corrected via OBC b1 (1st order); $T_{SM} \neq T_{SVS}$ Term Excluded)

Channel 8 Raw $\langle RVS \rangle_{40 \text{ scans}}$ vs AOI for 50 BCS Frames

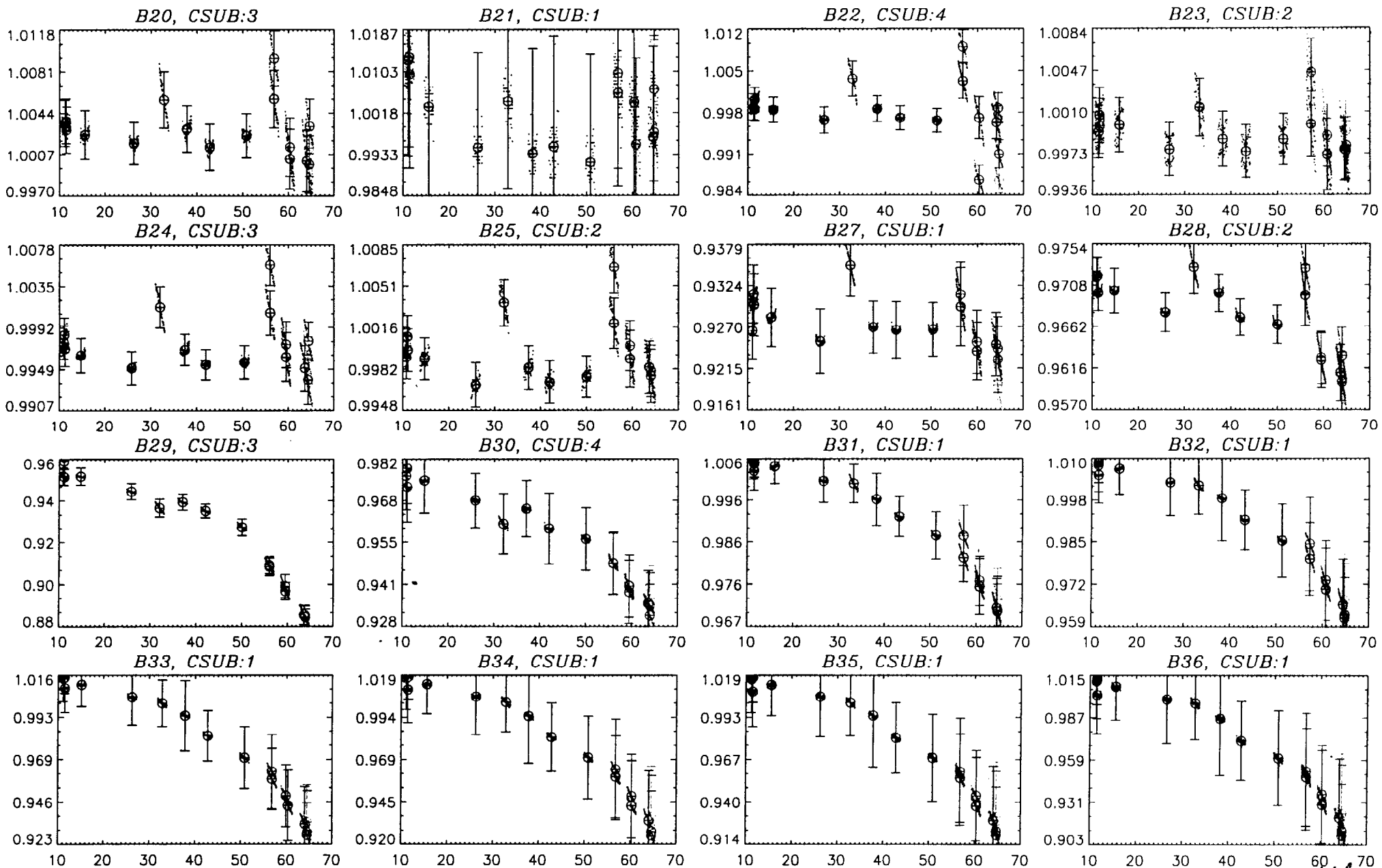
(320K_3 Data Set; Mirror A; w/50frame \times 40scan Average and 1- σ Error Bars; Optimum CSUB; Repeat AOIs in Color)



Instrument & Source Drift Corrected via OBC b1 (1st order); $T_{SM} \neq T_{SVS}$ Term Excluded)

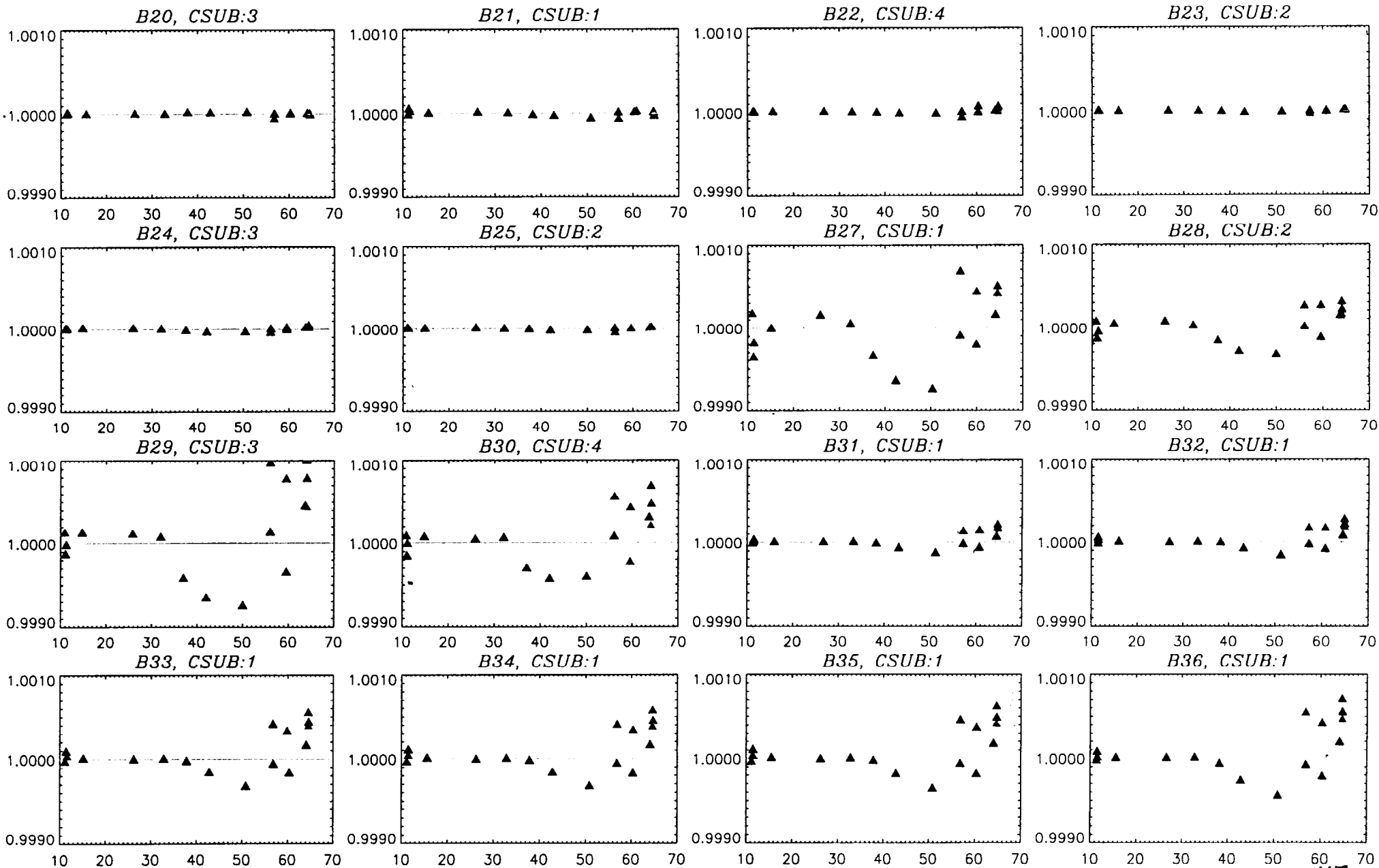
Channel 8 Raw $\langle RVS \rangle_{40 \text{ scans}}$ vs AOI for 50 BCS Frames

(320K_3 Data Set; Mirror A; w/50frame \times 40scan Average and $1-\sigma$ Error Bars; Optimum CSUB; Repeat AOIs in Color)



Note: Instrument & Source Drift Corrected via OBC b1 (1st order); $T_{SM} \neq T_{SVS}$ Term Included

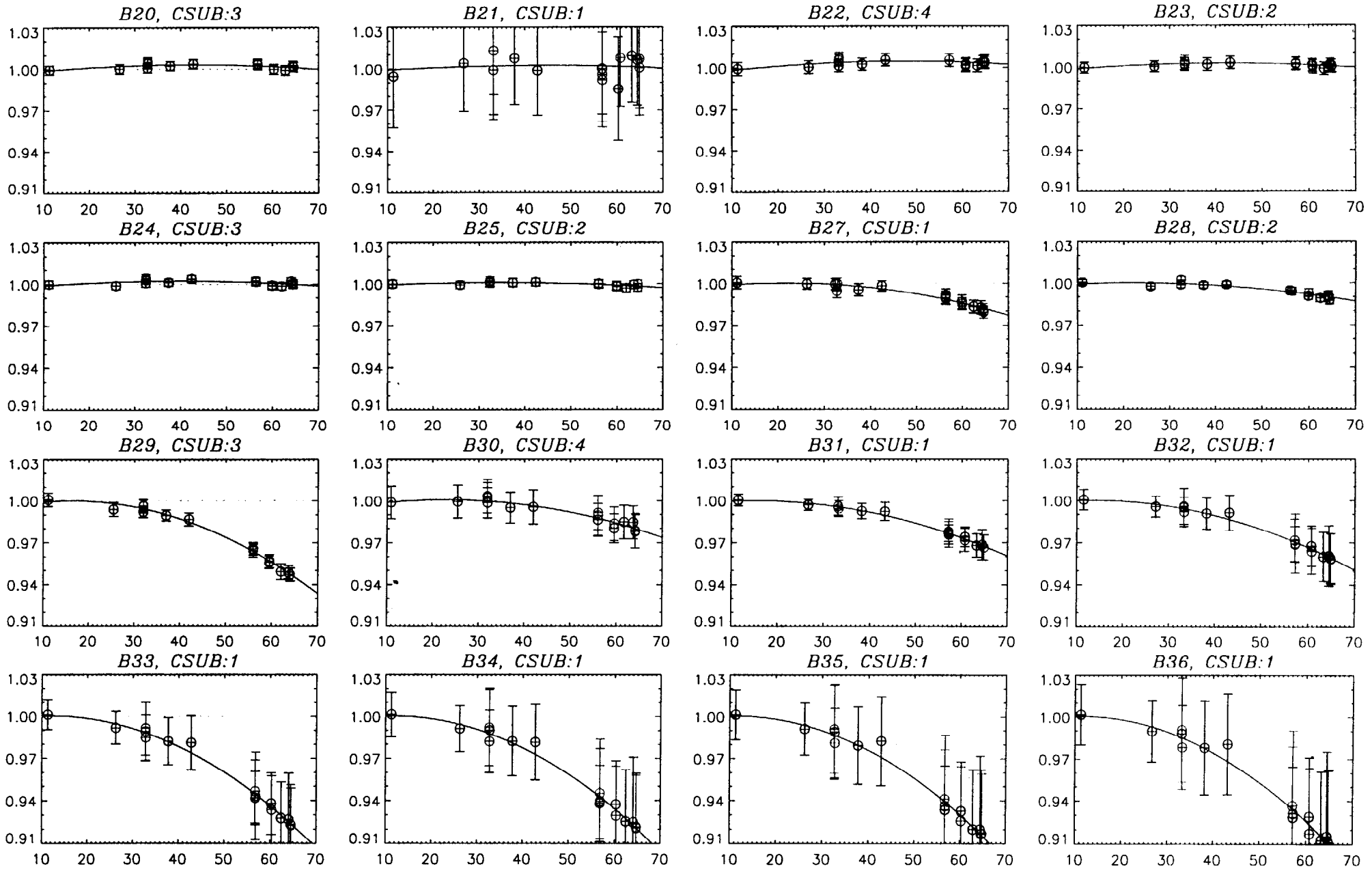
Channel 8 $\langle RVS \rangle_{T_{SM}=T_{SVS}} / \langle RVS \rangle_{T_{SM} \neq T_{SVS}}$ vs AOI for Data Set:[320K_3]
 (Mirror A; w/50frame×40scan Average; Repeat AOIs in Color)



Normalized RVS with weighted quadratic fit

- Quadratic function normalized at 10.75° AOI
- Channel 8 processed assuming $T_{sm}=T_{svs}$
- Channel 8 for 320K_3 data collect with $T_{sm}\neq T_{svs}$ correction

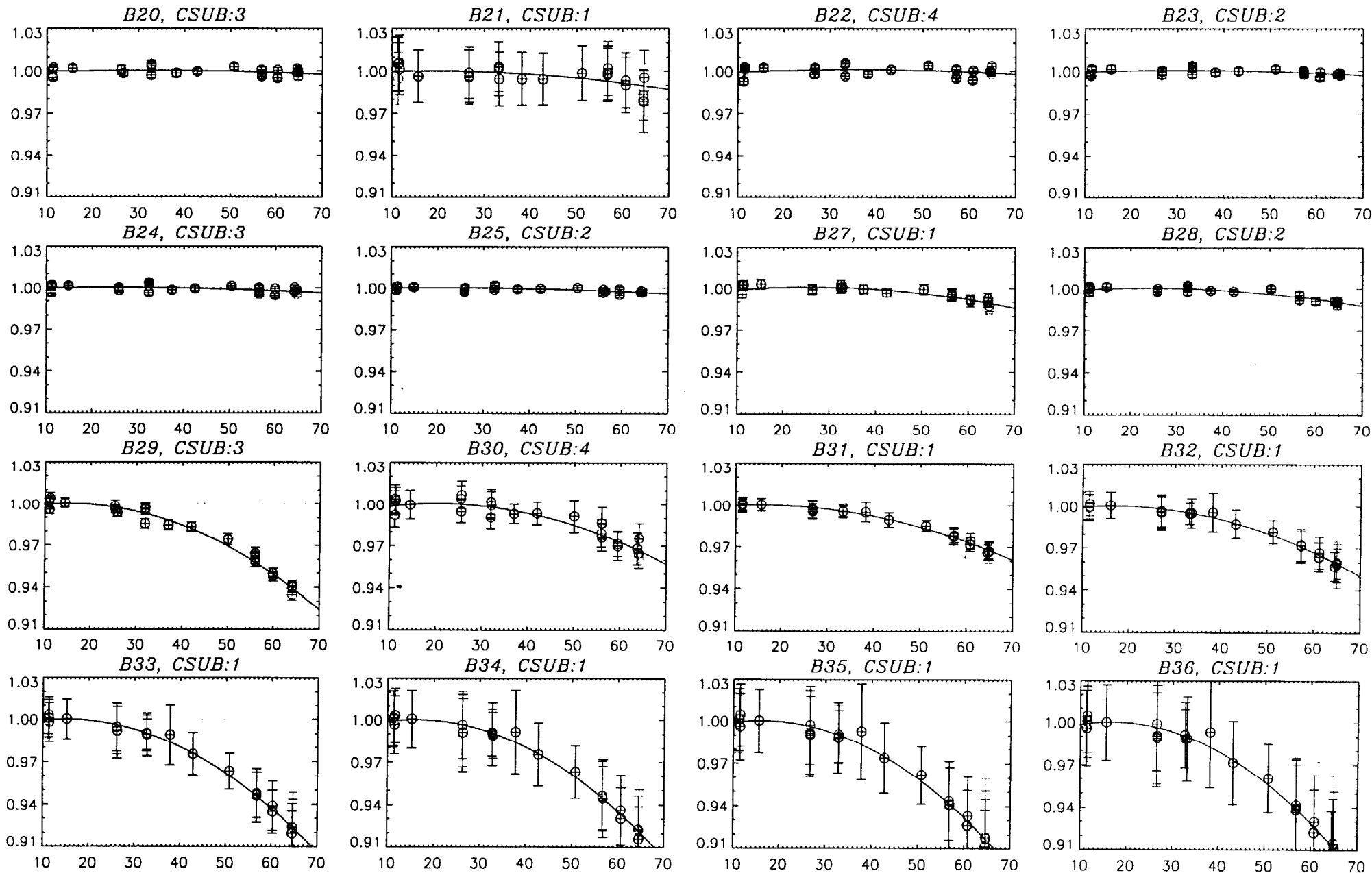
Channel 8 Normalized $\langle RVS \rangle_{40 \text{ scans}}$ @ 10.75° vs AOI for 50 BCS Frames with Quadratic Fit
 (310K_1 Data Set; Mirror A; w/50frame \times 40scan Average and $1-\sigma$ Error Bars; Optimum CSUB; Repeat AOIs in Color)



Note: Instrument & Source Drift Corrected via OBC b1 (1st order); $T_{SM} \neq T_{SVS}$ Term Excluded

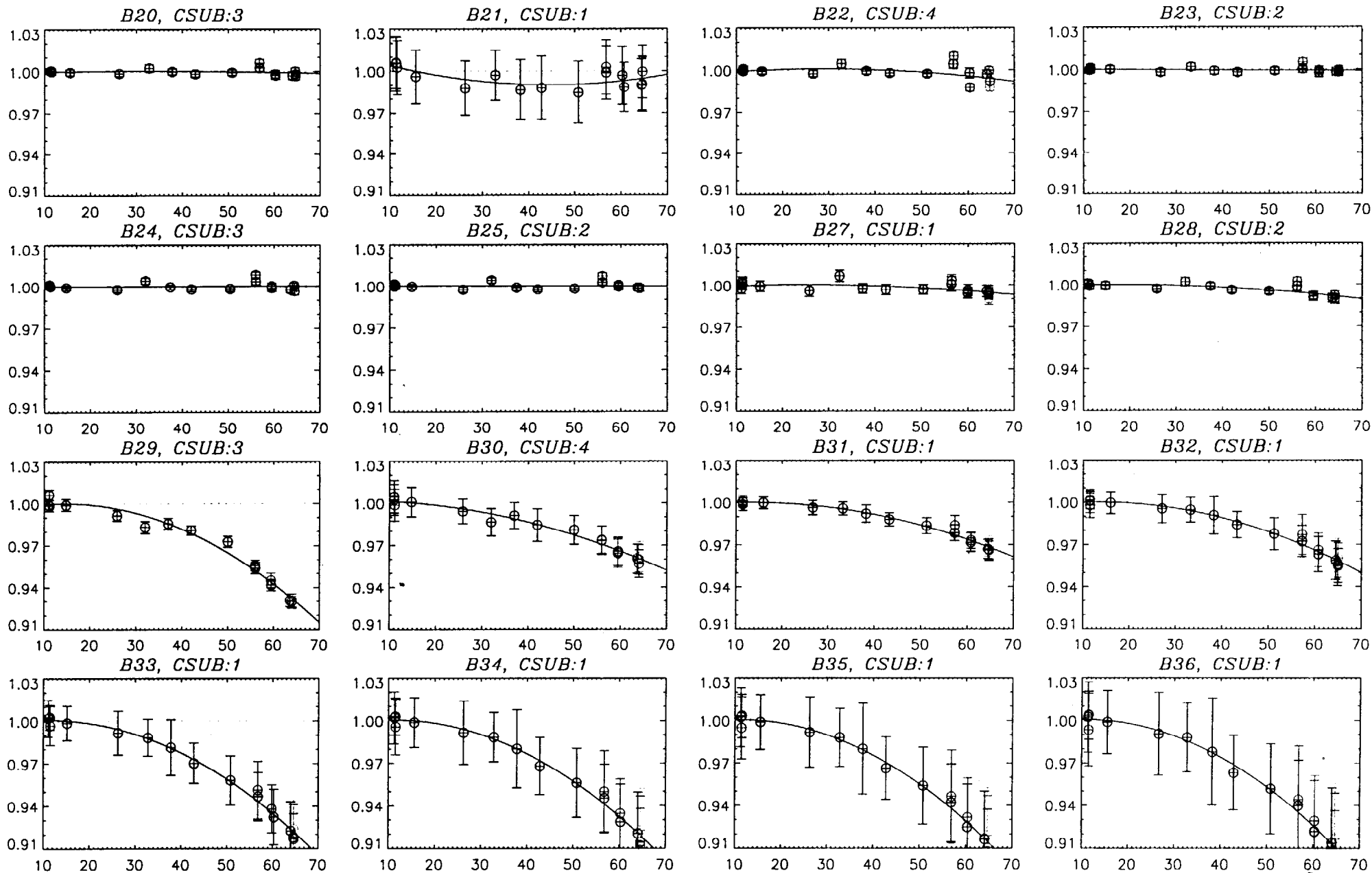
Channel 8 Normalized $\langle RVS \rangle_{40 \text{ scans}}$ @ 10.75° vs AOI for 50 BCS Frames with Quadratic Fit

(320K_2 Data Set; Mirror A; w/50frame \times 40scan Average and $1-\sigma$ Error Bars; Optimum CSUB; Repeat AOIs in Color)



Note: Instrument & Source Drift Corrected via OBC b1 (1st order); $T_{SM} \neq T_{SVS}$ Term Excluded

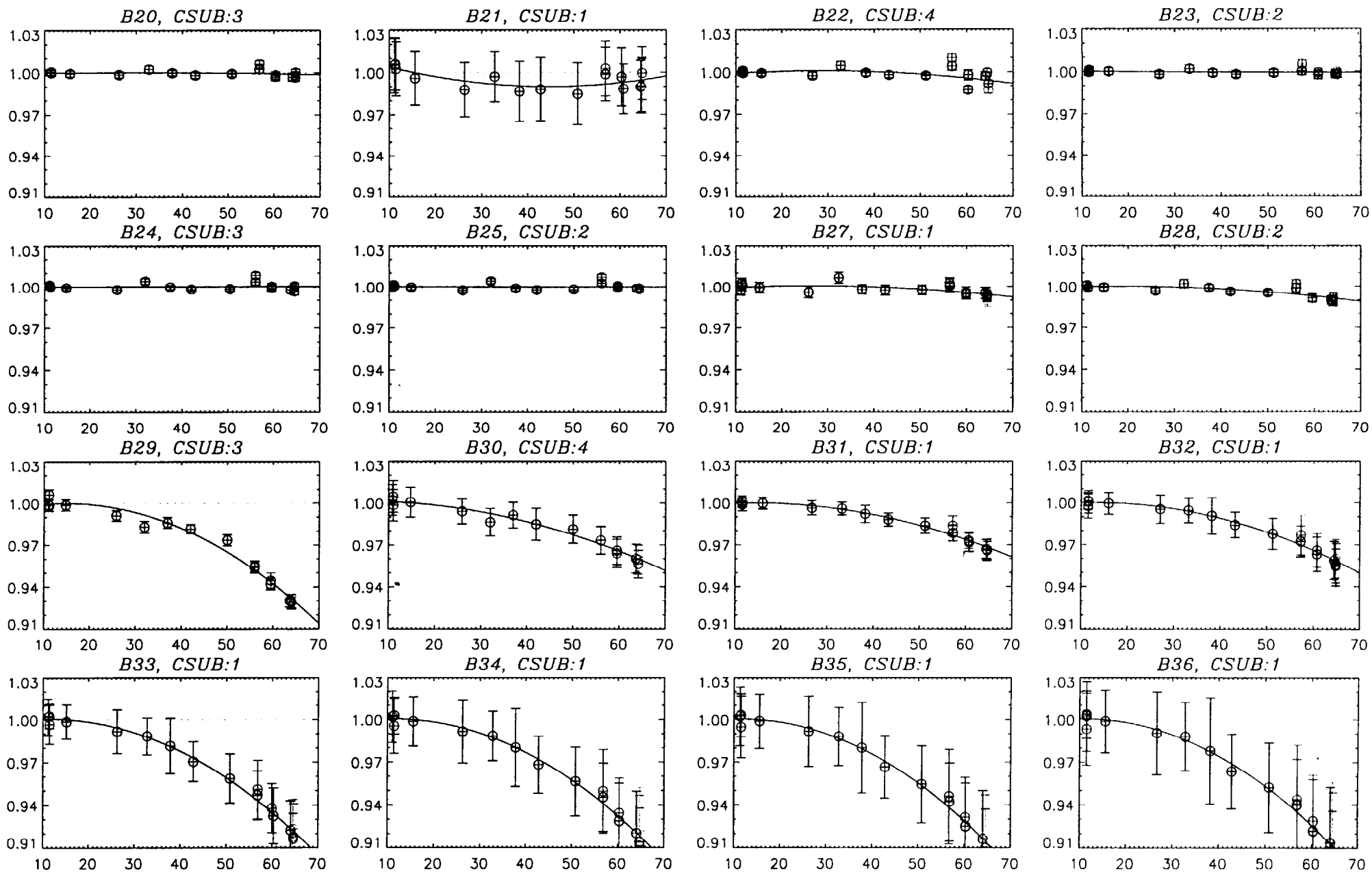
Channel 8 Normalized $\langle RVS \rangle_{40 \text{ scans}}$ @ 10.75° vs AOI for 50 BCS Frames with Quadratic Fit
 (320K_3 Data Set; Mirror A; w/50frame \times 40scan Average and 1- σ Error Bars; Optimum CSUB; Repeat AOIs in Color)



Note: Instrument & Source Drift Corrected via OBC b1 (1st order); $T_{SM} \neq T_{SVS}$ Term Excluded

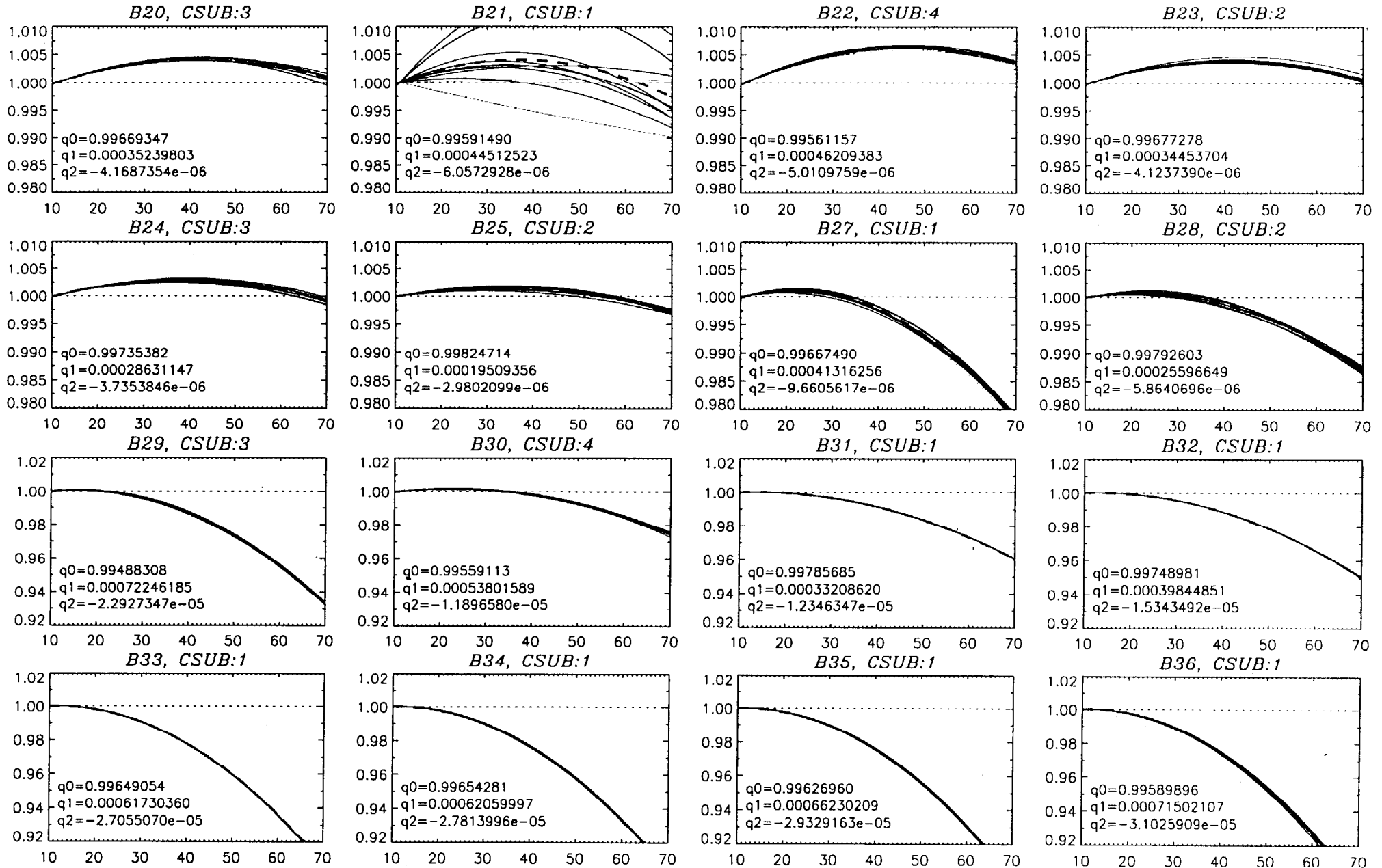
Channel 8 Normalized $\langle RVS \rangle_{40 \text{ scans}}$ @ 10.75° vs AOI for 50 BCS Frames with Quadratic Fit

(320K_3 Data Set; Mirror A; w/50frame \times 40scan Average and $1-\sigma$ Error Bars; Optimum CSUB; Repeat AOIs in Color)

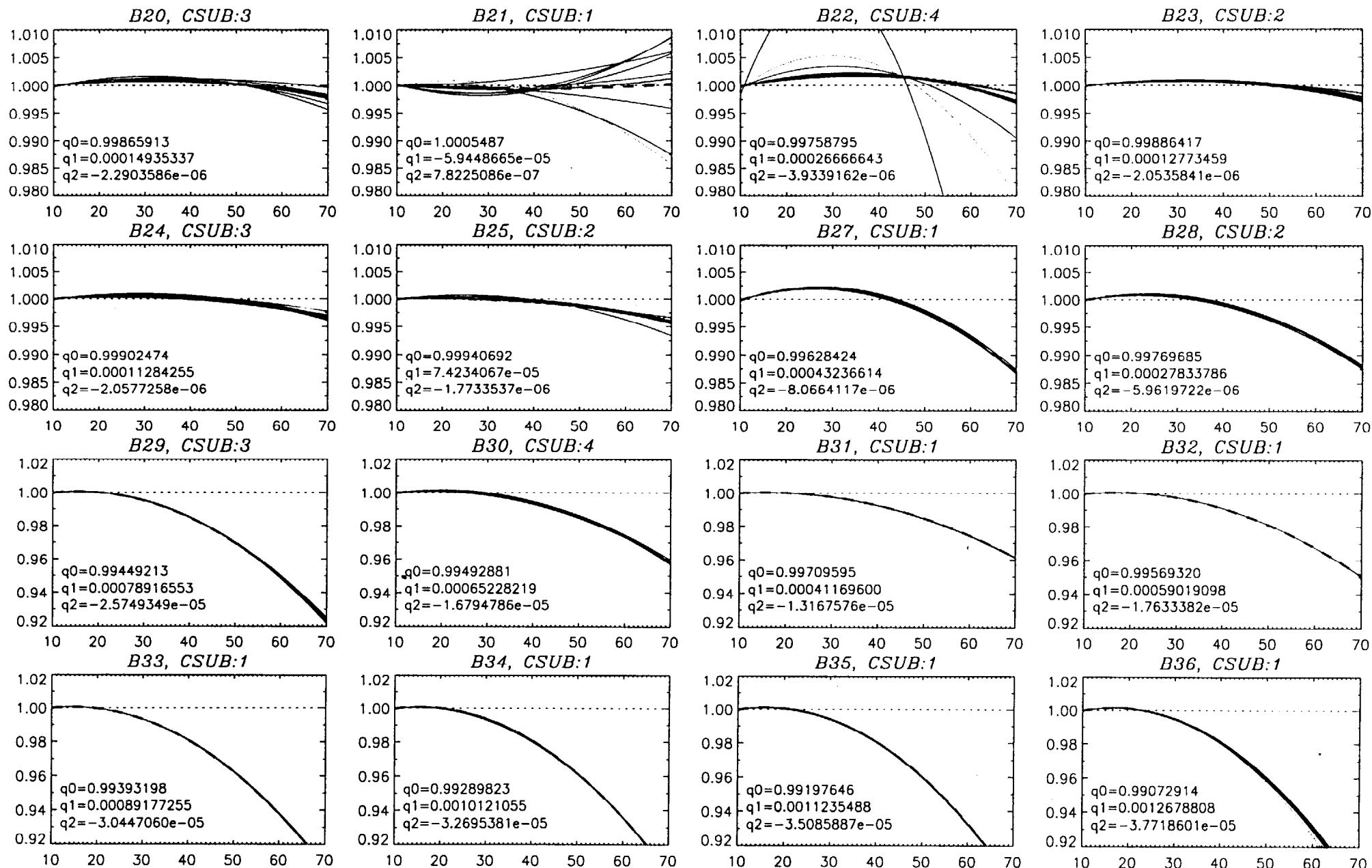


Note: Instrument & Source Drift Corrected via OBC b1 (1st order); $T_{SM} \neq T_{SVS}$ Term Included

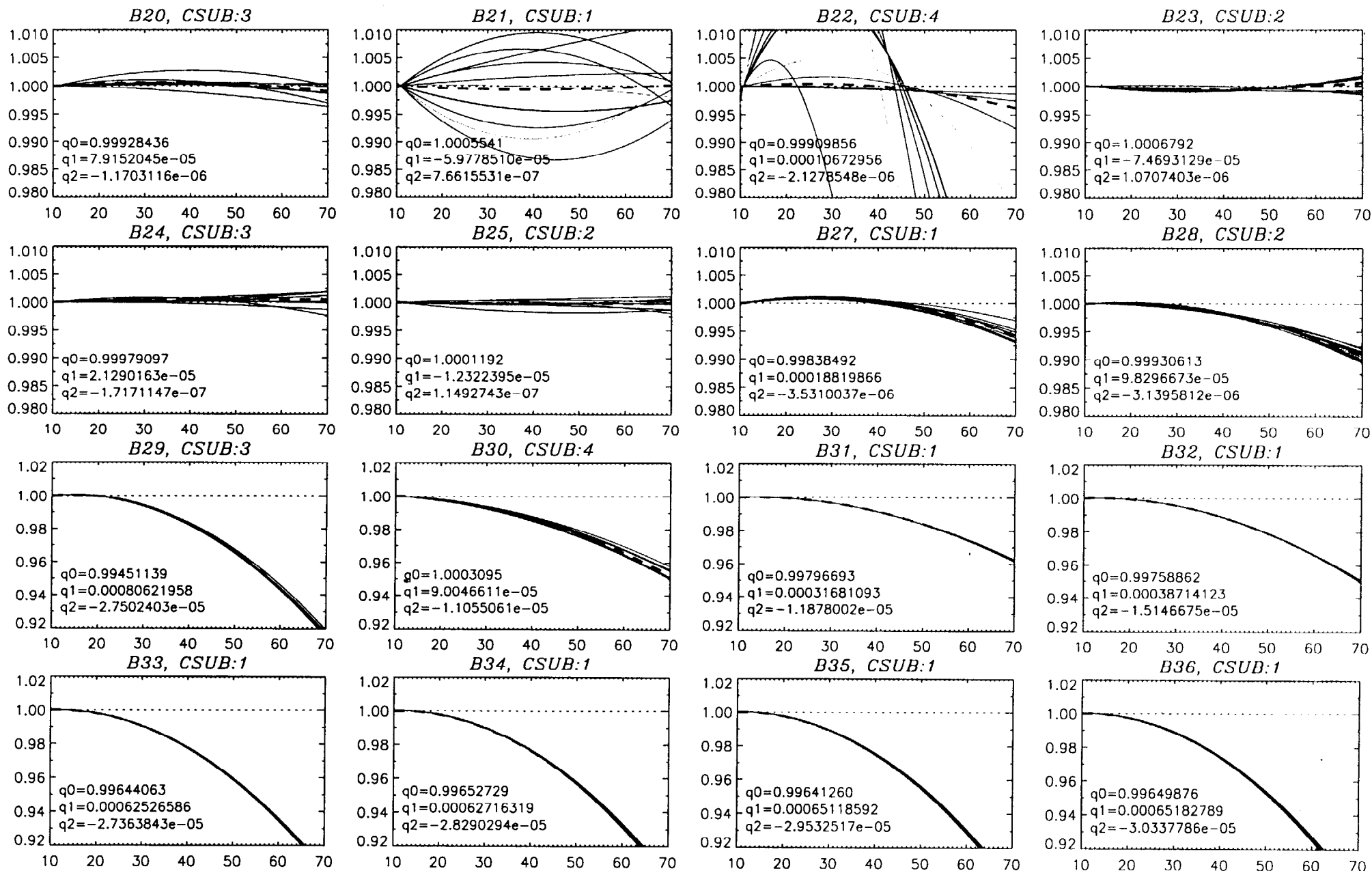
Normalized RVS (@ 10.75°) and Quadratic Fit vs AOI of 10 Channels for 310K_1 Data Set; Mirror A
 Polynomial coefficients result from the average (dashed line) of unsaturated channels



Normalized RVS (@ 10.75°) and Quadratic Fit vs AOI of 10 Channels for 320K_2 Data Set; Mirror A
 Polynomial coefficients result from the average (dashed line) of unsaturated channels



Normalized RVS (@ 10.75°) and Quadratic Fit vs AOI of 10 Channels for 320K_3 Data Set; Mirror A
 Polynomial coefficients result from the average (dashed line) of unsaturated channels



Quadratic Fit of Normalized RVS (@ 10.75°) of Unsaturated Channels vs AOI; Mirror A

_____ 310K_1 - - - - - 320K_2 - - - - - 320K_3 - - - - - Average of 3 Data Sets

